EVALUATION OF THE CANNABIDIOLIC ACID SYNTHASE (CBDAS) VARIANT'S ACTIVITY FROM HEMP IN TRANSGENIC *NICOTIANA BENTHAMIANA* PLANTS

SALMA SHUJAT
Master of Science, Pir Mehr Ali Shah Arid Agriculture University, Rawalpindi, 2013

A thesis submitted
in partial fulfillment of the requirements for the degree of

DOCTOR OF PHILOSOPHY

in

BIOMOLECULAR SCIENCE

Department of Biological Sciences
University of Lethbridge
LETHBRIDGE, ALBERTA, CANADA

EVALUATION OF THE CANNABIDIOLIC ACID SYNTHASE (CBDAS) VARIANT'S ACTIVITY FROM HEMP IN TRANSGENIC *NICOTIANA BENTHAMIANA* PLANTS

SALMA SHUJAT

Date of Defense: May 01, 2025

Dr. Igor Kovalchuk	Professor	MD, Ph.D.
Dr. Olga Kovalchuk	Professor	MD, Ph.D.
Thesis Co-Supervisors		
Dr. Dmytro Yevtushenko	Associate Professor	Ph.D.
Thesis Examination Committee Member		
Dr. Steve Wiseman	Associate Professor	Ph.D.
Thesis Examination Committee Member		
Dr. David Joly	Associate Professor	Ph.D.
External Examiner Université de Moncton		
Dr. Shelley Hoover	Associate Professor	Ph.D.
Chair, Thesis Examination Committee Member		

DEDICATION

With deep gratitude and love, I dedicate this study to the pillars of my strength, my beloved **Parents and Parents-in-law,** whose prayers and constant emotional support from afar have been with me throughout this journey.

To the love of my life, my husband, **Shujat Hussain**, your patience, encouragement, and steady support have been my most excellent source of strength. Your belief in me made me realize that I can have confidence in myself and achieve the dream of my life. Your guidance at every step over these past few years has meant the world to me, and I am forever grateful for your presence through every challenge and milestone.

To my precious children, **Irha Fatima and Muhammad Azlan**, your patience and understanding during my research, even when you were unintentionally neglected, have been remarkable. Your love and resilience inspire me daily. My dear little ones, I love you immensely.

I also dedicate this work to my supportive **siblings and in-laws**, whose encouragement and belief in me have been my greatest source of strength; I am eternally grateful for that.

ABSTRACT

Cannabis sativa L., historically controversial, has gained economic and scientific significance in Canada following legalization, primarily due to its primary cannabinoids: cannabidiol (CBD) and delta-9-tetrahydrocannabinol (THC). High-THC cannabis serves recreational and medicinal purposes, while high-CBD cultivars are increasingly valued in medical and cosmetic industries. Hemp, legally defined as cannabis containing less than 0.3% THC, is widely used in food, textiles, and biodegradable materials. Both cannabidiol and delta-9-tetrahydrocannabinol are synthesized through decarboxylation of their acidic precursors, cannabidiolic acid (CBDA) and delta-9-tetrahydrocannabinolic acid (THCA), respectively, which are derived from a common precursor, cannabigerolic acid (CBGA), through the enzymatic action of cannabidiolic acid synthase (CBDAS) and delta-9-tetrahydrocannabinolic acid synthase (THCAS). These enzymes exhibit partial promiscuity, meaning they can convert CBGA into multiple cannabinoids, including CBDA, THCA, and cannabichromenic acid (CBCA), typically in ratios ranging from 10:1:1 to 20:1:1. Thus, even in plants lacking the *THCAS* gene, trace amounts of THCA can be produced, potentially complicating regulatory classification under Health Canada's guidelines. Despite their structural similarities, bioinformatic analyses have identified unique functional variants of the CBDAS enzyme with differing specificity and activity.

This study evaluated four CBDAS variants, Del_1_108, X59_1_117, Joe_1_129, and CRS1_105, by expressing them in *Nicotiana benthamiana* via stable genetic transformation. After optimizing assay conditions (including incubation time, temperature,

and buffer composition), only Joe_1_129 and X59_1_117 showed enzymatic activity. Both variants catalyzed the exclusive conversion of CBGA to CBDA, with no production of THCA or CBCA, indicating enhanced specificity. Extended incubation (12–16 hours) further improved enzyme efficiency. While Joe_1_129 demonstrated higher conversion efficiency (2.46%), X59_1_117 exhibited better catalytic performance (1.14 vs. 0.89), suggesting functional specialization.

These results provide valuable insights into the evolution and function of CBDAS enzymes and support metabolic engineering strategies aimed at producing hemp cultivars with high CBDA and negligible THC content. Such advances have practical implications for pharmaceutical, cosmetic, and industrial applications, and future research integrating genomic, transcriptomic, and metabolomic approaches could further refine cannabinoid biosynthesis pathways.

.

STATEMENT OF ETHICAL AI

During the preparation of this work, the author used an AI tool (Chat GPT, Grammarly) to rephrase sentences to ensure clarity and make them more understandable and transparent for readers. The author didn't use AI to generate fake results, Graphs, or images. After using this tool/service, the author reviewed and edited the content as needed and take(s) full responsibility for the content of the publication.

ACKNOWLEDGMENTS

First and foremost, I would like to express my deepest gratitude to my supervisor, **Dr. Igor Kovalchuk**. He is an exceptional mentor and one of the kindest and most supportive individuals I have worked with within academia. His patience, encouragement, and ability to turn challenges into learning opportunities have been invaluable. He always took the time to listen, offering reassurance and guidance that helped me stay positive and focused. His continuous support and belief in my potential allowed me to grow as a researcher, providing me with opportunities to participate in various projects that enhanced my skills. I am genuinely grateful for his mentorship and the invaluable lessons he has imparted throughout this journey.

I would also like to thank **Dr. Olga Kovalchuk** and my committee members, **Dr. Dmytro Yevtushenko,** and **Dr. Steve Wiseman**, for their guidance and constructive feedback during my research/presentations. A special thank you to **Dr. Dmytro** for granting me access to lab instruments, which were essential for my work.

A special acknowledgment to **Dr. Dongping Li** and **Dr. Bo Wang**, whose presence in the lab was truly motivating. I would like to sincerely thank **Dr. Esmaeel** for his extensive knowledge and invaluable support in troubleshooting the challenges I encountered throughout my research. I would also like to express my heartfelt gratitude to **Dr. Slava Ilnytskyy** for his invaluable support during bioinformatics work. I truly appreciated his patience in teaching me and his willingness to always be available for discussions whenever I faced challenges. I would also like to thank **Rommy Rodriguez Juarez**, for her prompt and efficient technical assistance whenever required. I want to give a very special thanks to **Rocio Rodriguez Juarez**, whose dedication and willingness to help make a significant impact on my research during a stressful time. Her support and hard work were truly invaluable. Lastly, I would like to express my appreciation to the **lab team** and all those who contributed to my journey. Your support, advice, and motivation have played an essential role in making this accomplishment possible. Thank you all!

TABLE OF CONTENTS

LIST OF TABLES

LIST OF FIGURES

LIST OF ABBREVIATIONS

CBD: Cannabidiol

CBG: Cannabigerol

CBN: Cannabinol

THC: Δ9-Tetrahydrocannabinol

CBDA: Cannabidiolic acid

THCA: Δ9-Tetrahydrocannabinolic

CBCA: Cannabichromenic acid

CBGA: Cannabigerolic acid

CBDAS: Cannabidiolic acid synthase

THCAS: Δ9-Tetrahydrocannabinolic acid

AIDS: Acquired immunodeficiency syndrome

BBE: Berberine-bridge enzyme

PVs: Plant volatiles

DMAPP: Dimethylallyl diphosphate

IPP: Isopentenyl diphosphate

GPP: Geranyl diphosphate

ROS: Reactive Oxygen Species

TKS: Tetraketide synthase

PKS: Type III polyketide synthase

OAC: Olivetolic acid cyclase

OLA: Olivetolic acid

PT: Prenyltransferase

OLS: Olivetol synthase

DNA: Deoxyribonucleic acid

cDNA: complementary DNA

APT: Aromatic prenyltransferase

AA: Amino acid

FAD binding: Flavin-adenine dinucleotide

kDa: Kilodalton

Vmax: Maximum initial velocity

SNPs: Single nucleotide polymorphisms

AMT: *Agrobacterium*-mediated transformation

VIGS: Virus-induced gene silencing

RNAi: RNA interference

TALENs: Transcription activator-like effector nucleases

PMI: Phosphomannose-isomerase

GUS: ß-glucuronidase

GFP: Green fluorescence protein

PDS: Phytoene desaturase

CLCrV: Cotton leaf crumple virus

PEG: Polyethylene-glycol

pH: Power of hydrogen

MEP: Methylerythritol phosphate

MEV: Mevalonate

DMAPP: Dimethylallyl diphosphate

IPP: Isopentenyl diphosphate

CTAB: Cetyltrimethylammonium bromide

EDTA: Ethylenediaminetetraacetic acid

FOR: Forward

REV: Reverse

PCR: Polymerase chain reaction.

dNTP: Deoxyribose nucleotide triphosphate

UV: Ultraviolet rays.

V: volts

LB media: Luria-Bertani Media

ul: Micro litters

ml: Millilitre

mg/ml: Milligram/Milliliter

TAE: Tris-acetate EDTA

Rpm: Revolutions per minute

mM: milli Molar

µF: Microfarad

kV: Kilovolt

Ω: Ohm

NPK: Nitrogen, phosphorus, and potassium

µM: Micrometer

OD: Optical density.

MES: 2-(N-morpholino) ethane sulfonic Acid

MS: Murashige & Skoog Medium

IAA: Indole-3-Acetic Acid

6-BAP: 6-Benzylaminopurine

NAA: 1-Naphthaleneacetic Acid

DTT: Dithiothreitol

SDS: Sodium Dodecyl Sulfate

PMSF: Phenylmethylsulfonyl Fluoride

MMA: 10 mM $MgCl_2$, 10 mM MES pH 5.6, 150 µM acetosyringone

µL: Microliter.

PBST: Phosphate buffered saline Tween-20.

ECL: Enhanced chemiluminescence

mM: Millimolar

HPLC: High-performance liquid chromatography

LS-MS: Liquid chromatography-mass spectrometry

nm: Nanometer

GAPDH: Glyceraldehyde-3-phosphate dehydrogenase

IP: Immunoprecipitation

F1: First filial generation

F2: Second filial generation

SVs: structural variations

His: Histidine

Cys: Cysteine

Tyr: Tyrosine

CHAPTER 1: INTRODUCTION

1.1 Cannabis and Industrial Hemp: Diversity, Applications, and Emerging Potential

Cannabis, scientifically known as *Cannabis sativa* L., belongs to the *cannabaceae* family and is a remarkably diverse and polymorphic plant species originally native to Eurasia (Clarke and Merlin, 2016; Groom et al., 2014). Its global distribution encompasses various habitats, altitudes, soil, and climate conditions (Clarke and Merlin, 2016). Cannabis has a long history of use, valued for its psychoactive and therapeutic properties as well as its industrial applications. Cannabis use includes textile manufacturing, paper production, construction materials, cosmetics, and the food industry (Salami et al., 2020; Schultz et al., 2020). In medicine, cannabis has found application in alleviating chronic pain associated with cancer, mitigating the side effects of chemotherapy, addressing issues related to anorexia and AIDS, managing inflammatory conditions, and providing relief from conditions like epilepsy, spasticity in Tourette's syndrome, skin diseases, and multiple sclerosis, among others (Devsi et al., 2020; Gerasymchuk et al., 2022).

Industrial hemp (*Cannabis sativa* subsp. *sativa*) is an ancient crop originating from Central Asia, historically cultivated for its fiber, seeds, and medicinal properties (Rupasinghe et al., 2020). Its decline in the 20th century was largely due to regulatory confusion with psychoactive cannabis; however, recent legalization in many countries has renewed interest in its agricultural and commercial potential. Hemp seeds are a source of high-quality proteins, essential fatty acids, and bioactive compounds, making them valuable for functional foods and nutraceuticals (Callaway, 2004; Rupasinghe et al., 2020). The plant

also produces non-psychoactive phytocannabinoids such as CBD, which interact with the endocannabinoid system in human and are being studied for their anti-inflammatory, neuroprotective, and anxiolytic properties (ElSohly & Slade, 2005; Rupasinghe et al., 2020). Botanically, hemp differs from medical cannabis in morphology and chemical composition, with hemp bred to have tall stalks and low levels of tetrahydrocannabinol (THC < 0.3%) (Small & Marcus, 2002). Genetically, this distinction results from variations in cannabinoid synthase genes that control THC and CBD biosynthesis (van Bakel et al., 2011). The industrial hemp market is growing rapidly, driven by demand for sustainable materials, dietary supplements, and therapeutic products. Breeding programs across Europe and North America are now focused on improving yield, pest resistance, and cannabinoid profiles to support standardized production (Rupasinghe et al., 2020).

The use and exploration of cannabis have often been topics of debate. Recent legislative changes in many countries have legalized cannabis for medical and recreational purposes (Cox, 2018; Pacula and Smart, 2017), and with the plant's notable therapeutic potential, this has created a pressing need for research efforts in the field of cannabis. Despite being in its early stages, there is a significant and rapidly growing interest in cannabis research, evident in the rising number of publications and citations on the subject. Over 100 cannabinoids have been identified, including Δ9-tetrahydrocannabinol (THC), cannabidiol (CBD), cannabichromene (CBC), cannabigerol (CBG), cannabinol (CBN), and others. These cannabinoids, along with volatile compounds like terpenes, which contribute to the distinctive aroma of cannabis, are synthesized primarily within the trichomes found on the plant's flowers and leaves (Linder et al., 2022; Pattnaik et al., 2022).

Female cannabis flowers are known for their biochemical synthesis of cannabinoids within glandular trichomes. In contrast, male flowers typically contain fewer cannabinoids due to a lower density of trichomes (Livingston et al., 2020). Trichomes are primarily found on the bracts and leaves of both male and female plants and the undersides of the anther lobes in male flowers (Mahlberg et al., 1984). Due to these differences, female cannabis plants are more valuable to cultivators due to more glandular trichomes and, as a result, more cannabinoids found within the plant. Simultaneously, pollination of female cannabis plants can induce seed development in females, resulting in reduced energy used to develop female flowers and glandular trichomes. As such, cultivators commonly separate or destroy male cannabis plants or utilize feminized seeds (Owen et al., 2023).

1.2 Cannabis Biology and Classification

There exists a notable debate within the field of botanical taxonomy regarding the precise number of species that constitute the cannabis genus. However, genomics can settle this debate (McPartland, 2018). Traditionally, informal taxonomic systems have classified cannabis into three distinct groups: *C. sativa* subsp. Sewdativa (recognized for its high CBD content), *C. sativa* subsp. Indica (known for its high THC content), and *C. sativa* subsp. Ruderalis (a wild-type cultivar with roughly equal levels of THC and CBD) (McPartland, 2018). However, a more refined approach based on chemical characteristics, known as chemotaxonomy, further divides *C. sativa* into three chemotypes primarily differentiated by their THC: CBD ratios(Small and Beckstead, 1973). The THC: CBD ratio serves as a crucial indicator for distinguishing plants with high THC content from those with low THC content. The pioneering work of Fetterman et al., in 1971 was instrumental in developing this concept, enabling the differentiation of fiber- and drug-type plants based

on their THC: CBD ratios (Fetterman et al., 1971). Chemotype 1, commonly called the drug type, exhibits a THC: CBD ratio greater than 1 and THC content exceeding 0.3% of the total dry weight. Chemotype 2 represents an intermediate type characterized by a THC: CBD ratio close to 1. In contrast, Chemotype 3, known as the fiber type, typically possesses low THC content and high CBD content, with a THC: CBD ratio considerably less than 1, often at or below 0.1. Additionally, two distinct chemotypes have been identified: Chemotype 4, characterized by high CBG content; and Chemotype 5, where all cannabinoid levels are low. As a result, a THC: CBD ratio of 0.1 or less renders Chemotype 3 non-psychoactive. It's noteworthy that the commercial market offers approximately 600 different cannabis varieties (Rahn et al., 2016), and for many of these varieties, the genetics remain only partially understood.

1.3 Genetics of Cannabinoid Production in Cannabis: Inheritance and Gene Regulation

Cannabis, which is diploid with nine autosomal pairs and one pair of sex chromosomes (X and Y), (Ming et al., 2011), was recently sequenced with a draft genome showing an estimated size of ~808 Mb–900 Mb (Laverty et al., 2019; Singh et al., 2021; van Bakel et al., 2011). Within the genome, particular focus has been placed on the cannabinoid synthase paralogs that are responsible for the psychoactive and medicinal phytocannabinoids. The cannabinoid synthase paralogs are arranged in tandem arrays and are embedded in long terminal repeat retrotransposons on chromosome 7 (Grassa et al., 2018). The origin of the cannabinoid synthase has been speculated to likely represent isoforms originating from a single genetic locus B (de Meijer et al., 2003). It is supported by patterns of segregation in genome-wide association studies (Welling et al., 2020). In

2003, de Meijer and colleagues proposed a genetic framework to elucidate the production of THC and CBD within *C. sativa* populations (de Meijer et al., 2003). They conceptualized cannabinoid yield per crop area as a multifaceted trait influenced by factors such as total above-ground biomass, the proportion of biomass consisting of inflorescence, overall cannabinoid content, and the purity of cannabinoids. Given that the production of THC and CBD is closely tied to the presence of enzymes responsible for deacidification, it appeared that the enzymes themselves adhered to straightforward Mendelian additivity at a synthase locus (de Meijer et al., 2003). Individuals harboring two B_T alleles tended to produce tetrahydrocannabinolic acid synthase (THCAS). Conversely, those with two B_D alleles tended to produce cannabidiolic acid synthase (CBDAS). Meanwhile, individuals carrying one B_T and one B_D allele generated both THC and CBD. Substantiating this hypothesis, the sequencing of *THCAS* and *CBDAS* genes revealed an 89% genetic similarity between them (Taura et al., 1995, 1996). Moreover, de Meijer and colleagues figured out that a homozygous genotype, marked by two loss-of-function alleles (B_0) at the same synthase locus, regulated the accumulation of the precursor CBG in adult plants (de Meijer et al., 2009). Intriguingly, they observed that the expression of CBC was susceptible to environmental factors like light, and its inheritance did not conform to a simple additive or dominant genetic model (de Meijer et al., 2009). Consequently, de Meijer and colleagues detailed the inheritance patterns of THC:CBD ratios and CBC production (de Meijer et al., 2003, 2009). They introduced a mathematical model to portray cannabinoid abundance as a potentially intricate quantitative trait. While de Meijer and colleagues probed into the genetic basis of cannabinoids, their examination primarily focused on a straightforward additive model. More complex genetic effects remained largely unexplored until research

was conducted by Weiblen and colleagues (Weiblen et al., 2015). This subsequent work identified that the enzymes participating in cannabinoid biosynthesis, seemingly originating through gene duplication events, represent compelling candidates for targeted breeding initiatives and genetic engineering endeavors. Furthermore, the THC:CBD ratio in most genotypes and populations is fundamentally governed by the cannabinoid synthase alleles present in the plant, while environmental factors and cultivation conditions can influence total cannabinoid levels (Chandra et al., 2017; Toth et al., 2020). In 2020, Campbell et al. showed the production of phytocannabinoids is influenced by two additive genetic loci (Campbell et al., 2020). Their analysis utilized data from cultivars with pure THC or CBD chemotypes and hybrid progeny, allowing them to estimate composite genetic effects on cannabinoid concentration variations (Campbell et al., 2020). In contrast to previous research, this study revealed distinct findings concerning the nonadditive aspects of cannabinoid inheritance. THC concentration appeared to be a polygenic trait, with both additive and dominant genetic effects contributing to its expression patterns. On the other hand, CBD concentration may be influenced by cytoplasmic genomes and additive genes. Maternal and genetic additive effects influenced CBC expression (Campbell et al., 2020). These findings suggest that the inheritance of cannabinoids is more intricate than previously assumed with cytogenetic and maternal factors potentially influencing cannabinoid ratios and concentrations. Furthermore, emerging evidence confirms and strongly supports a highly complex genetic model (de Meijer et al., 2003, 2009; Staginnus et al., 2014; Weiblen et al., 2015). Variations among genetically uniform F1 offspring from parents with specific alleles displayed considerable variation in cannabinoid levels, highlighting the impact of environmental factors. Furthermore, THC

and CBD expression depend on linked loci and gene duplication on chromosome 6 for synthesis. Intriguingly, efforts to reduce THC expression in hemp cultivars have not resulted in its complete elimination. In summary, these findings underscore the complexity of cannabinoid inheritance, surpassing the explanatory power of simple genetic models.

1.4 Biochemistry and Evolution of THCAS, CBDAS, and CBCAS in Cannabis: Catalytic Efficiency and Substrate Specificity

Many studies have suggested that *THCAS* may have evolved from *CBDAS* through gene duplication (Onofri et al., 2015; Shoyama et al., 2012; Taura et al., 2007). Both enzymes exhibit similarities in their reaction mechanisms, relying on molecular oxygen to oxidize cannabigerolic acid (CBGA) and generating hydrogen peroxide as a byproduct. Notably, the domain present in these enzymes bears a striking resemblance to the C-terminal berberine-bridge-enzyme (BBE) domain, a critical enzyme in the alkaloid biosynthesis pathway of *Eschscholzia californica* (Onofri et al., 2015).

Although THCA synthase and CBDA synthase have been extensively studied since their initial characterization nearly two decades ago (Taura et al., 1995; Taura et al., 1996), research on CBCA synthase remains in its early stages. Cannabichromene (CBC-C5), a rare cannabinoid that has recently garnered increased attention, is the most abundant among its class and is currently being investigated in multiple clinical studies for its potential anti-inflammatory, immunoprotective, antibacterial, and antifungal effects (Davis and Hatoum, 1983; DeLong et al., 2010; Eisohly et al., 1982; Turner and Eisohly, 1981). The gene responsible for encoding CBCA synthase was only recently identified, and its enzymatic activity was confirmed through expression in *Komagataella phaffii* (Laverty et al., 2019). CBCAS shares a high degree of similarity with THCAS, exhibiting 93% amino acid

identity and 96% nucleotide sequence identity. According to kinetic analyses conducted by Laverty et al. (2019), CBCAS demonstrates a stronger substrate affinity, with a Km of 9.3 μM, in contrast to 137 μM reported for THCAS. However, its catalytic efficiency is notably lower, with a kcat of 0.02 s^{-1} compared to 0.2 s^{-1} for THCAS (Taura et al., 1995; Taura et al., 2007). While the catalytic efficiency (kcat/Km) of CBCAS is marginally higher, THCAS performs significantly better under high substrate concentrations. This suggests that for industrial applications involving elevated substrate levels, enhancing the turnover rate of CBCAS could greatly improve its utility. The exact molecular basis for these kinetic differences remains unclear, as no crystal structure of CBCAS has yet been resolved. One of the primary challenges in working with CBCA synthase is its intricate folding requirements, which include the incorporation of a covalently bound FAD cofactor and the presence of at least six surface-exposed N-glycosylation sites. These features often lead to heterogeneous mannosylation when the protein is expressed in *K. phaffii*. However, due to its 93% sequence identity with THCAS, a reliable homology model of the protein can be constructed.

The enzymatic process for THCAS and CBDAS begins with transferring a hydride ion from the CBGA substrate to the isoalloxazine ring of the FAD coenzyme, initiating the reaction. Another piece of evidence supporting their shared ancestry is that both enzymes display some degree of promiscuity; each enzyme can convert CBGA into CBDA and THCA in varying ratios, with the most common ratios being ~10:1 and ~20:1. Consequently, even in the absence of a *THCAS* gene, a plant can still contain THCA, suggesting *CBDAS* produces THCA in small amounts. Moreover, it is plausible that only a limited number of amino acid residues determine the product specificity of both enzymes

due to their functional similarities in med catalytic mechanisms (Taura et al., 2007). Beyond their sequence similarities, THCAS and CBDAS also share comparable biochemical and structural properties. Notably, enzyme promiscuity has led to regulatory considerations, such as those outlined in the Cannabis Act by Health Canada and within the United States for the classification of hemp cultivars (Cox, 2018).

1.5 Biosynthesis of Cannabinoids in Cannabis

Despite ongoing research, there is still a lack of clarity regarding the molecular mechanisms underlying cannabinoid biosynthesis (Fellermeier and Zenk, 1998). In summary, cannabinoids share a common initial pathway that involves tetraketide synthase (TKS) (Kearsey et al., 2020). TKS, a type III polyketide synthase (PKS), catalyzes the sequential condensation of hexanoyl-CoA with three molecules of malonyl-CoA, resulting in the formation of 3,5,7-trioxododecaneoyl-CoA (Taura et al., 2007). This compound, 3,5,7-trioxododecaneoyl-CoA, then undergoes cyclization and aromatization facilitated by olivetolic acid cyclase (OAC). This transformation leads to olivetolic acid (OLA) formation as coenzyme A is detached (Gagne et al., 2012). Subsequently, an aromatic prenyltransferase (PT) inserts a prenyl group into the highly nucleophilic 2-resorcinol position, producing CBGA (Fellermeier and Zenk, 1998). Cannabigerolic acid (CBGA) serves as the central biosynthetic precursor for the major cannabinoids, as it is enzymatically converted into cannabidiolic acid (CBDA), tetrahydrocannabinolic acid (THCA), and cannabichromenic acid (CBCA) by their respective synthases. These acidic cannabinoids are subsequently decarboxylated into their neutral forms, CBD, THC, and CBC, through non-enzymatic processes such as heat or light exposure (Fellermeier and Zenk, 1998). OLA is the fundamental polyketide nucleus in synthesizing cannabinoids

(Gagne et al., 2012; Z. Tan et al., 2018; Taura, 2009). Initially, it was believed that OLA biosynthesis was solely governed by TKS, where spontaneous cyclization and aromatization occurred after adding the third malonyl group (Z. Tan et al., 2018). However, a breakthrough in understanding this process came when Taura and colleagues utilized a cDNA encoding olivetol synthase (OLS) from *C. sativa* (Taura, 2009). Surprisingly, their recombinant OLS did not produce OLA, the expected compound, but instead exclusively generated its decarboxylated form known as olivetol. This observation was further substantiated by experiments involving crude enzyme extracts obtained from flowers and early-growth leaves, the primary cannabinoid-producing tissues of *C. sativa*, which also exclusively produced olivetol.

These findings strongly suggested that OLA biosynthesis does not solely depend on OLS and may involve the participation of other enzymes. However, it is worth noting that olivetol is not detected in *C. sativa*, leading to the hypothesis that olivetol might be an artifact of *in vitro* enzyme assays (Taura, 2009). The puzzling situation of OLA not being producible in a lab setting, while its lab-created by-product olivetol doesn't occur naturally has been clarified by the finding that OAC plays a crucial role. OAC facilitates the substrate's intramolecular C2 → C7 aldol condensation without decarboxylation. Kearsey et al. (2020) further confirmed that in the absence of OAC, a nonenzymatic C2 → C7 decarboxylative aldol condensation of the tetraketide intermediate occurs resulting in the formation of olivetol instead of OLA (Kearsey et al., 2020). It's essential to emphasize that OLS and OAC do not directly interact; instead, the metabolite must diffuse from one enzyme to the other through the cytosol. Subsequently, OLA converts into CBGA by adding GPP, a process catalyzed by the enzyme APT (Lercker et al., 1992). GPP itself is

formed through the condensation of IPP and DMAPP by GPP synthase (Bohlmann and Gershenzon, 2009; Davis and Croteau, 2000). CBGA serves as a central intermediate, giving rise to THCA, CBDA, and cannabichromenic acid (CBCA) through a series of enzymatic reactions (Fig. 3) (Shoyama et al., 2012; Z. Tan et al., 2018). It was previously noted that the significant difference between THCAS and CBDAS arises from their primary mode of action during proton transfer (Tahir et al., 2021). CBDAS extracts a proton from the terminal methyl group of CBGA, while THCAS targets the cyclization pattern and, ultimately, the cannabinoid profile of a given cannabis cultivar (Taura et al., 2007). A more comprehensive understanding of these pathways is essential as it could pave the way for their deliberate manipulation, either within the plant itself or through recombinant vectors, to enable the selective production of specific cannabinoids. Over the past two decades, there has been significant progress in cannabinoid natural product chemistry. However, substantial research remains to be undertaken to produce the desired cannabinoids in sufficient quantities and with high purity.

1.6 Genetic and Enzymatic Basis of Cannabinoid Biosynthesis in Cannabis

Recent advancements in genome sequencing of cannabis and hemp have made it possible to systematically analyze genes responsible for encoding the enzymes involved in the cannabinoid biosynthesis pathway. Single-nucleotide polymorphisms (SNPs) in the coding regions of *CBDAS* synthases play a key role in determining plant chemotypes. A deep understanding of how these genetic variations impact enzyme activity and cannabinoid accumulation can aid in breeding new cultivars with desirable cannabinoid profiles.

The *THCAS* gene consists of a 1,635-nucleotide open reading frame (ORF) that encodes a 545-amino-acid (AA) polypeptide, including a 24-AA signal peptide and is classified

within the p-cresol methyl-hydroxylase superfamily (Quimby et al., 1973). Similarly, *CBDAS* is a single-exon gene that encodes a 516-AA protein, featuring a 28-AA signal peptide. Both enzymes share two primary domains: an FAD-binding domain and a BBE-like domain. The FAD coenzyme interacts with the His^{114} and Cys^{176} residues within domain I. Mutations in key active site residues, such as His^{292} and Tyr^{417}, have been shown to reduce enzymatic activity (Shoyama et al., 2012*).*

CBDAS catalyzes the oxidative cyclization of CBGA to form CBDA, which can be further decarboxylated to CBD (Taura et al. 1996, 2007*a*). CBDAS also possesses His^{114} and Cys^{176} flavin-binding sites. It has a FAD binding site composed of amino acid sequence (Arg-Ser-Gly-Gly-His). Similarly, mutation of His^{114} residue results in the loss of CBDAS activity (Taura et al., 2007b). Cannabichromenic acid synthase (CBCAS) catalyzes stereoselective cyclization of CBGA to CBCA. CBCAS does not require molecular oxygen for the oxidocyclization of CBGA (Morimoto et al., 1998).

The CBDAS enzyme shares a high amino acid identity (84%) with the THCAS enzyme (Andre et al., 2016). This enzyme synthesizes CBDA stereospecifically from CBGA through FAD via an oxygen-dependent mechanism, which is very similar to the mechanism of action of the THCAS enzyme. Enzymatic reactions catalyzed by both enzymes start with the transfer of a hydride ion from the substrate CBGA to the isoalloxazine ring of the FAD coenzyme. Interestingly, a difference of about 16% in the amino acid sequence between THCAS and CBDAS, primarily at specific active site residues, is sufficient to determine their distinct product specificities (Taura et al., 2007b). Biochemically, THCAS and CBDAS are monomeric with a native protein mass of 74 kDa and similar Pi, Vmax, and Km for CBGA substrate.

In a study, phylogenetic analysis of amino acid sequences of THCAS and CBDAS from in-house sequenced cultivars demonstrated lower levels of divergence for THCAS as compared to CBDAS among cultivars. Among 29 analyzed cultivars, they detected only 8 and 18 unique sequences for THCAS and CBDAS, respectively (Sing et al., 2021). This agrees with a previous study suggesting a recent evolution of *THCAS* from the *CBDAS* group (Onofri et al., 2015). Alternatively, the artificial selection of plants with the highest level of THCA and with the most active THCAS reduced the number of THCAS variants in the cannabis population. Interestingly, previous genotyping studies have revealed that hemp and marijuana are significantly different at the genome level (Sawler et al., 2015), and it has also been proven that both environmental and genetic factors are responsible for such chemotype diversity in cannabis (Bócsa et al., 1997; de Meijer et al., 2003; Hillig, 2005). Environmental factors such as the amount of light received by plants and their quality, nutrients, and temperature have been shown to modulate the accumulation of cannabinoids in a plant. At the same time, it has been reported that the CBD:THC ratio remains constant irrespective of plant development and ambient conditions (Pacifico et al., 2008). Therefore, analysis of the cannabinoid profile in leaves of developing plants allows us to deduce the chemotype of a plant before its maturity.

Among cannabinoids, CBD is an isomer with a different cyclic system from THC. In recent years, it has attracted much attention as a powerful antiepileptic drug for the treatment of intractable epilepsy in children (García-Peñas et al., 2021). The significant difference between these reactions is reflected in the proton transfer step: the CBDAS enzyme extracts a proton from the methyl group at the end of CBGA, while the THCAS enzyme extracts a

hydroxyl group (Andre et al., 2016). Given their similar sequences and reactions, it is speculated that the subtle differences in active sites among these cannabinoid synthetases can regulate oxidative cyclization reactions, forming different ring systems (Andre et al., 2016). At present, CBD, used as a therapeutic drug, is generally extracted from plants or chemically synthesized (Mücke et al., 2018). The amino acid mutations of proteins can cause changes in their spatial three-dimensional structure, which may lead to functional changes. Therefore, mutations in the key amino acids involved in the interaction between CBDAS and substrate CBGA cause changes in CBDAS enzyme activity by altering their interaction relationship. The results provide a theoretical basis for enhancing the affinity between the enzyme and substrate, which lays a foundation for the industrial production and application of recombinant CBDAS and improving the yield of biosynthetic CBD. Some investigators suggest that sequence variation among *THCAS* gene copies influences the ratio (van Bakel et al., 2011; Onofri et al., 2015), while others propose that a nonfunctional *CBDAS* allele in the homozygous state alters the ratio in favor of THC (Weiblen et al., 2015). Current explanations for differences among cultivars in the THC:CBD ratio focus on cannabinoid synthase gene loci (Sirikantaramas et al., 2004; van Bakel et al., 2011; Onofri et al., 2015; Weiblen et al., 2015). In spite of recent advances in genome sequencing, precisely how cannabinoid synthase genes influence the THC:CBD ratio and the overall abundance of cannabinoids (potency) is poorly understood (van Bakel et al., 2011). Among the obstacles to understanding the relationship between cannabinoid synthase gene diversity and phenotypes is genomic complexity which has frustrated attempts to assemble complete chromosomes until recently (Laverty et al., 2019; Kovalchuk et al., 2020).

1.7 Biosynthesis and Bioactivity of Terpenoids in Cannabis

The cannabis plant produces a unique category of compounds known as cannabinoids, characterized by their terpenophenolic nature. According to Chandra et al. (2017), 565 constituents have been identified from *Cannabis sativa*, with 120 falling under phytocannabinoid classification (Chandra et al., 2017). Additionally, these plants undergo biosynthesis, generating a diverse range of lipophilic volatile metabolites through processes like reduction, methylation, and acylation, which involves the removal of hydrophilic components (Pichersky et al., 2006). These plant volatiles (PVs) serve various functions, including regulating interactions with both biotic and abiotic factors. They can attract pollinators, provide protection against pests and pathogens, and fulfill other ecological roles (Dudareva et al., 2013). Terpenoids, among PVs, stand out as the most significant and abundant chemical group. They are further categorized into isoprenes (C5), monoterpenes (C10), and sesquiterpenes (C15). Terpenoids are synthesized through the utilization of dimethylallyl diphosphate (DMAPP) and isopentenyl diphosphate (IPP), which are derived from distinct biosynthetic pathways in different cellular compartments. These pathways share geranyl diphosphate (GPP) as a common precursor with cannabinoids (Nagegowda, 2010; Russo, 2011). Cannabis terpenoids, with their essential role in determining the flavor and fragrance of the plant, have garnered recent attention from researchers (Russo and Marcu., 2017). Comparative studies between terpenoid-rich essential oils and CBD have confirmed the latter's superior bioactivity and medicinal properties (Gallily et al., 2018). Compared to CBD, terpenoids exhibit transient immunosuppressive effects and lower bioactivity levels, such as reactive oxygen species ROS scavenging properties. Moreover, several individual phytochemicals from cannabis,

including terpenoids such as β-myrcene, β-caryophyllene, limonene, and α-pinene, have shown potential as bioactive molecules (Russo and Marcu, 2017). In addition, other non-terpenoid compounds like cannabisin B, isolated from hemp seed hulls, have demonstrated biological activity; for example, cannabisin B has been shown to induce autophagy in human hepatoblastoma HepG2 cells (T. Chen et al., 2013).

Terpenoid profiles, like those of cannabinoids, can be used to classify different cannabis chemovars (Fischedick, 2017). Their biosynthesis is regulated by terpene synthases, organized in large gene families, with their activity being spatially and temporally distributed. This makes them ideal targets for genetic engineering (Tholl, 2006). Terpenoids are highly potent metabolites, and even when inhaled at very low doses, they can affect the behavior of animals and humans. Their potential synergy with cannabinoids, known as the "entourage effect", has also been proposed (Russo, 2011). Terpenes are likely among the key contributors to this effect, alongside other phytochemicals such as flavonoids and stilbenes. (Russo and Marcu, 2017). Studies have highlighted the fundamental role that cannabis mono- and sesquiterpenoids play in the potency of flower extracts (Russo and Marcu, 2017).

1.8 Advancements in Genetic and Biotechnological Approaches for Optimizing Cannabinoid Biosynthesis

In recent years, with the rapid development of genetic engineering, protein engineering, and various omics technologies, technology for the directed evolution of enzyme molecules has been continuously improved. The glycosylation pattern, C-terminal BBE domain, and product specificity of CBDAS and THCAS were studied by site-directed mutagenesis (Zirpel et al., 2018). In amino acid mutagenesis experiments, the

selection of mutation sites is highly random. If the function of the mutated protein can be predicted, the experiment's reliability can be significantly improved (Steinbrecher et al., 2017)

The most frequent genetic variation within a population's DNA sequence is Single nucleotide polymorphisms (SNPs). In the context of the Cannabidiolic Acid Synthase (*CBDAS*) gene in cannabis, SNPs can have substantial impacts on the structure and function of the CBDAS enzyme, which is pivotal in the biosynthesis of cannabidiolic acid (CBDA), the precursor to CBD. SNPs in the *CBDAS* gene can lead to amino acid substitutions in the enzyme, potentially altering its three-dimensional structure. This can affect the enzyme's active site, where the conversion of CBGA to CBDA occurs. Depending on the nature of the SNP, the enzyme's catalytic efficiency may be enhanced, reduced, or even abolished. For example, a SNP that results in a non-conservative amino acid change could disrupt hydrogen bonding or hydrophobic interactions within the enzyme, leading to a less stable or less active enzyme conformation. Conversely, some SNPs may confer a beneficial change that improves enzyme stability or affinity for its substrate.

The effects of SNPs on *CBDAS* activity are crucial for determining the overall yield of CBD in cannabis plants. Plants with CBDAS variants that have reduced enzyme activity due to deleterious SNPs might produce lower levels of CBD, which could affect the plant's suitability for industrial purposes. On the other hand, SNPs that enhance CBDAS activity might be targeted in breeding programs aimed at developing high-CBD cannabis strains. Recent studies have identified several SNPs in the *CBDAS* gene across different cannabis cultivars, linking specific genetic variants to variations in CBD content. For instance, a

study by Onofri et al. (2015) demonstrated that certain SNPs in the *CBDAS* gene correlate with decreased enzyme activity, leading to lower CBDA and, consequently, CBD levels in the plant. Understanding these genetic variations provides valuable insights into the molecular mechanisms underlying cannabinoid biosynthesis and offers potential strategies for optimizing cannabis strains through selective breeding or genetic engineering. Biotechnological methods, including genetic transformation, have the potential to advance *C. sativa* breeding significantly. Comparable strategies in other plant species have resulted in improved varieties with more excellent resistance to biotic and abiotic stresses, enhanced nutritional and processing qualities, and higher productivity (Gosal and Wani, 2018). Current progress in cannabis molecular biology, including systems biology, has significantly enhanced our comprehension of the cannabinoid biosynthesis pathway (Hesami et al., 2020; Hurgobin et al., 2021). These developments have opened the door to employing biotechnological methods for cannabinoid production in various non-native hosts, such as yeast, bacteria, and plant cells, as well as enzymatic systems by constructing a comprehensive biosynthetic pathway by assembling its genes into a single artificial gene cluster (Bharadwaj et al., 2021). Furthermore, transformation and tissue regeneration techniques can be utilized on cannabis to modify the genome. Importantly, recent breakthroughs in computational, molecular, and synthetic biology tools present an opportunity to rapidly understand and exploit the specialized metabolic potential of plants (Arya et al., 2020).

In cannabis cultivation, gene editing techniques represent a promising opportunity using transformation methods, which include projectile bombardment or *Agrobacterium*-mediated transformation (AMT) with *in vitro* tissue culture for regeneration. Once

incorporated, the transferred (desired) genes can be engineered using various strategies, including overexpression, virus-induced gene silencing (VIGS), or RNA interference (RNAi), offering researchers a precise way to control gene activity. However, transgenes often incorporate randomly within the cannabis genome, which cause genetic variability. Recent improvements in gene editing tools, such as TALENs, CRISPR-Cas9, and other precision nucleases, have emerged as game-changers. These tools allow for direct and specific genome alterations, eliminating the randomness associated with conventional methods.

1.9 Advancements in Gene Editing and Transformation Techniques for Cannabis Cultivation

Gene editing components are delivered to plants through Agroinfiltration using *Agrobacterium tumefaciens*. While agroinfiltration is one method for delivering genetic material, the transformation of cannabis hairy roots is more likely achieved through *Agrobacterium rhizogenes*-mediated co-cultivation. For example, one of the studies by Wahby et al. (2013) reports the successful establishment of *Agrobacterium rhizogenes*-mediated hairy root cultures in *Cannabis sativa* L. using co-cultivation techniques. The researchers used hypocotyl explants from intact hemp seedlings and infected them with various *Agrobacterium* strains containing either root-inducing (Ri) or tumor-inducing (Ti) plasmids. These explants were co-cultivated under controlled *in vitro* conditions, resulting in hairy roots and tumor tissue induction. Notably, the transformed hairy roots exhibited rapid growth, extensive lateral branching, dense root hair formation, and did not require exogenous phytohormones for proliferation, typical characteristics of hairy root cultures. Molecular confirmation through PCR analyses demonstrated successful T-DNA

integration from the *Agrobacterium* plasmids. Additionally, hairy roots transformed with the AR10GUS strain showed positive *β-glucuronidase* (GUS) staining, verifying transgene expression (Wahby et al., 2013). Other techniques, such as vacuum infiltration and nanoparticle-based approaches, can also be employed to deliver molecules of interest into the plant cell (Ahmed et al., 2021; Sorokin et al., 2020) or to silence undesirable genes in cannabis (Schachtsiek et al., 2019). Before applying this technique to *C. sativa*, it is essential to establish an efficient transformation protocol capable of regenerating transgenic plants. In this context, some efforts have been made to transform *C. sativa*. Notably, successful Agrobacterium-mediated transformation (AMT) has been documented in stem and leaf-derived callus suspension cultures from four hemp varieties, expressing the *phosphomannose-isomerase* (PMI) gene. (Feeney and Punja, 2003, 2015). While agroinfiltration is one method for delivering genetic material, the transformation of cannabis hairy roots is more likely achieved through *Agrobacterium rhizogenes*-mediated co-cultivation. Furthermore, studies have documented the successful establishment of *Agrobacterium rhizogenes*-mediated hairy root cultures in three hemp varieties and two drug-type varieties, exhibiting β-glucuronidase (GUS) positive staining (Wahby et al., 2013, 2017). These studies also reported both *in vivo* and *in vitro* infections of hypocotyl and cotyledonary node explants using *Agrobacterium* strains carrying Ri and Ti plasmids. AMT has also been successfully performed on leaf, male and female flowers, stem, and root tissues from eight hemp varieties using vacuum infiltration. This transformation was confirmed by detecting β-glucuronidase (GUS) activity and green fluorescent protein (GFP) expression in the modified tissues (Deguchi et al., 2020). In the previous study, silencing of the *phytoene desaturase* (PDS) gene was conducted, leading to an albino

phenotype in leaves and male and female flowers. Additionally, *Agrobacterium tumefaciens*-mediated transformation of *C. sativa* seedlings from three medical cannabis varieties has been documented, resulting in transient expression of the *GUS* gene (Sorokin et al., 2020). In addition, nanoparticle-based transient gene transformation of trichomes and leaf cells from one hemp variety, in which transcription of soybean genes and localization of fluorescent-tagged transcription factor proteins were detected, has also been achieved (Ahmed et al., 2020a). Finally, transient transformation with *A. tumefaciens* and Cotton leaf crumple virus (CLCrV) induced gene silencing of *PDS* and *magnesium chelatase subunit I (ChII)* genes in leaves from one hemp variety (Schachtsiek et al., 2019), and GFP-transient expression through polyethylene-glycol (PEG)-mediated protoplast transformation have also been obtained (Beard et al., 2021). However, despite the successful genetic transformation of different non-regenerating explants, *C. sativa* recalcitrance to plant regeneration has prevented the recovery of transgenic plants (Feeney and Punja, 2017; Wrobel et al., 2018). It was only recently that the regeneration of one *C. sativa* transformed plant has been reported (Zhang et al., 2021).

Nowadays, *in vitro*-based biotechnological methods are applied for breeding to improve plant genotypes through rapid multiplication, micropropagation of disease-free plants, production of plant-derived metabolites, and gene transformation (Hesami et al., 2020b). Genetic transformation (genetic engineering) is one of the key biotechnological tools to improve plant performance. The *Agrobacterium* strain, *Agrobacterium* cell density, immersion time, type and concentration of antibiotics to kill *Agrobacterium*, type, and concentration of the selected antibiotics, the concentration of acetosyringone, duration of co-cultivation, pH, and temperature of co-cultivation, and wounding treatments are the key

factors that can affect *Agrobacterium*-mediated gene transformation and should be taken into account in all gene delivery studies (Liu et al., 2020). The interaction between the plant genotype and the abovementioned factors challenges implementing the transformation strategies. This leads to genotype-dependency in gene transformation studies, meaning the different responses of different cultivars to a specific protocol. As an *in vitro* procedure, AMT is a multi-factorial biological system that is highly variable and complex, making it a non-deterministic and a non-linear process.

1.10 Use of tobacco as a heterologous expression system

Tobacco is a model plant for *Agrobacterium*-mediated genetic transformation due to the simplicity of its transformation procedures. The traditional technique does not require expensive machinery or complicated procedures. Some significant advantages of using tobacco for genetic transformation include the following.

(1) Tobacco plants can be easily regenerated from tobacco leaf pieces through organogenesis (Constantin et al. 1977).

(2) Short acclimatization time and a high trans-potting survival rate: up to 100% of the in vitro-raised plants transferred from lab to greenhouse condition were successfully established ex vitro. The acclimatization is brief, taking only a matter of days (Chandra et al. 2010).

(3) Easy crossing: Hand-pollination is easily accomplished due to large flower size.

(4) Longevity: By removing the flowering buds or tips, plants continue growing in greenhouse conditions for extended periods, which provides supplemental experimental material, particularly for the W38 tobacco species.

(5) Prolific seed production for sustaining lines and testing results.

(6) Increased biomass has the potential for molecular farming to produce recombinant proteins due to tobacco's high biomass yield (Twyman et al. 2003).

(7) Efficiency of transient transformation assays (Ma et al. 2012).

Due to the advantages mentioned above, most plant research scientists view tobacco as a prime choice for genetic transformation in proof-of-concept experiments with the added benefit of multiple, practical uses.

I used *Nicotiana benthamiana* as a model plant to evaluate enzyme activity for two main reasons. First, developing transgenic cannabis plants is challenging due to the absence of well-established tissue culturing protocols and techniques in the literature. Second, the entourage effect in cannabis plants occurs when multiple compounds, such as terpenes, flavonoids, and minor cannabinoids, interact synergistically, complicating the isolation of pure enzymatic activity from CBDA synthase, as it is difficult to attribute observed effects to a single compound in such a chemically complex system. Model organisms such as Nicotiana benthamiana (tobacco plant) are often used to develop transgenic plants to overcome this challenge. Tobacco provides a genetically tractable and chemically simpler system, enabling researchers to express cannabinoid synthase genes like CBDA synthase in isolation. This allows precise characterization of enzyme function and facilitates metabolic engineering efforts to produce specific cannabinoids in a controlled environment.

CHAPTER 2: HYPOTHESIS AND OBJECTIVES

2.1 Objectives

This study has the following objectives,

1. Identifying and isolating genes encoding *CBDAS* variants in industrial hemp cultivars.
2. Stable integration of identified *CBDAS* variant genes into the genome of *N. benthamiana* plants.
3. Molecular analyses of transgenic plants and evaluation of the CBDAS variant's activities in a heterologous host.

2.2 Hypothesis

I hypothesized that some variants can efficiently convert CBGA into CBDA, CBCA, and THCA compared to wildtype and other variants. To improve enzyme properties for cannabinoid production, previously a postdoc in Kovalchuk's lab analyzed all 26 sequences to evaluate the glycosylation pattern, effects on the C-terminal berberine bridge (BBE) domain, the active sites, and the specificity of the enzymes. After some bioinformatic analyses, several polymorphisms were identified that likely changed the level of CBDA produced. Those included: S116A is an SNP present at the activation site of CBDAS variants that should result in an approximately 2.6-fold increase in CBDA production compared with CBDAS wild-type; amino acid substitutions of T74S, N168S, N196S, and K474Q that would result in an almost 80% increase in CBDA production; conversely, the amino acid substitutions G375R, and P476S should impair CBDAS activity. My role was to investigate the effect of these CBDAS variants on the production

level of CBDA and THCA through a stable transformation of the gene variant in the *Nicotiana benthamiana* plant.

CHAPTER 3: MATERIALS AND METHODS

3.1 Analysis of CBDAS Variants Activity

3.1.1 Molecular Cloning and Characterization of the *CBDAS* Gene in *Cannabis sativa*

3.1.1.1 *Plant Material and Growth Conditions*

The varieties of *Cannabis sativa* (X59_1_117, Del_1_108, CRS1_105, Joe_1_129) were sourced from donated seeds. The plants were grown and controlled to ensure the best possible growth and development. The plants were grown under controlled conditions at 25 °C with an 18-hour light and 6-hour dark photoperiod to promote healthy growth. I maintained these conditions in greenhouses and growth chambers to ensure vigorous plant growth. Plants that were 4 weeks old had their leaves sampled for cloning and cannabinoid extraction.

3.1.1.2 *Genomic DNA Extraction*

With some modifications, the cetyltrimethylammonium bromide (CTAB) technique suggested by Murray and Thompson (1980) was used to extract genomic DNA from *Cannabis sativa* leaf tissues.

A 500 mL working solution of DNA extraction buffer contained 31.8 g of sorbitol, 6 g of Trizma base, and 0.84 g of EDTA, adjusted to pH 7.5 and supplemented with 1.9 g/500ml sodium bisulfite at the time of use. The Nucleic Lysis Buffer was prepared by mixing 50 mL of 1M Tris (pH 7.5), 50 mL of 0.25M EDTA, 100 mL of 5M NaCl, and 5g of CTAB in 50 mL of double-distilled water (DDW), adjusting the pH to 7.5 with HCl and bringing

the final volume to 250 ml. CTAB was heated to dissolve completely. A 5% Sarkosyl solution was prepared by dissolving 50 g of N-Lauroyl sarcosine (Sigma L-5125) in 1 L of DDW.

The Total Extraction Solution was prepared before DNA isolation by combining 10 mL of DNA Extraction Buffer (38 mg of sodium bisulfite per 10 mL), 10 mL of Nucleic Lysis Buffer, and 4 mL of 5% Sarkosyl solution. For DNA extraction, ~100 mg of frozen leaf tissue was homogenized in 600 µL of Total Extraction Solution, and the samples were incubated at 65°C for 60 minutes, with gentle inversion every 15 minutes. 600 µL of chloroform was added to remove cellular debris, and the mixture was gently inverted and shaken for 5 minutes under a fume hood. The centrifugation of samples was done at 12,000 g for 10 minutes at room temperature, and the upper aqueous phase was transferred to a new tube with great care, avoiding contamination from the protein-rich interphase. The chloroform extraction step was repeated to ensure purity. Genomic DNA was precipitated by adding 2/3 volume (400 µL) of isopropanol, followed by overnight incubation at -20°C. Centrifugation at 4°C at 12,000 g for 5 minutes pelted the precipitated DNA. It was then twice rinsed with 70% ethanol (1mL) and centrifuged at 12,000 g for 5 minutes. After 10 minutes of air drying at room temperature, the DNA pellet was reconstituted in 40 µL of nuclease-free water. A NanoDrop spectrophotometer was used to measure the extracted DNA's concentration and purity. A 260/280 absorbance ratio of ~1.8–2.0 indicated high-quality DNA suitable for downstream molecular analyses.

3.1.1.3 *Primer Design for CBDAS Gene Amplification*

The cannabidiolic acid synthase (*CBDAS*) gene sequences were analyzed bioinformatically, and specific primers (Table 1) were designed using NCBI Primer-

BLAST. The forward and reverse primers (Figure 1), including known variants, were selected to amplify the full-length *CBDAS* gene. The primers were synthesized commercially and subsequently used for PCR amplification from the extracted genomic DNA.

Table 1. Primers used for PCR-based amplification of the *CBDAS* gene.

Sequence Name	Seq 5'-3'
IPB-173-FOR	AAAGGATCCATGACATTCTCCTTTTG
IPB-174-REV	AAAGGTACCATGAGATGCCGTGGAAG
1- Promoter For	CCGCATAGAAATAGAAGGCGAAGAG
1- CBDAS Rev	CTCCTCCACCAAAGTGTCCACC
2- CBDAS For	CAAGCACGTATTTGGGGTGAGAAG
2- Terminator Rev	CGCGATAATTTATCCTAGTTTGCGC

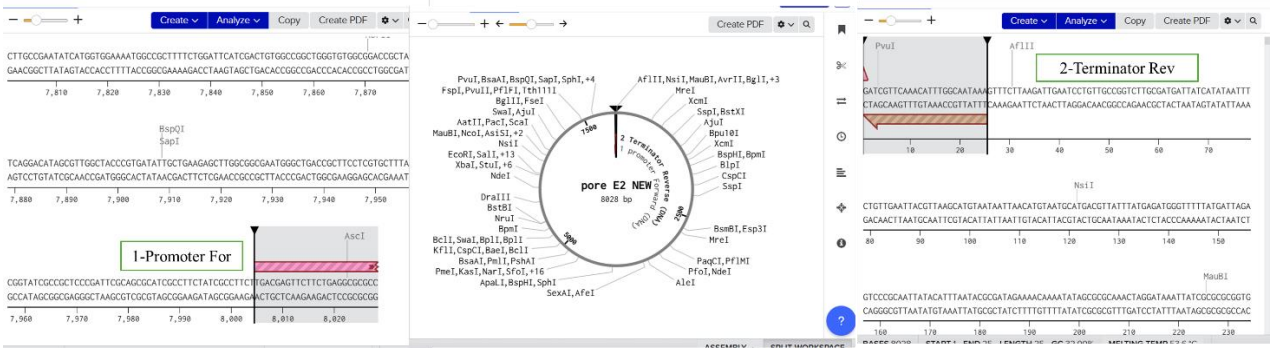

Figure 1. The illustration depicts the locations of the 1-Promoter Forward and 2 2-Terminator Reverse primer sequences, which were utilized together with the 1-*CBDAS* Reverse and 2-*CBDAS* Forward primer sets. This graphic was created using Benchling software to accurately map the primer's positions on the pORE-E2 vector.

3.1.1.4 *Amplification of the CBDAS Gene Using PCR*

The *CBDAS* gene was amplified from genomic DNA utilizing Phusion High-Fidelity DNA Polymerase (Fisher Thermo Scientific) to guarantee high precision and reduce errors during the amplification process.

Each PCR reaction was prepared in a total volume of 100 µL, containing approximately 500 ng of genomic DNA, 1X Phusion HF buffer, 0.2 mM of each dNTP, 0.5 µM of forward IPB-173 and reverse primers IPB-174, and 1 unit of Phusion DNA polymerase. The PCR cycling conditions were optimized as follows: an initial denaturation step at 98°C for 30 seconds, followed by 35 cycles of denaturation at 98°C for 10 seconds, annealing at 64°C for 30 seconds, and extension at 72°C for 1 minute per kilobase of the expected amplicon size. A final extension was performed at 72°C for 10 minutes to ensure complete amplification of the target sequence.

Following amplification, the PCR products were analyzed by agarose gel electrophoresis to confirm the presence and size of the amplified fragments. A 1% agarose gel was prepared in 1X TAE buffer (40 mM Tris, 20 mM acetic acid,01 mM EDTA, pH 8.0) and stained with GelRed. Approximately 5 µL of each PCR product was mixed with 1 µL of 6X loading dye and loaded onto the gel alongside a DNA ladder (e.g., 1 kb or 100 bp ladder) for size reference. Electrophoresis was carried out at 100 V for 30–45 minutes, and the gel was visualized under UV light using a gel documentation system. A single, distinct band at the expected size confirmed the successful amplification of the *CBDAS* gene.

3.1.1.5 *Purification of PCR Product*

The *CBDAS* gene fragment that was amplified was purified utilizing a commercially available PCR purification kit, like the Monarch PCR purification kit, according to the instructions provided by the manufacturer. The PCR product was combined with the binding buffer and passed through a silica membrane column, enabling the DNA to adhere to the membrane. Following a wash with the designated wash buffer, the DNA was eluted in 30 µL of nuclease-free water. The concentration of the purified PCR product was measured using a spectrophotometer or Nanodrop. 200 ng of the purified sample was then employed for cloning experiments.

3.1.1.6 *Double Digestion of Insert and Vector*

The *CBDAS* gene fragment (insert) and the pORE-E2-CFLAG vector were both subjected to double digestion using FastDigest *BamHI* and *KpnI* restriction enzymes (provided by Thermo Scientific). For the insert, a reaction mixture was created with a total volume of 30 µL, which included 200 ng of purified PCR product, 1X FastDigest buffer, 1 µL of *BamHI,* and 1 µL of *KpnI*. Likewise, 1 µg of pORE-E2-CFLAG plasmid DNA was digested under identical conditions. The reactions were kept at 37°C for 15 minutes, followed by heating at 80°C for 20 minutes to inactivate the enzymes. The digested products were then purified using a commercial PCR purification kit and quantified in preparation for the ligation step.

3.1.1.7 *Ligation of Insert into Vector*

The ligation reaction was performed to insert the *CBDAS* gene into the digested pORE-E2-CFLAG vector. A total volume of 20 µL was used to prepare the reaction mixture, which

included 100 ng of the digested vector, 60 ng of the digested insert, 1X T4 DNA ligase buffer, and 1 µL of T4 DNA ligase (Thermo Scientific). The mixture was subsequently incubated at 22°C for 5 minutes to promote the ligation of the insert with the.

3.1.2 Preparation of *E. coli* Competent Cells and Transformation with pORE-E2

To prepare *E. coli* competent cells with optimal transformation efficiency, a strain like DH5α was utilized. A single colony of *E. coli* was transferred into a small amount of Luria-Bertani (LB) broth and incubated overnight at 37°C while shaking. The next day, the overnight culture was moved to a larger volume of fresh LB broth (usually between 50–100 mL) and cultivated at 37°C with shaking until it reached the mid-log phase, corresponding to an OD_{600} of 0.4–0.6. After the culture attained the desired density, it was chilled on ice for 10–15 minutes.

During this time, all necessary solutions and equipment, including centrifuge tubes, pipettes, and a 1 mM calcium chloride ($CaCl_2$) solution, were pre-chilled. The cells were harvested by centrifugation at 4°C for 10 minutes at 3,000–4,000 × g, and the supernatant was carefully removed without disturbing the cell pellet. The pellet was then gently resuspended in a small volume of ice-cold 1 mM $CaCl_2$ solution, typically 1/10th of the original culture volume, and incubated on ice for 30 minutes, with occasional gentle swirling. Following the incubation, the cells were further cooled by placing them back on ice. The competent cells were then divided into 200 µL aliquots in pre-chilled microcentrifuge tubes and flash-frozen using liquid nitrogen or a dry ice/ethanol bath. The aliquots were stored at -80°C for future use.

For transformation, an aliquot of competent cells was thawed on ice, and 10 µL of the ligation mixture (containing the pORE-E2 vector with *CBDAS* variants) was added. The mixture was incubated on ice for 30 minutes, followed by a heat shock at 42°C for 30–90 seconds, and then immediately cooled on ice for a few minutes. 1 mL of pre-warmed LB medium was added to the mixture, and the cells were incubated at 37°C with shaking for 2 hours to allow for recovery.

Following recovery, the transformed cells were plated on LB agar plates containing 50 mg/ml kanamycin as a selection marker and incubated overnight at 37°C. The next day transformed colonies were observed. Five-milliliter overnight cultures were then initiated by inoculating single colonies into LB broth. These 5 mL cultures were grown overnight and used for plasmid isolation and further experiments.

It's worth noting that keeping the cells at 4°C overnight enhanced their viability. Nonetheless, key factors for effective transformation included collecting the cells during the log phase of growth, utilizing pre-chilled materials, and consistently ensuring the cells remained on ice.

3.1.2.1 *Isolation of Plasmid and Confirmation by Agarose Gel Electrophoresis*

Plasmid isolation was performed using the Plasmid Miniprep Kit by New England biolabs, according to the manufacturer's instructions. The final elution volume was 50 µL.

To confirm successful plasmid isolation, agarose gel electrophoresis was performed. A 1% agarose gel was prepared using 60 mL of 1X TAE buffer. For gel preparation, 0.6 g of agarose was added to 60 mL of 1X TAE buffer in a gel flask, which was then heated in a microwave oven for approximately 30 seconds until the agarose was completely dissolved.

The solution was then allowed to cool to room temperature, after which 3 µL of GelRed was added for DNA staining. The gel solution was poured into a casting tray and left undisturbed for at least 30 minutes to solidify.

For sample preparation, 3 µL of loading dye, 3 µL of plasmid DNA, and 4 µL of distilled, autoclaved water were mixed thoroughly. The prepared samples were then loaded into the gel wells. Electrophoresis was performed at 80 V for 30 minutes in a gel electrophoresis chamber filled with 1X TAE buffer. After 30 minutes, the gel was visualized under UV light using a gel documentation system, confirming the presence of the isolated plasmid.

3.1.2.2 *PCR-Based Confirmation*

A PCR validation was conducted to verify the existence of the *CBDAS* gene in the extracted plasmid. The plasmid preparation was diluted tenfold in autoclaved distilled water, and 2 µL of this diluted plasmid DNA was used as the template for PCR amplification. The reaction mixture for PCR was prepared in a total volume of 25 µL, which included 10 µL of PCR master mix, 1 µL of forward primer (IPB 173), 1 µL of reverse primer (IPB-174), 5 µL of nuclease-free water, and 2 µL of the diluted plasmid DNA. Four PCR tubes containing this mixture were placed into a thermocycler for amplification. The PCR conditions were set as follows: initial denaturation at 94°C for 3 minutes, denaturation at 94°C for 1 minute, annealing at 64°C for 40 seconds, extension at 72°C for 40 seconds, and a final extension at 72°C for 7 minutes. This process was repeated for 30 cycles. After the PCR, the amplified products were analyzed by agarose gel electrophoresis to confirm the presence of the expected DNA fragment.

3.1.2.3 *Restriction Digestion-Based Confirmation*

To perform the restriction enzyme digestion, the following reaction mixture was prepared: 1 µL of each restriction enzyme *(BamHI* and *KpnI*), 2 µL of the buffer, 14 µL of water, and 2 µL of DNA, resulting in a total volume of 20 µL. The mixture was incubated at 37°C for 15 minutes to allow the enzymes to act. After incubation, the enzymes were inactivated by heating the mixture at 80°C for 20 minutes. The samples were run on gel electrophoresis, and the digested products were visualized under the UV in the gel documentation system.

3.1.3 Transformation of *Agrobacterium* Cells (EHA 105) with *pORE-E2* Harboring the Variants of the *CBDAS* Gene

3.1.3.1 *Preparation of Competent Cells of Agrobacterium (EHA105)*

To prepare competent *Agrobacterium* EHA105 cells for transformation, a single colony from an *Agrobacterium* plate was used to grow a bacterial culture in 5 mL of LB medium containing rifampicin (25 mg/mL) and kanamycin (50 mg/mL). The culture was incubated at 28°C in a shaker overnight. The next day, 5 mL of the overnight culture was transferred to 250 mL LB media with the same antibiotics. This culture was incubated at 28°C with vigorous shaking at 250 rpm for 5-6 hours until the OD_{600} reached 0.5-0.8. The cultures were then placed on ice for 15 minutes. The tubes were centrifuged at 5000g for 15 minutes at 4°C, and the supernatant was discarded. The pellet was initially washed with wash buffer (20 mM $MgCl_2$, 50 mM $CaCl_2$, filtered and stored at 4°C), but since the plan was to perform electroporation later, 10% glycerol was used to wash the pellet instead of the wash buffer.

After dissolving the pellet in 10% glycerol, the tubes were kept on ice for 15 minutes, followed by a second centrifugation. 10% glycerol was used to resuspend the pellet stored on ice overnight in an ice bucket at 4°C. The following day, 100-200 µL aliquots of the competent cells were transferred into Eppendorf tubes (2mL) and stored at -80°C for future use.

3.1.3.2 *Electroporation of pORE-E2 in Agrobacterium Strain EHA105*

The competent *Agrobacterium* cells were taken out of the ultra-low temperature freezer set at -80°C and allowed to thaw on ice for 15 minutes. Forty microliters of the competent cells were transferred into Eppendorf tubes, and 2 µL of plasmid DNA was introduced into the mixture. The remaining 60 µL of competent cells were kept aside as a control. The combination of competent cells and plasmid DNA was then placed into chilled electroporation cuvettes (BioRad) featuring a 2 mm gap. The Gene Pulser (BioRad) was configured with the following parameters: capacitance set to 25 µF, voltage at 2.4 kV, resistance at 200 Ω, and a pulse duration of about 5 milliseconds (automatically adjusted by the Gene Pulser). The cells underwent pulsing in the BioRad Gene Pulser, after which 1 mL of LB media was promptly added to the electroporation cuvette. The resulting mixture was transferred to Eppendorf tubes and incubated in a shaker at 28°C for 2-3 hours. Once the incubation period was over, the cells were spread onto LB plates supplemented with antibiotics kanamycin (50 mg/L) and rifampicin (25 mg/L). The plates were then placed in an incubator at 26-28°C for 2-3 days to facilitate colony formation from the transformed cells.

3.1.3.3 *Confirmation of Plasmid Presence in Agrobacterium*

Single colonies collected from transformed plates were used to grow a 5-10 mL culture of *Agrobacterium* in LB using rifampicin (25 mg/mL) and kanamycin (50 mg/mL). The inoculated cultures were placed in an incubator shaker at 28°C overnight or for two days if no growth was observed in the cultures. These cultures were used to perform colony PCR of *Agrobacterium*

3.1.3.4 *PCR-based Confirmation*

For colony PCR of *Agrobacterium*, 10 µL of overnight culture was heated at 98°C in a thermal cycler for 3 minutes to release the plasmid, followed by cooling to room temperature. Two microliters of this mixture were then used in a 25 µL PCR reaction. The reaction mixture was prepared by adding 6 µL of 10X reaction buffer, 1.25 µL of each primer (forward (IPB 173) and reverse (IPB 174)), 2-5 µL of bacterial culture, and 6.5 µL of distilled, autoclaved water to achieve a final volume of 25 µL. Initial denaturation was performed at 94°C for 3 minutes. Denaturation was then performed at 94°C for 1 minute, followed by annealing at 64°C for 40 seconds. The extension was performed at 72°C for 40 seconds, and the final extension was carried out at 72 °C for 10 minutes.

3.1.4 Development of Transgenic *Nicotiana benthamiana* Plants via *Agrobacterium*-Mediated Transformation

3.1.4.1 *Plant Material*

To grow *Nicotiana benthamiana* plants for stable transformation in a greenhouse, I maintained a temperature range of 22–28°C during the day and 18–22°C at night, with humidity levels between 50–70% and 12–16 hours of light daily. The plants were grown in well-draining soil with a pH of 5.5–6.5 and were fertilized with NPK 20-20-20 to promote healthy growth. I collected samples after 6 weeks of germination, although in some cases, I collected them later, at around 8 or 9 weeks, for transformation (Figure 2).

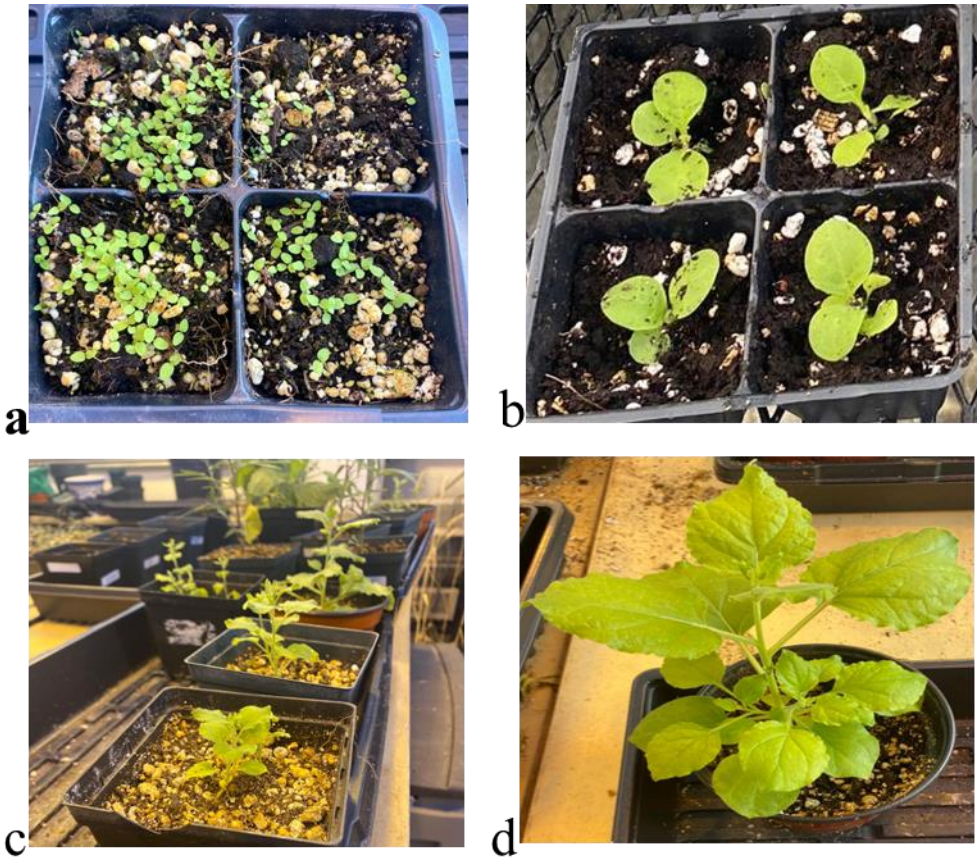

Figure 2. The developmental phases of *N. benthamiana* seedlings that were set up for *Agrobacterium*-mediated transformation under controlled growing conditions. The plants were cultivated in a temperature-regulated greenhouse at 25°C, following a 16-hour light and 8-hour dark photoperiod, and were watered regularly to promote healthy growth before transformation. (a) Young seedlings just a few days post-sowing in soil. (b) 7-day-old

seedlings transplanted into larger containers to encourage proper root growth and vigorous early development. (c) Two-week-old seedlings replanted into yet larger pots to facilitate ongoing vegetative growth. (d) *N. benthamiana* plants four weeks after germination, at the ideal stage for sample collection and explant preparation for *Agrobacterium*-mediated transformation.

3.1.4.2 *Preparation of Infection Media for Agrobacterium-Mediated Transformation*

To grow colonies from glycerol stocks of transformed bacteria harboring the pORE-E2 plasmid with *CBDAS* variants, I inoculated the bacteria in an LB medium supplemented with 25 mg/mL rifampicin and 50 mg/mL kanamycin. After two days, I prepared a 10 mL culture of *Agrobacterium* from a single colony in an LB medium with the same antibiotics and incubated it overnight on a shaker. If adequate growth was not seen after one day, I let the culture continue growing for another day. Subsequently, 3 mL of the culture was transferred to fresh LB medium containing the antibiotics, and 20 µM acetosyringone was added. The culture was incubated at 28°C with shaking at 200 rpm for 6-7 hours until OD_{600} reached the desired level of OD_{600} 0.6. After the 6 hours, I measured the OD of the bacterial culture and centrifuged it at 4000 g for 15 minutes at 19°C. I removed the supernatant, resuspended the pellet in infiltration buffer (10 mM $MgCl_2$, 10 mM MES pH 5.6, 150 µM acetosyringone(MMA)), and allowed the culture to rest for 2 hours. In an alternative method, the pellet was washed twice with 10 mM $MgSO_4$ after centrifugation and then resuspended in 25 mL of MS medium. After assessing the OD_{600} of the infectious media, 200 µM acetosyringone was added.

3.1.4.3 *Preparation of Explants*

Fresh leaves were harvested from 7 to 8-week-old seedlings and underwent surface sterilization. Following a thorough rinse with distilled water, the leaves were immersed in a 1% bleach solution, which included three drops of Tween 20, and was agitated for 30 minutes. They were washed thrice with distilled, autoclaved water and then treated with 3% H_2O_2 for 5 minutes. Afterward, the leaves were rinsed again 3 to 4 times with water. The leaves were then cut into small discs and placed on plain MS media until they were ready for transformation.

3.1.4.4 *Agrobacterium-Mediated Transformation*

The vacuum infiltration technique was utilized to introduce *Agrobacterium* into the explants (Figure 3). The pressure was maintained at 600 ppm for 30 minutes. Following this, the explants were dried using filter paper and transferred to co-cultivation media (MS, 0.2 mg/L IAA, 2mg/L 6-BAP), where they were kept in the dark for 3-4 days. After 4 days, the explants underwent a wash using washing media that contained 250 mg/mL timentin to remove any residual *Agrobacterium*. Two rinses with standard MS media followed this step to further confirm the elimination of the bacteria.

The explants were then transferred to the shooting media (MS, 0.2 mg/L IAA, 2.5 mg/L 6-BAP, 200 mg/L kanamycin, and 250 mg/L timentin) and placed in growth chambers with conditions of 70% relative humidity, a 16/8-hour light/dark cycle, and a temperature of 25°C. Subculturing was performed every three weeks. When small shoots were observed, the explants were moved to rooting media (½ MS, 250 mg/L timentin, 100 mg/L kanamycin). Once small roots developed, the plants were transferred to soil (Figure 4). The

pots were kept in the growth chamber for several weeks to acclimate the regenerated plants to the new environment before being moved to the greenhouse.

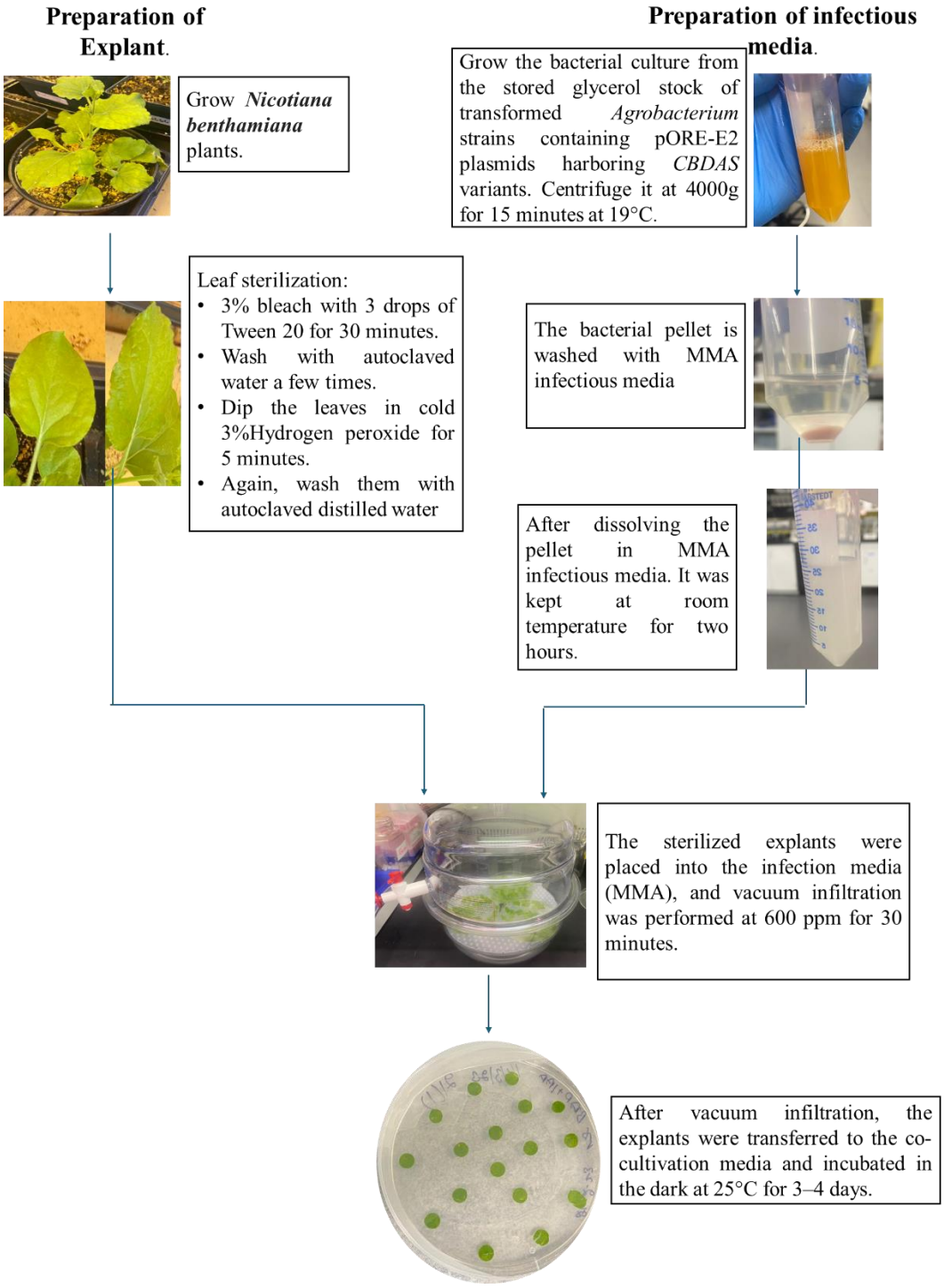

Figure 3. The flowchart illustrates the stages of *Agrobacterium*-mediated transformation of *N. benthamiana* explants with pORE-E2 harboring *CBDAS* variants gene. This procedure consists of three main phases: (1) Explant leaf preparation, which includes surface sterilization to maintain sterile conditions; (2) Preparation of *A. tumefaciens* infection media (10 mM $MgCl_2$, 10 mM MES pH 5.6, 150 µM acetosyringone(MMA)),, wherein the bacterial cells are pelleted, washed, and the infection media is formulated with 150µM acetosyringone to boost bacterial virulence; and (3) *Agrobacterium*-mediated transformation, during which explants are subjected to vacuum infiltration for optimal bacterial absorption, followed by their placement on co-cultivation media to enable gene integration.

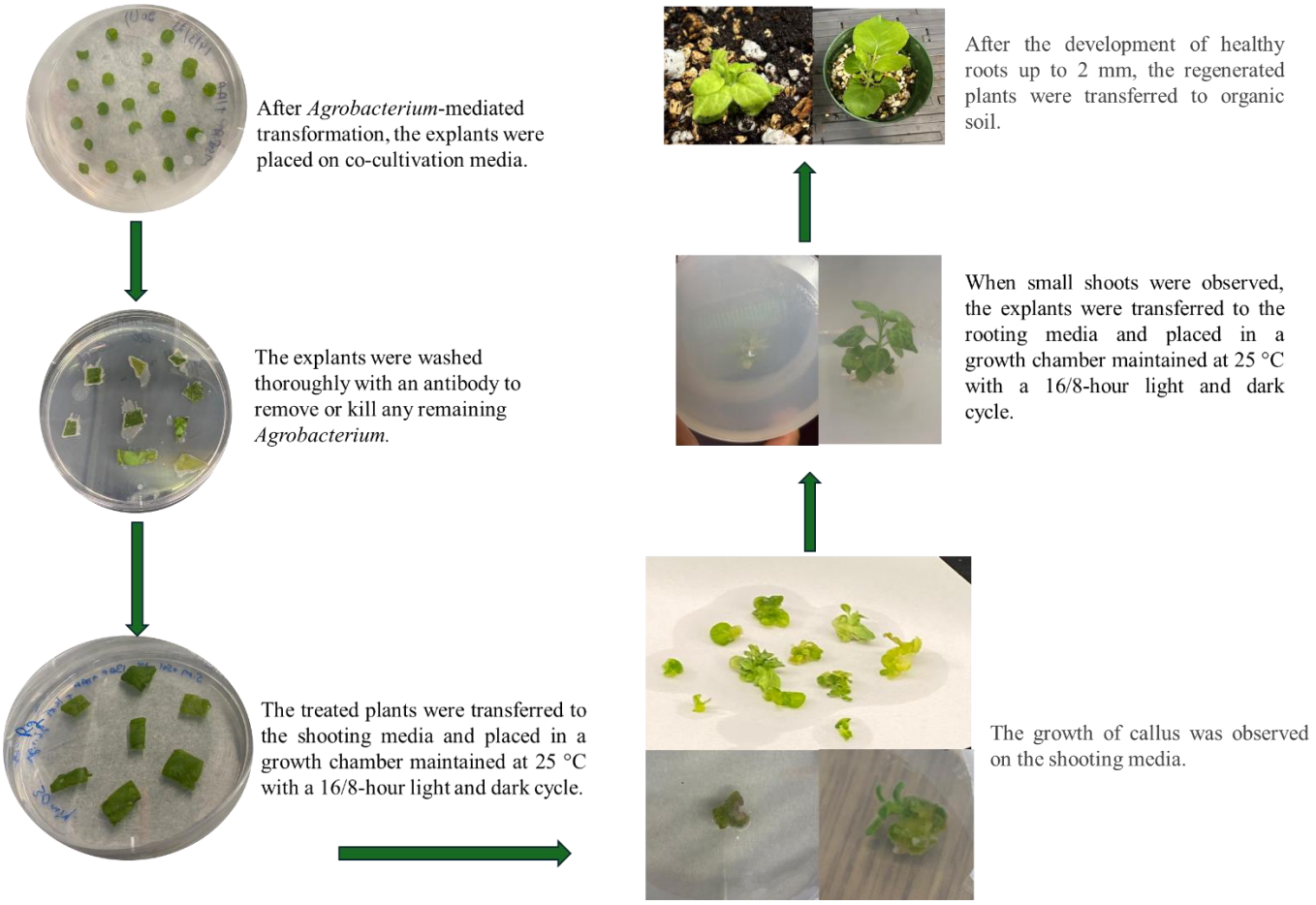

Figure 4. A flowchart depicting the various phases of regenerating *N. benthamiana* plants via tissue culture. The explants were incubated on co-cultivation media in the dark for 3–4 days at a temperature of 25°C and then moved to media for shooting and rooting. The plants were kept in growth chambers with a light/dark cycle of 16/8 hours at 25°C. When the roots reached around 2 mm in length, the regenerated plants were moved to organic

soil and allowed to acclimatize in the growth chamber for a few weeks to avoid abrupt environmental changes.

3.1.5 Molecular Confirmation of Transgenic *Nicotiana benthamiana* Plants via PCR

After a few weeks, I collected the samples for the regenerated plants and did the DNA extraction using the CTAB method mentioned above. The DNA was of poor quality. I cleaned the DNA using a DNA clean and concentrator kit by Zymo research. PCR was performed using the *CBDAS*-specific primers (IPB 173 and IPB 174). The reaction mixture consisted of 6 µL of master mix, 1 µL of forward primer (1PB 173), 1 µL of reverse primer (IPB174), 3-5 µL of DNA, and 9 µL of water. The PCR conditions were as follows: initial denaturation at 95°C for 2 minutes, denaturation at 95°C for 30 seconds, annealing at 64°C for 30 seconds, extension at 72°C for 1 minute, and final extension at 72°C for 5 minutes. A total of 35 cycles were performed.

3.1.6 Protein Extraction

Protein extraction was performed on transgenic plant samples, which PCR confirmed. For the transgenic plants, samples were collected at different stages, including the early vegetative stage, late vegetative stage, and after flowering. Fully expanded, fresh leaves from healthy transgenic plants were collected. After removing the major veins, the samples were ground in liquid nitrogen using a pestle and mortar. To improve the extraction, lysis buffer (50 mM Tris-HCl, 150 mM NaCl, 1% Nonidet P-40, and 1 tablet/50 mL protease inhibitor) was added. For every 1 g of ground sample, 500 mL to 1 L of lysis buffer was added. The tubes were vortexed and kept on ice. The samples were then centrifuged at 40,000g for 15 minutes at 4°C. The supernatant was collected, and the protein

concentration was measured using the Bradford assay. A diluted sample for the Bradford assay was prepared in a 1:10 ratio (6 µL of protein and 54 µL of distilled autoclaved water).

3.1.7 Protein Purification

To purify the CBDAS protein from the total extracted protein, I used the Dynabeads Protein G Immunoprecipitation Kit, following the manufacturer's protocol with some modifications. These modifications were implemented to optimize the purification process and enhance protein yield while maintaining specificity. Protein purification was carried out by incubating 4-5 µL of antibody DYKDDDDK tag mouse (1:50) with 600-700 µL of extracted protein samples for at least 4 hours at 4°C, with continuous rotation at low speed. After 4 hours, 50 µL of agarose bead suspension was added to the mixture, and the incubation was continued overnight with rotation at 4°C. The following day, the tube was placed on a magnet plate, and the supernatant was removed. This lysate was saved for further analysis if needed. The magnetic beads-antibody-antigen complex was washed three times with 20 µL of wash buffer, with agitation at 4°C for 5 minutes after adding the wash buffer between each wash. The supernatant was removed after each wash, and the beads were resuspended by pipetting. After the third wash, the magnetic beads-antibody-antigen complex was resuspended in 100 µL of wash buffer and transferred to a new tube. To elute the protein, the tubes were placed on a magnet plate, the supernatant was removed, and the beads were resuspended in 50 µL of elution buffer (0.2 M glycine, pH 2.6). The samples were incubated for 10 minutes with frequent rotation. The elute was pooled, and neutralization was performed by adding 20% of Tris's total elute volume (30 µL) (pH 8.00). The contents of the tube were mixed gently to ensure neutralization. The purified samples were then stored at -80°C.

3.1.8 Western Blot Analysis

Protein samples were prepared for SDS-PAGE by adding 1% SDS and loading dye, followed by denaturation at 95°C for 5 minutes. A 10% acrylamide SDS-PAGE gel (1.5 mm thick) was prepared, and 60–65 µL of each sample was loaded into the wells. The gel was run at 60V for 1.5 hours to ensure proper separation of protein bands, then at 100V until the proteins reached the bottom of the gel. Following electrophoresis, proteins were transferred onto a PVDF using a wet transfer system at 100V for 2 hours.

After transfer, the membrane was stained with 5 mL of Ponceau S stain for 5 minutes to confirm protein transfer, then destained by rinsing with water or washing 3–4 times with 1X PBS buffer. Blocking was performed using 1X PBST containing 5% skim milk for at least 1 hour at room temperature to prevent non-specific binding. The membrane was then incubated overnight at 4°C with shaking in the primary antibody, diluted at 1:1000 in 1X PBST containing 5% BSA. Following incubation, the membrane was washed 3–4 times with 1X PBST for 7 minutes each. Next, it was incubated with the secondary antibody, diluted at 1:5000 in blocking buffer (1X PBST with 5% skim milk), for 2 hours at room temperature with gentle shaking. After secondary antibody incubation, the membrane was washed 3–4 times with 1X PBST for 7 minutes each.

An enhanced chemiluminescence (ECL) substrate was applied to detect the target protein, and the signal was visualized using an image viewer.

3.1.9 Sephadex Gel Filtration

Gel filtration using Sephadex G-25 was performed to remove salts, detergents, and other contaminants from protein samples. Sephadex G-25 was prepared by swelling 6.25 g of Sephadex in 10 mL of 25 mM sodium acetate buffer (pH 4.65). The Sephadex was allowed to swell overnight. The column was equilibrated with 2 mL of the Sephadex buffer, and once the Sephadex settled, 2 mL of 25 mM sodium acetate buffer was added drop by drop along the walls of the column. Pressure was applied to allow the buffer to leak out slowly, leaving just enough to cover the Sephadex gel, ensuring it did not dry out.

Next, 300 µL of the protein sample was applied to the column, and pressure was applied slowly to elute the sample, which was labeled as "elute 1." Then, 800 µL of elution buffer (25 mM sodium acetate buffer, pH 4.6) was added drop by drop to elute the protein further, labeled as "elute 2," containing the purified protein. The samples were analyzed using a 1 mm SDS-PAGE gel to confirm successful protein purification and stained with Coomassie Blue. The gel was stained overnight in Coomassie Blue solution, and the following day it was washed with washing buffer (50/50 methanol and water).

3.1.10 Enzyme Assay

The enzyme was incubated with CBGA (plant extract) in a buffer at 30°C, 550 rpm for 4 hours or overnight. After the enzyme assay, the samples were filter-sterilized by passing them through a 1.2 µm filter. Liquid-liquid extraction was then performed by adding two volumes of ethyl acetate, mixing the samples thoroughly, and spinning them down. The top layer was collected for further analysis. The samples were left to dry under a nitrogen atmosphere overnight. I performed the enzyme assay multiple times, adjusting different

parameters each time. The details of these changes are provided in the table 2. The next day, the samples were resuspended in 300 µL of acetonitrile, mixed well, and prepared for HPLC and LC-MS analysis.

Table 2: A summary of the optimization process for CBDAS enzyme activity assays.

Enzyme assay	**CBGA concentration**	**Buffer**	**Protein/enzyme concentration**	**Total volume**	**Conditions**
Assay 1	200 uM (43.2 ul in total volume)	100 uM sodium citrate, (450 ul) 0.1% Triton X prepared 10 % stock solution of 100 mM sodium citrate) (6 ul in total reaction)	100 ul	600 ul	30°C, at 500 rpm shaking for 4 hours
Assay 2	200 uM, 32.4 ul	50 mM Sodium citrate pH 5, 167 ul	100 ul	300 ul	37°C at 500 rpm for 4 hours.

Assay 3	200 uM, 32.4 ul	50 mM sodium citrate buffer pH 4.5	100 ul	300 ul	30°C at 500 rpm for 30 minutes, 2 hours and 4 hours
Assay 4	200 uM (21 ul)	No buffer for (some samples) but for the other 25 mM sodium acetate at pH 4.86	200 ul	300 ul	30°C at 500 rpm for 4 hours and overnight.

3.1.11 HPLC Conditions

After optimizing various factors, research assistant Rocio Rodriguez developed a refined HPLC protocol, named Kovalchuk's Cannabis Jan 30B, for accurate cannabinoid profiling. The mobile phase consisted of 10 mM ammonium formate (pH 5.19) and acetonitrile, with a carefully adjusted gradient to ensure optimal separation. The flow rate was set at 0.9 mL/min, and the column temperature was maintained at 30°C. The analysis was conducted using an Agilent Poroshell column, while UV detection was performed at 220 nm, 230 nm,

and 254 nm. The system operated within a 400 to 600 bar pressure range, ensuring stable performance.

The concentration of cannabinoid standards used for analysis included CBDA (Acetonitrile), CBGA (Acetonitrile), and THCA (Acetonitrile) at 20 ppm each. The combined CBGA and CBDA standards were prepared at 10 ppm each. The sample concentration for the last run was 5 ppm. The total run time was 15 minutes, with no additional post-run equilibration. These conditions were carefully selected to provide high precision, reproducibility, and effective compound separation for enzyme activity assessment.

3.1.12 Enzyme Activity Evaluation and Conversion Efficiency

Ultimately, I evaluated enzyme activity and conversion efficiency by analyzing the transformation of CBGA (substrate) into CBDA (product). The data was obtained through HPLC analysis for CBGA and CBDA levels and Western blot analysis for enzyme normalization using ImageJ. The intensity of the CBDAS (55 kDa) bands was normalized by using GAPDH (36 kDa) as a loading control. The membrane was first stained with Ponceau stain to achieve this, which binds to total proteins, confirming equal loading across lanes. ImageJ software was then used to measure the area, and the mean intensity of both CBDAS and GAPDH bands was measured. The integrated density was used to measure band intensity, which was obtained by dividing the area by the mean intensity. The intensities of the CBDAS bands were divided by their matching GAPDH band intensities to accommodate variations in protein loading. This guaranteed a more realistic representation of enzyme activity. The formula followed was:

Normalized Intensity = 55 kDa CBDAS band intensity/ 36 kDa GAPDH band intensity

Retention times (Rt) for CBGA and CBDA were recorded for the HPLC study to guarantee correct peak identification. The peak regions were then measured to estimate both the amount of CBDA produced and the starting concentration of CBGA. We evaluated substrate conversion and enzyme performance using these values.

We divide the CBDA peak area by the normalized protein intensity to ascertain enzyme activity using the following formula:

Enzyme Activity= Peak Area/Normalized Protein Intensity

I got conversion efficiency with this formula:

Conversion Efficiency (%) = (CBDA Peak Area/ CBGA Peak Area + CBDA Peak Area) ×100

These analyses allowed us to identify the most effective sample for enzyme activity and the sample with the highest substrate conversion.

CHAPTER 4: RESULTS

4.1 Analysis of *CBDAS* Variants Activity

4.1.1 Cloning of *CBDAS* Variants into pORE-E2 and Successful Transformation in *E. coli* Competent Cells

After initial bioinformatic analyses, we identified 26 distinct functional sequences of *CBDAS* variants from various *Cannabis sativa* cultivars. I selected four specific *CBDAS*

variants for this study to further investigate enzyme activity: Del_1_108, CRS1_105, X59_1_117, and Joe_1_129.

The cloning of the *CBDAS* gene into vectors has been previously documented. The insertion of cannabinoid biosynthesis genes into vectors facilitates the expression of functional proteins in a host organism, such as *Agrobacterium tumefaciens* or *E. coli* (Taura et al., 2007). The vector pORE-E2, designed for protein expression and purification, contains a C-terminal FLAG tag, which allows for the convenient purification of the expressed protein using antibody-based techniques such as immunoprecipitation and Western blotting (Coutu et l., 2007). The four selected *CBDAS* variants were successfully cloned into the pORE-E2-CFlAG vector. This was done by amplifying the *CBDAS* sequences (Figure 5), digesting the vector and gene with *BamHI* and *KpnI,* and then ligating. The recombinant plasmid pORE-E2-CFlAG containing these variants was effectively introduced into *E. coli* competent cells (Figure 6), and the presence of the plasmid was verified through colony PCR (Figure 7). The plasmid pORE-E2 harboring *CBDAS* variants gene was purified from transformed colonies of *E. coli* through miniprep and verified by restriction digestion (Figure 8). It was subsequently used to transform the competent cells of *Agrobacterium.*

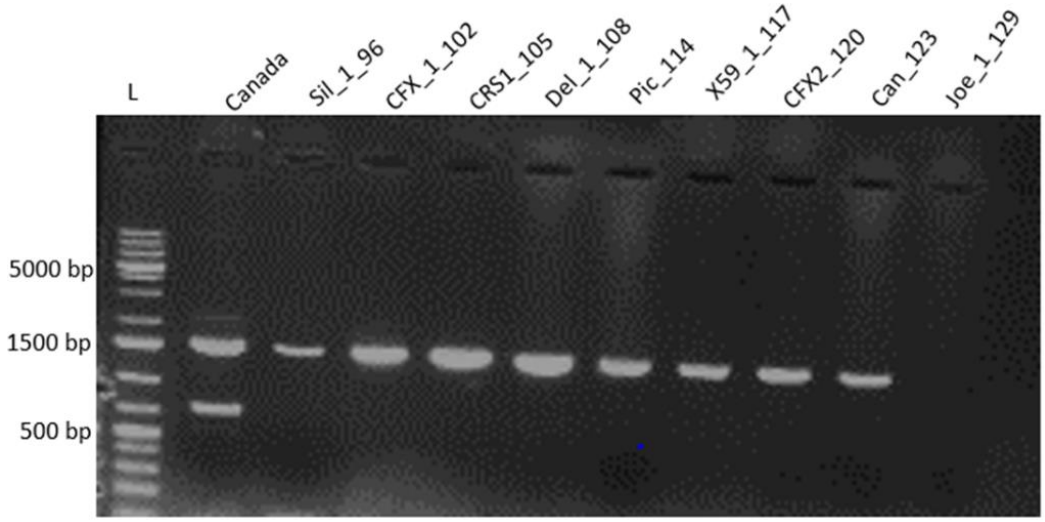

Figure 5. Amplification of *CBDAS* variant sequences through PCR using total genomic DNA from various *Cannabis sativa* L. samples with the forward IPB173 and reverse primers IPB174. "L" indicates the DNA ladder. “Canada”, “Sil_1_96”, “CFX_1_102”, “CRS1_105”, “Del_1_108”, “Pic_114”, “X59_1_117”, “CFX2_120”, “Can_123”, “Joe_1_129” are individual cultivars used for amplification of *CBDAS* variants. The anticipated band size of the *CBDAS* variant gene is 1500 bp, which was successfully amplified by the primers.

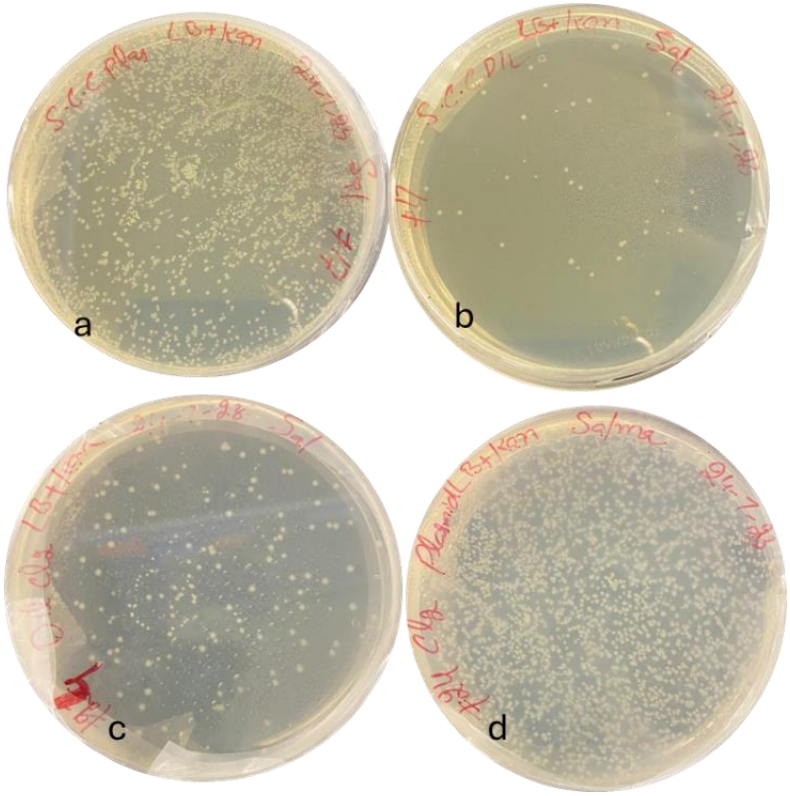

Figure 6. Development of *E. coli* colonies on LB agar enriched with 50 mg/mL kanamycin after heat-shock transformation with pORE-E2 containing various *CBDAS* variants. (a,b) *E. coli* DH5α competent cells transformed with pORE-E2 featuring the Del_1_108 *CBDAS* variant. (c,d) *E. coli* DH5α competent cells transformed with pORE-E2 incorporating the Joe_1_129 *CBDAS* variant. The colonies were allowed to grow at 37°C for 16-18 hours, and the emergence of kanamycin-resistant colonies identified successful transformation.

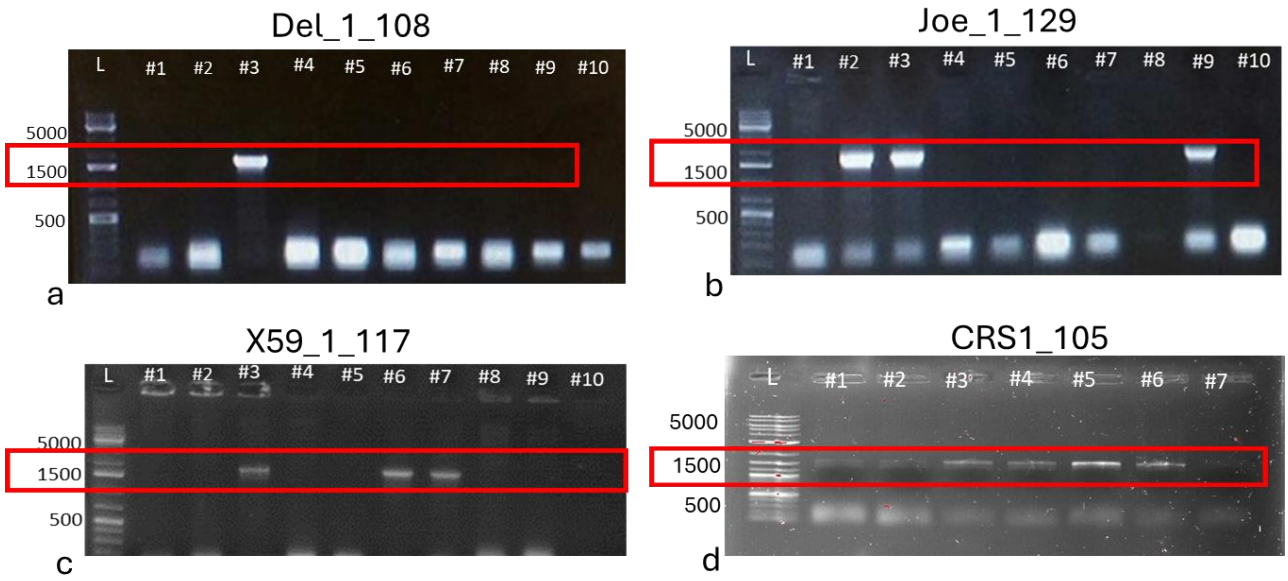

Figure 7. Confirmation of *E. coli* DH5α competent cells that were transformed with the pORE-E2 vector containing *CBDAS* variants was carried out using PCR. Amplification of the *CBDAS* variants gene was done via PCR using the primers IPB173 (forward) and IPB174 (reverse). The appearance of a clear band at 1500 bp indicates that the *CBDAS* gene has been successfully integrated into the *E. coli* host. (a) PCR results confirm the Del_1_108 *CBDAS* variant. (b) PCR results confirm the Joe_1_129 *CBDAS* variant. (c) PCR results confirm the X59_1_117 *CBDAS* variant. (d) PCR results confirm the CRS1_105 *CBDAS* variant. A DNA ladder (L) served as a reference for molecular size.

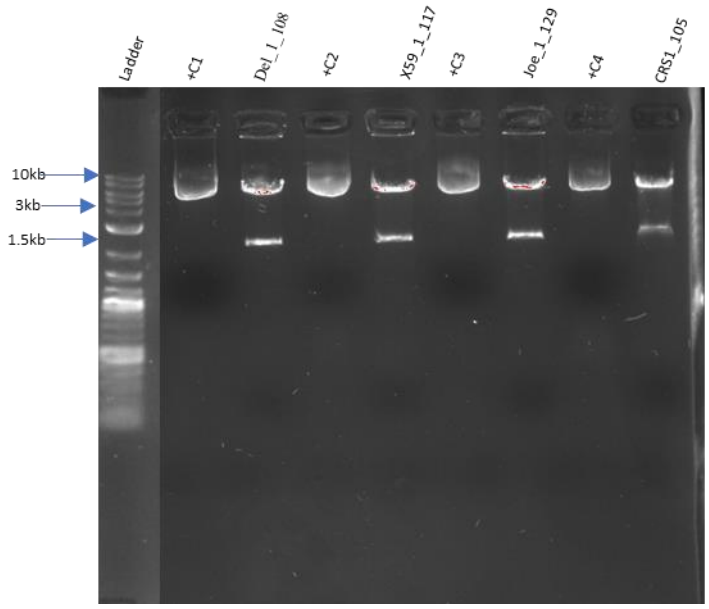

Figure 8. The isolated plasmid PORE-E2 containing *CBDAS* variants from *E. coli* colonies was verified through restriction digestion. The plasmid underwent treatment with *BamHI* and *KpnI*, yielding the expected fragment profile. Lanes +C1, +C2, +C3, and +C4 demonstrate that the mini-prepped plasmid PORE-E2 containing CBDAS variants acts as a positive control for the *CBDAS* variants Del_1_108, X59_1_117, JOE_1_129, and CRS1_105, respectively. The undigested plasmid +C produces a band approximately 9 kb in size. In contrast, the digested plasmid results in a fragment of about 7.5 kb, along with the *CBDAS* insert of 1.5 kb, confirming the presence of the expected variant.

4.1.2 *A. tumefaciens* Strain EHA105 Cells Transformed with Plasmid pORE-E2 Harboring *CBDAS*

Competent cells of *A. tumefaciens* were successfully transformed with the recombinant plasmid pORE-E2 containing *CBDAS* variants using the electroporation method. I recovered many colonies on the plate with selection antibiotics (Figure 9) at 25 mg/mL rifampicin and 50 mg/mL kanamycin. A few colonies from the plates of each *CBDAS* variant were chosen to perform colony PCR to verify whether they were transformed

(Figure 10). Following confirmation, I prepared glycerol stocks and stored them at -80 degrees.

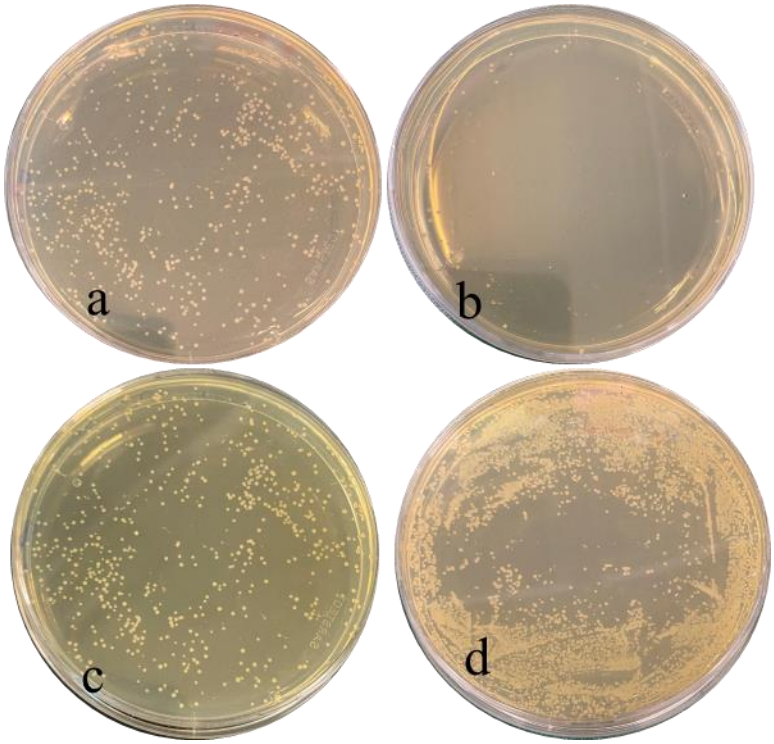

Figure 9. The development of *A. tumefaciens* colonies on LB media enriched with 50 mg/mL kanamycin and 25 mg/mL rifampicin followed electroporation-mediated transformation with pORE-E2 containing various *CBDAS* variants. Transformed EHA105 cells were incubated at 28°C in a dark environment for 2–3 days to promote colony growth under selective conditions. (a) EHA105 cells that were transformed with pORE-E2 featuring the Del-1-108 *CBDAS* variant. (b) EHA105 cells that were transformed with pORE-E2 containing the JOE_1_129 *CBDAS* variant. (c) EHA105 cells that were transformed with pORE-E2 harboring the X59_1_117 *CBDAS* variant. (d) EHA105 cells that were transformed with pORE-E2 carrying the CRS1_105 *CBDAS* variant. Colonies indicate successful transformation, plasmid uptake, and stable maintenance under antibiotic selection.

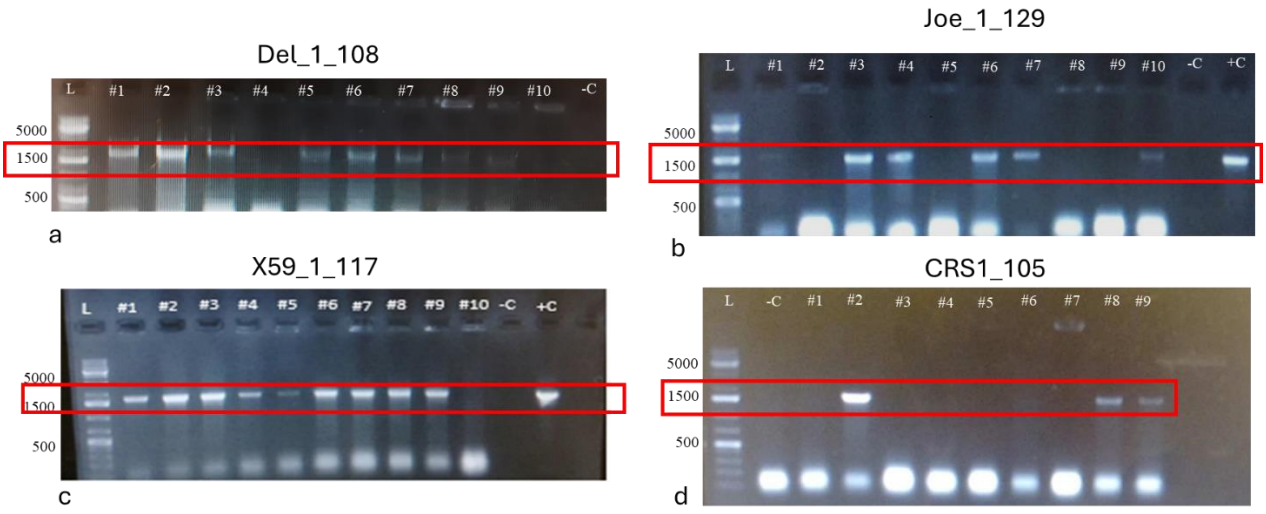

Figure 10. PCR-based validation of transformed *A. tumefaciens* EHA105 competent cells containing the pORE-E2 vector with *CBDAS* variants. The successful transformation is demonstrated by the appearance of a 1500 bp PCR product, indicating the presence of the *CBDAS* insert in the transformed cells. (a) PCR results for Del_1_108. (b) PCR results for Joe_1_129. (c) PCR results for X59_1_117. (d) PCR results for CRS1_105. +C indicates miniprepped *E. coli*-transformed cells utilized for *Agrobacterium* transformation, serving as a positive control. -C signifies the negative control, where template DNA or pORE-E2 was not included in the reaction. L refers to the DNA ladder utilized for size assessment. Detecting a 1500 bp band in the experimental lanes confirms effective transformation of *A. tumefaciens* with the *CBDAS* carrying pORE-E2 vector.

4.1.3 Development of Transgenic Plant via *Agrobacterium*-mediated Transformation

After successfully infecting explants of *Nicotiana benthamiana* leaves with transformed *A. tumefaciens* carrying recombinant pORE-E2 plasmid harboring different *CBDAS* variants, I successfully regenerated five plants for X59_1_117, Joe_1_129, and Del_1_108; however, I was only able to regenerate two plants for CRS_1_105 (Figure 11).

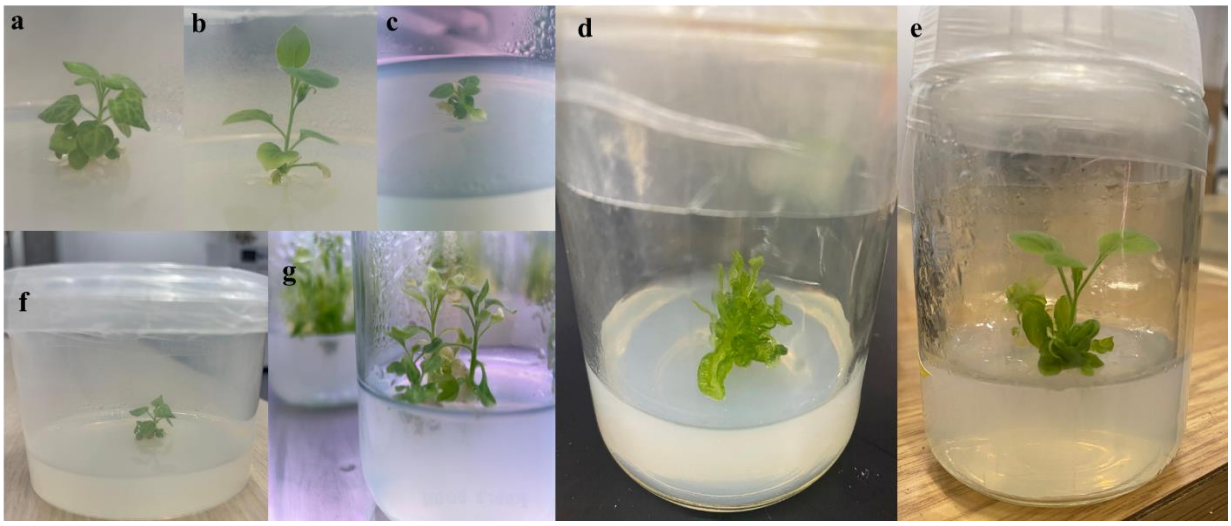

Figure 11. Regeneration of *Nicotiana benthamiana* plants was achieved on ½ MS rooting media that included 250 mg/L timentin and 100 mg/L kanamycin after transforming with pORE-E2 containing various *CBDAS* variants. The plants were grown under controlled conditions at 25°C with a photoperiod of 16 hours of light and 8 hours of darkness to encourage root development and evaluate successful regeneration. (a) Regenerated *N. benthamiana* plants corresponding to the *CBDAS* variant Del-1-108. (b) Regenerated *N. benthamiana* plants associated with the *CBDAS* variant Joe_1_129. (c, f) Regenerated *N. benthamiana* plants related to the *CBDAS* variant X59_1_117. (d, e) Regenerated *N. benthamiana* plants linked to the CBDAS variant CRS1_105. (g) Regenerated *N. benthamiana* plants transformed with pORE-E2 that did not have a *CBDAS* insert, serving as a control group. The existence of rooted plants under selective conditions indicates successful transformation and regeneration.

Two protocols were employed to prepare infectious media for *Agrobacterium*-mediated transformation. In the first protocol, the bacterial pellet was washed with 10 mM $MgSO_4$, resuspended in MS media supplemented with 200 uM acetosyringone, and used immediately for transformation. This approach resulted in fewer transformed explants; 2 or 3 transformed explants survived out of 20 treated leaf disks. Many explants failed to survive co-cultivation or died on shooting media. In contrast, the second protocol, which involved resuspending the pellet in infiltration buffer (10 mM $MgCl_2$, 10 mM MES pH 5.6,

150 µM acetosyringone) and incubating for 2 hours before use, yielded more efficient transformation results. 7 to 8 transformed explants survive out of 20 treated leaf disks.

To assess the effectiveness of various infection media in *Agrobacterium*-mediated transformation, I conducted a statistical analysis comparing the success rates of two protocols. The first protocol achieved an average transformation rate of 11% (2.2/20 explants), while the second protocol produced a markedly higher rate of 34% (6.8/20 explants) (Table 3). In this study, the null hypothesis (H_0) stated that there is no significant difference in transformation efficiency between the two infection methods utilized for AMT. This implies that any differences observed in transformation rates between the first and second methods are attributable to chance. However, after applying an independent t-test, the derived t-value (-8.69) is considerably large in magnitude, signifying a significant difference between the two methods. Furthermore, the very low p-value (0.0000239) is significantly below the conventional significance level ($p < 0.05$), indicating that the noted difference is not merely the result of random variation. Given that the t-value and p-value point to a highly significant difference, we reject the null hypothesis (H_0) and infer that the second method notably improves transformation efficiency, likely due to the improved conditions in the modified infection media (Table 4). These findings demonstrate that the second protocol, incorporating a 2-hour incubation period in infiltration buffer ($MgCl_2$, MES, acetosyringone), substantially improves transformation efficiency by facilitating bacterial adhesion and T-DNA transfer.

Table 3: Transformation efficiency of two Infection protocols used in *Agrobacterium*-mediated transformation

Replications	**First Protocol (10 mM $MgSO_4$, MS+ 200 uM Acetosyringone) %**	**Second Protocol (10 mM $MgCl_2$, 10 mM MES pH 5.6, 150 µM acetosyringone) %**
Replication 1	10% (2/20)	30% (6/20)
Replication 2	15% (3/20)	35% (7/20)
Replication 3	5% (1/20)	40% (8/20)
Replication 4	15% (3/20)	35% (7/20)
Replication 5	10% (2/20)	30% (6/20)
Average transformation rate	11%	34%

Table 4: Detailed statistical calculations for the t-Test demonstrating the significant difference between two infection protocols in *Agrobacterium*-mediated transformation

Statistic	**Formula**	**First Protocol (Low Efficiency)**	**Second Protocol (High Efficiency)**
Mean Efficiency (%)	$\bar{X}=\sum Xi/n$	10+15+5+15+10/5 =11%	30+35+40+35+30/5 =34%
Variance (s^2)	$S^2= \sum(Xi-\bar{X})^2/n$	$(10-11)^2+(15-11)^2+(5-11)^2+(15-11)^2+(10-11)^2/4$ =17.5	$30-34)^2+(35-34)^2+(40-34)^2+(35-34)^2+(30-34)^2/4$ =17.5
Standard Deviation (s)	$s= \sqrt{s^2}$	$\sqrt{17.5}$=4.18	$\sqrt{17.5}$ = 4.18
Sample Size (n)		5	5
Standard Error (SE)	$SE=\sqrt{s_1^2/n_1+s_2^2/n_2}$	$\frac{\sqrt{17.5}}{5}+\frac{17.5}{5}=\sqrt{7}$ = 2.645	
T Test(t)	$t=X1^{-}-X2^{-}/SE$	11-34/2.645= -8.69	
Degrees of Freedom (df)	$df=\frac{(s_1^2/n_1+s^{22}/n_2)^2}{\frac{(s_1^2/n_1)^2}{n_1-1}+\frac{(s_2^2/n_2)^2}{n_2-1}}$	$\frac{(3.5+3.5)^2}{\frac{(3.5)^2}{4}+\frac{(3.5)^2}{4}}$ =8.00	
p-Value (p)	Based on t-distribution table	0.0000239	

Statistical Significance.	If $p<0.05$, then significant	Yes	

Despite maintaining optimal environmental settings in the growth chamber (70% relative humidity, 16/8-hour light/dark cycle, and 25°C), explants on the shooting media exhibited poor survival rates, often turning yellow or brown and dying within a few days. To address this, some jars containing explants on shooting media were moved to the lab bench, where they showed improved growth without yellowing or browning. However, growth was slow, likely due to the lab's lack of controlled light conditions.

Subsequently, explants were transferred to an older growth chamber (Thermo Forma) equipped with blue and white light spectra, unlike the previous chamber (PERCIVAL), which only had white light. This change resulted in the successful regeneration of plants (Figure 11), suggesting that the light spectrum plays a critical role in explant survival and growth. (Data not shown)

To address the problem with explants on the shooting media, I adjusted the levels of plant growth regulators and applied 3.5 mg/L 6-BAP, 0.5 mg/L NAA, and 2 mg/L $AgNO_3$, in addition to antibiotics. However, despite these changes, the small leaf-like formations continued to develop into enlarged callus-like masses instead of properly formed leaves and shoots. The higher concentrations of 6-BAP and NAA encouraged excessive callus development rather than promoting shoot elongation. At the same time, $AgNO_3$ was effective in alleviating ethylene stress but did not sufficiently counteract the strong effects of auxins and cytokinin, resulting in stunted and abnormal shoot structures.

4.1.4 Regeneration of Controls

Two controls were included to validate the transformation process. The first control (C1) involved untreated tobacco leaf explants that were surface-sterilized and placed directly on co-cultivation and shooting media (IAA,6-BAP, and 200 mg/ml kanamycin, 250 mg/ml timentin) without exposure to *Agrobacterium* or dark conditions. These explants died on shooting media after one or two weeks, confirming the suitability of the media, antibiotics, and conditions for tissue culture (Figure 12 a, b).

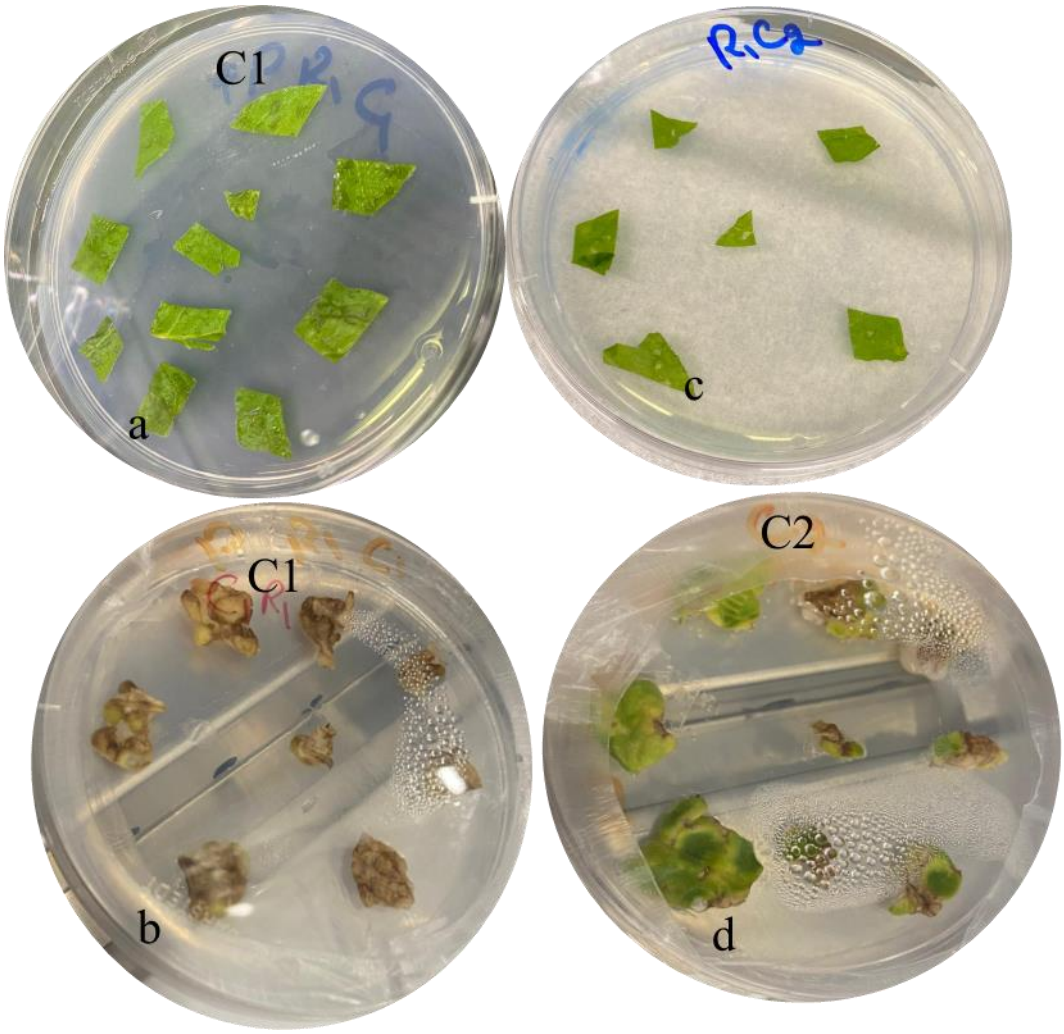

Figure 12. Experimental controls for *N. benthamiana* tissue culture aimed at verifying media composition, antibiotic selection, and transformation protocols. (a) C1 control: Untreated tobacco leaf explants are surface-sterilized and directly placed onto co-cultivation and shooting media without prior exposure to *Agrobacterium* or dark conditions. (b) These explants did not survive and perished after one to two weeks, demonstrating the effectiveness of the antibiotic selection and tissue culture media conditions. (c) C2 control: Explants exposed to *A. tumefaciens* carrying the empty pORE-E2 vector (which lacks the *CBDAS* insert). These samples were subjected to the same treatments as the experimental explants, including dark conditions during co-cultivation. (d) After one to two weeks, these explants exhibited callus formation on the shooting media, indicating that the transformation and co-cultivation conditions were favorable for plant tissue regeneration.

The second control (C2) consisted of explants treated with *Agrobacterium* containing the empty pORE-E2 vector (without the *CBDAS* insert) (Figure 12 c, d). These explants were

treated identically to the experimental samples, including exposure to dark conditions during co-cultivation. The results from this control helped rule out potential effects of the vector backbone or *Agrobacterium* treatment on explant survival and regeneration (Figure 11 g).

4.1.5 Molecular Confirmation of Transgenic *Nicotiana benthamiana* Plants via PCR

Following the successful regeneration of transformed *Nicotiana benthamiana* plants that incorporated *CBDAS* variant genes from four distinct variants, the subsequent step involved verifying whether the *CBDAS* gene was present or absent. Genomic DNA extraction was done by using CTAB method. The successful amplification of the *CBDAS* gene in the regenerated plants validated the transgene integration into the *Nicotiana benthamiana* genome. (Figure 13).

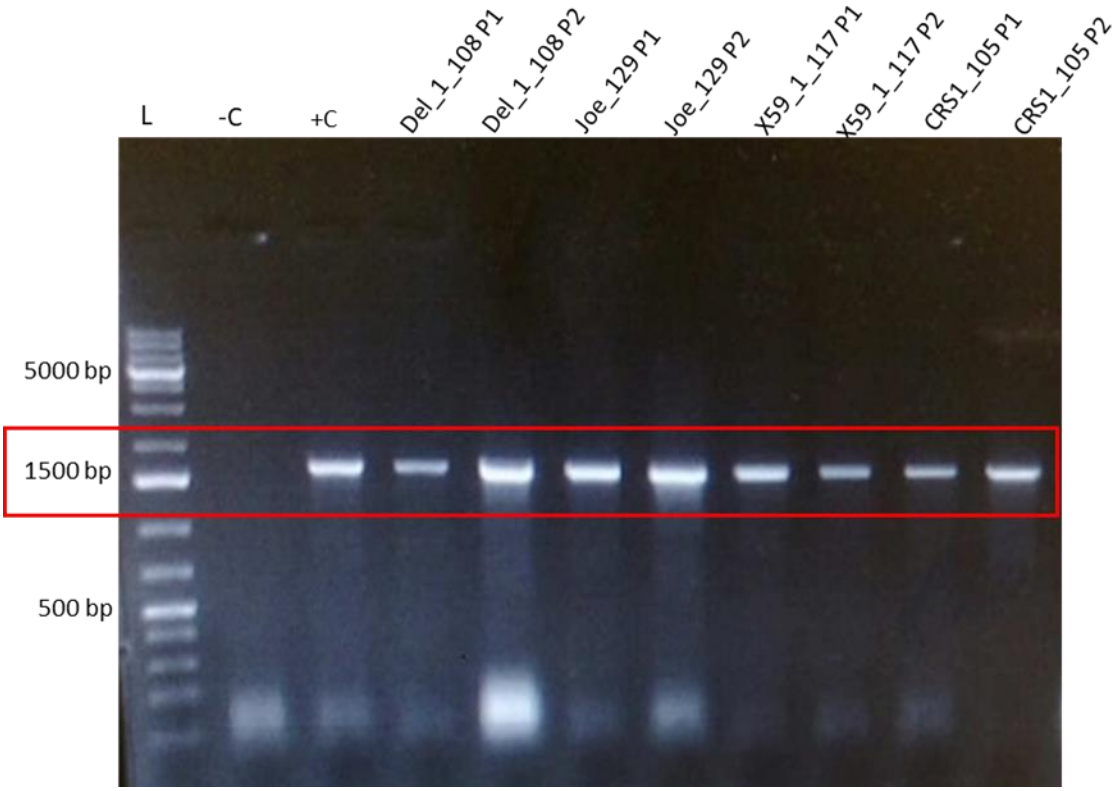

Figure 13. The results of gel electrophoresis from PCR amplification of genomic DNA obtained from regenerated *N. benthamiana* plants were analyzed to verify the existence of *CBDAS* inserts. After four weeks of transitioning regenerated plants from rooting media into soil, DNA was isolated using the CTAB method. Lanes P1 and P2 display genomic DNA from two separate regenerated plants with distinct *CBDAS* variants, validating their status as transgenic. The lane labeled +C represents the pORE-E2 vector containing the *CBDAS* insert, acting as a positive control(miniprep). The -C refers to Control 2, a plant regenerated through tissue culture and contains only the pORE-E2 vector without a *CBDAS* insert. The L indicates the DNA ladder utilized for size determination. Identifying 1500 bp PCR bands in both P1 and P2 supports the successful integration of *CBDAS* within the regenerated plants**.**

4.1.6 Total Protein Extraction and Immunopurification

Fresh leaf samples from transgenic tobacco plants were frozen in liquid nitrogen to prevent protein degradation. Two lysis buffers were tested for protein extraction. The first buffer, consisting of 50 mM Tris-HCl (pH 8.0), 10 mM EDTA, 2% SDS, 1% DTT, and protease

inhibitors (1 mM PMSF, 1 µg/mL Leupeptin, 1 µg/mL Aprotinin), failed to yield detectable protein, likely due to insufficient cell lysis or protein solubility issues. In contrast, the second buffer, containing 50 mM Tris-HCl (pH 8.0), 150 mM NaCl, 1% Nonidet P-40, and one protease inhibitor tablet per 50 mL of buffer, proved highly effective, resulting in successful protein extraction with clear and detectable protein bands (Figure 14). A small amount of lysis buffer was added during tissue grinding in a pre-chilled mortar and pestle to optimize the process further. This modification helped maintain protein integrity and significantly improved extraction efficiency. Overall, combining the second lysis buffer and adding buffer during grinding provided optimal conditions for protein extraction, ensuring high-quality results for downstream analyses.

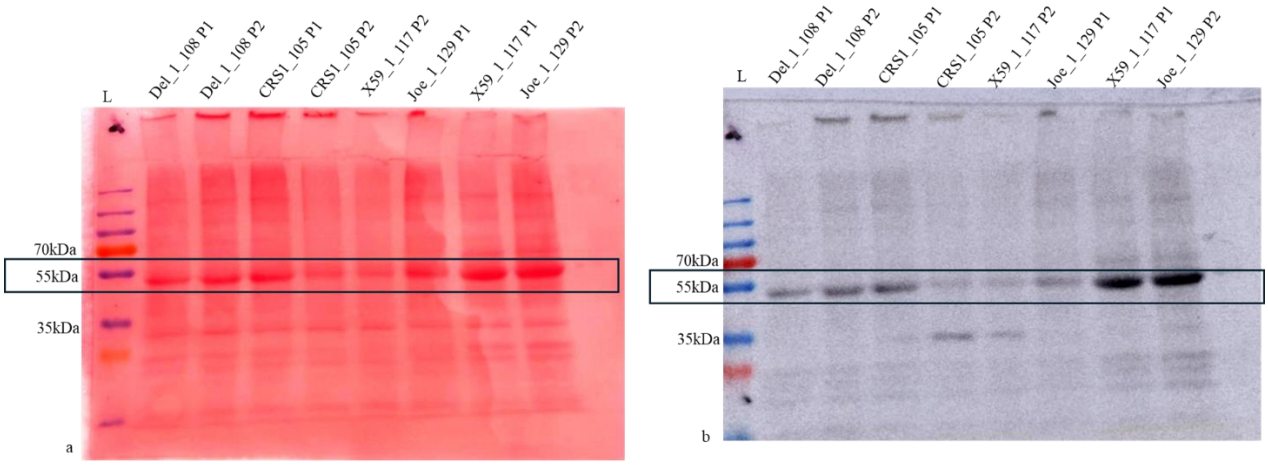

Figure 14. The image shows the results of Western blot analysis conducted on transgenic *N. benthamiana* plants that express various *CBDAS* variants. A total of 40 µg of total soluble protein (TSP) was resolved on a 10% SDS-PAGE gel and then transferred to PVDF membrane (a) Ponceau S staining of the PVDF membrane illustrates the total protein loading. It verifies the existence of protein bands across the samples. The uniform banding pattern indicates consistent protein transfer throughout the lanes. (b) The Western blot detection through ECA analysis reveals bands around 55 kDa, confirming the expression of *CBDAS* inserts in the transgenic plants. Lanes P1 and P2 represent individual transgenic

plants (Plant 1 and Plant 2) for different *CBDAS* constructs. The distinct bands observed in these lanes suggest that the target protein has been successfully expressed.

After confirming the successful expression of the *CBDAS* gene in the total extracted protein from transgenic tobacco plants for all four *CBDAS* variants, I purified the protein using the Dyna beads Agarose G immunoprecipitation kit (Figure 15).

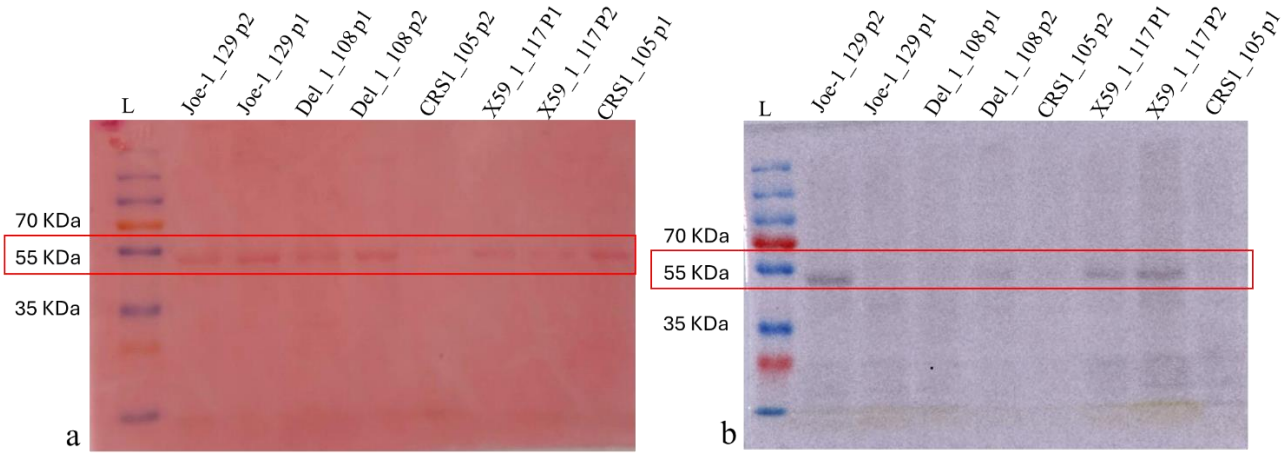

Figure 15. Analysis of immunopurified CBDAS-expressed protein derived from transgenic *N. benthamiana* plants. The purification was performed by using the Agarose G Immunoprecipitation Kit (Thermo Fisher) to extract CBDAS protein from total protein samples. (a) The membrane stained with Ponceau reveals protein bands in the immunopurified samples corresponding to various *CBDAS* variants. Only bands at 55 kDa can be seen, though their low intensity suggests inadequate recovery of the desired CBDAS protein. (b) Western blot analysis employing ECA detection confirms the existence of CBDAS-expressed protein at 55 kDa. Nevertheless, only a limited number of bands were observed, indicating that the protein concentration in specific samples was too low for the primary antibody to detect. P1 and P2 denote Plant 1 and Plant 2, which have different *CBDAS* inserts. The findings suggest that the immunopurification procedure resulted in a low yield of CBDAS protein, impacting detection efficiency.

4.1.7 Sephadex G-25 Gel Filtration

Gel filtration using Sephadex G-25 successfully purified the protein by removing salts, detergents, and other contaminants. The initial lysate was discarded, while the eluted fractions were collected and labeled "Elute 1" and "Elute 2." As expected, elute 1 contained a lower protein concentration, primarily consisting of the equilibration buffer (25 mM sodium acetate, pH 4.6). In contrast, elute 2 had a significantly higher protein concentration, confirming that most purified protein was successfully eluted in this fraction.

SDS-PAGE analysis followed by Coomassie blue staining further validated the purification process. The stained gel revealed zero or very minimal protein presence in elute 1, while elute 2 displayed a strong, distinct protein band, confirming the successful separation and concentration of the target protein. These results demonstrate that Sephadex G-25 gel filtration effectively purified the protein, with elute 2 containing the highest yield of the desired sample (Figure 16).

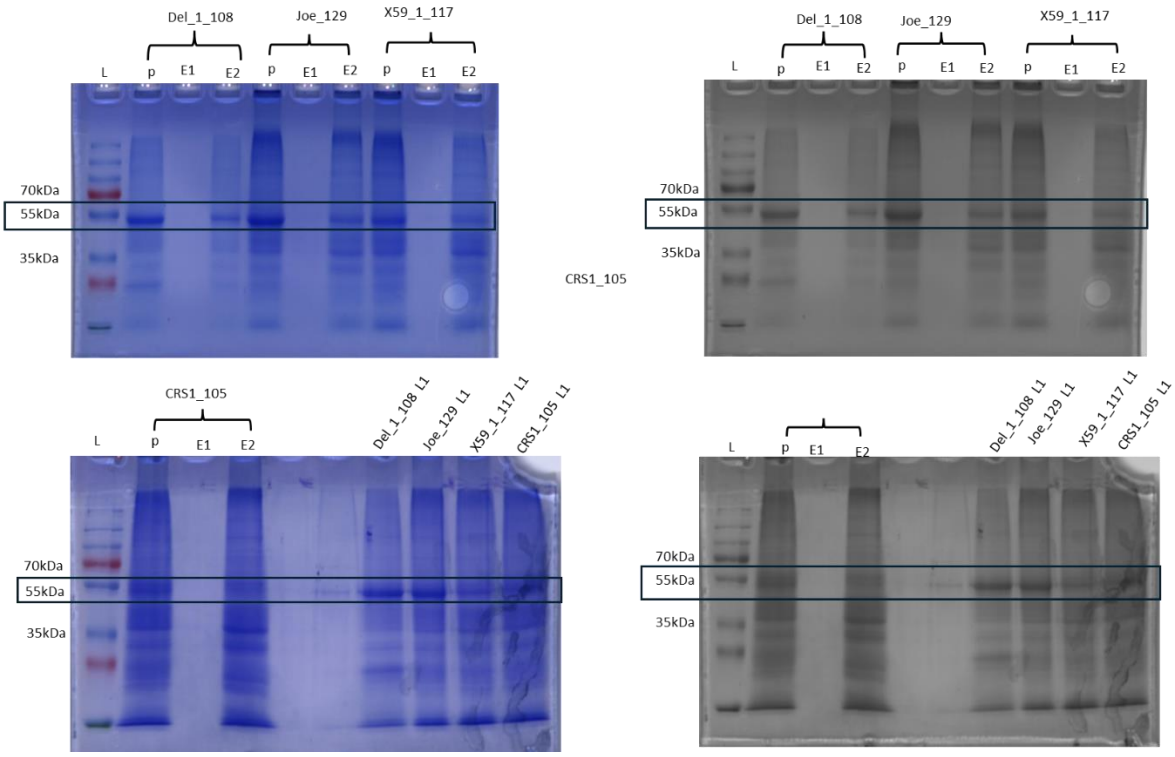

Figure 16. Analysis of protein samples via SDS-PAGE stained with Coomassie Blue after Sephadex-25 gel filtration. Protein fractions were isolated to assess the distribution and purification of proteins containing the *CBDAS* insert. "P" indicates the total protein extracted from each *CBDAS* insert sample, while "L1" refers to the lysate prior to purification. "E1" and "E2" represent the first and second eluates collected post-Sephadex gel filtration, respectively. A total of 20 µg of protein from each fraction was applied to a 10% SDS-PAGE gel and then stained with Coomassie Blue to visualize the separation of proteins and evaluate the efficiency of purification.

4.1.8 Enzyme Assay Optimization and Analysis

To evaluate CBDAS's enzymatic activity, a series of enzyme assays were performed under varying conditions, as summarized in Table 2.

The first enzyme assay used 100 mM sodium citrate buffer with 0.1% Triton X. However, the resulting chromatograms were poor, likely due to issues with column performance and pH inconsistencies in the solutions.

For the second attempt, LC-MS was employed to analyze the samples. The samples were subjected to Sephadex gel filtration before the enzyme assay to avoid interference from detergents, salts, and other contaminants. Additionally, the samples were filter-sterilized to remove particulate pollutants after enzyme assay. Liquid-liquid extraction was performed using 2 volumes of total reaction 600 ul of acetonitrile, and the samples were dried and reconstituted in 150 µL of acetonitrile. The temperature for this assay was set at 37°C. Despite these optimizations, the chromatograms only revealed the presence of the substrate, with no detectable product peaks.

HPLC was used for analysis in the third enzyme assay. Although the buffer was adjusted to 50 mM sodium citrate at pH 4.5, the temperature was set back to 30 °C. This time, the incubation time varied from 30 minutes to 2 hours to 4 hours. No desired product peaks were observed in the chromatograms, indicating that the enzymatic reaction was still not optimal.

Significant modifications were made for the fourth enzyme assay, including using 25 mM sodium acetate buffer at pH 4.86 for some samples (labeled as B). In contrast, others were run without a buffer (labeled as A, Table 2). This adjustment and extended incubation times (4 hours and overnight) yielded positive results (Figure 17). The chromatograms showed clear peaks for only CBDA and CBGA, confirming the successful detection of the CBDAS enzyme product, while no peak was detected for THCA.

4.1.9 HPLC Results

The iterative optimization of enzyme assay conditions, including buffer composition, pH, and sample preparation methods, was critical to achieving successful results. The final

assay demonstrated that using sodium acetate buffer at pH 4.86 and extended incubation times significantly improved the enzymatic activity and detection of the desired product. The retention times for the standards were confirmed as follows: CBDA (20 ppm) at 4.3 minutes, CBGA (20 ppm) at 4.624 minutes, THCA (20 ppm) at 6.095 minutes, CBGA (10 ppm) at 4.6 minutes, and CBDA (10 ppm) at 4.3 minutes. When analyzing the enzyme activity of four different CBDAS variants under varying conditions, the results revealed minimal conversion of CBGA into CBDA. For the 4-hour incubation (Joe_1_129), the CBGA peak area was 40.8, while the CBDA peak area was only 0.344, indicating very low conversion efficiency. In the overnight incubation (Joe_1_129), the CBGA peak area increased to 51.5, and the CBDA peak area was 1.3, suggesting that prolonged incubation did not improve conversion. Still, the ratio with which the CBGA converts into the CBDA increased from 0.8% (for 4 hours of incubation) to 2 %. Finally, the overnight incubation with 25 mM sodium acetate buffer Joe_1_129 (B) resulted in a CBGA peak area of 85.6 and a CBDA peak area of 2; the conversion rate was the same 2 % as without buffer. This indicates that the buffer did not enhance the reaction or inhibit the activity (Figure 17).

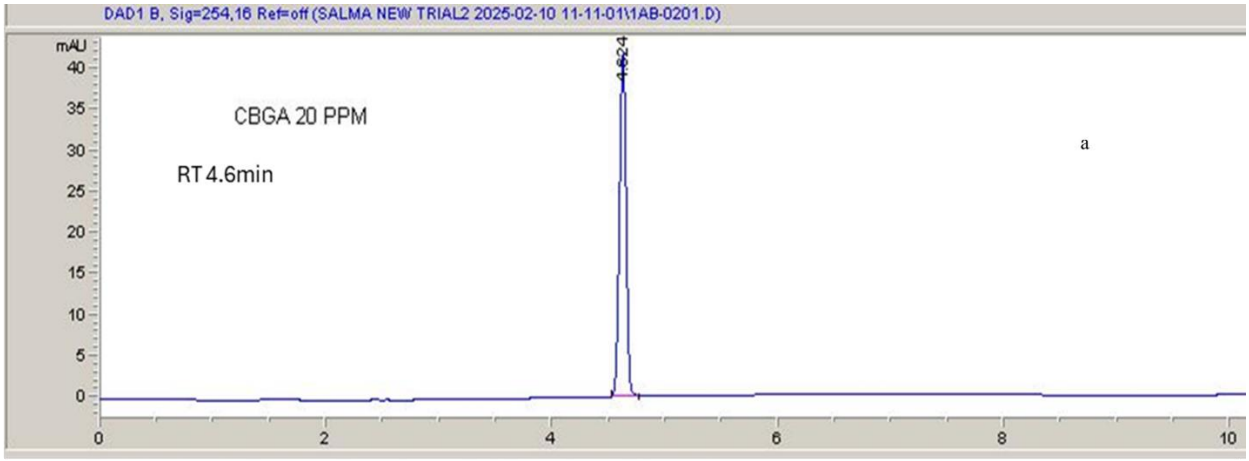
DAD1 B, Sig=254,16 Ref=off (SALMA NEW TRIAL2 2025-02-10 11-11-01\1AB-0201.D)
mAU
CBGA 20 PPM
RT 4.6min
a

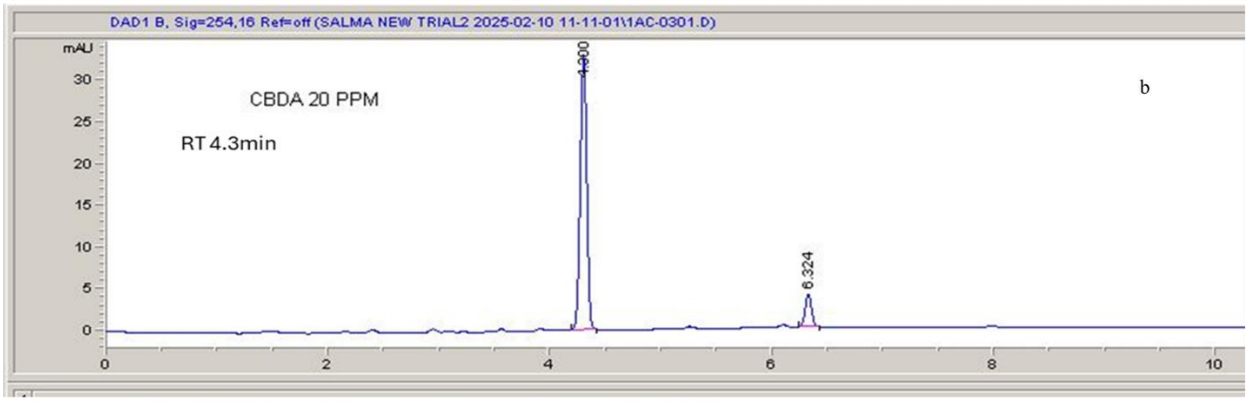
DAD1 B, Sig=254,16 Ref=off (SALMA NEW TRIAL2 2025-02-10 11-11-01\1AC-0301.D)
mAU
4.300
CBDA 20 PPM
RT 4.3min
6.324
b

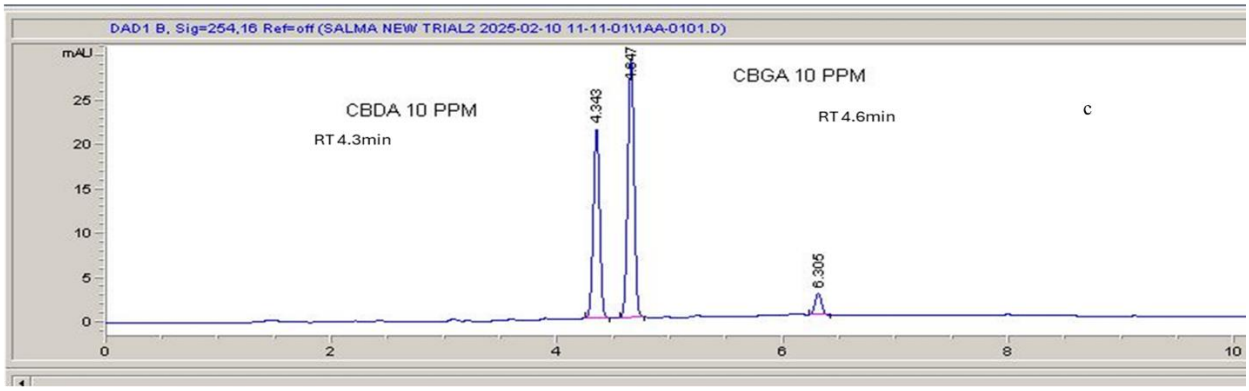
DAD1 B, Sig=254,16 Ref=off (SALMA NEW TRIAL2 2025-02-10 11-11-01\1AA-0101.D)
mAU
CBDA 10 PPM
RT 4.3min
4.343
4.647
CBGA 10 PPM
RT 4.6min
6.305
c

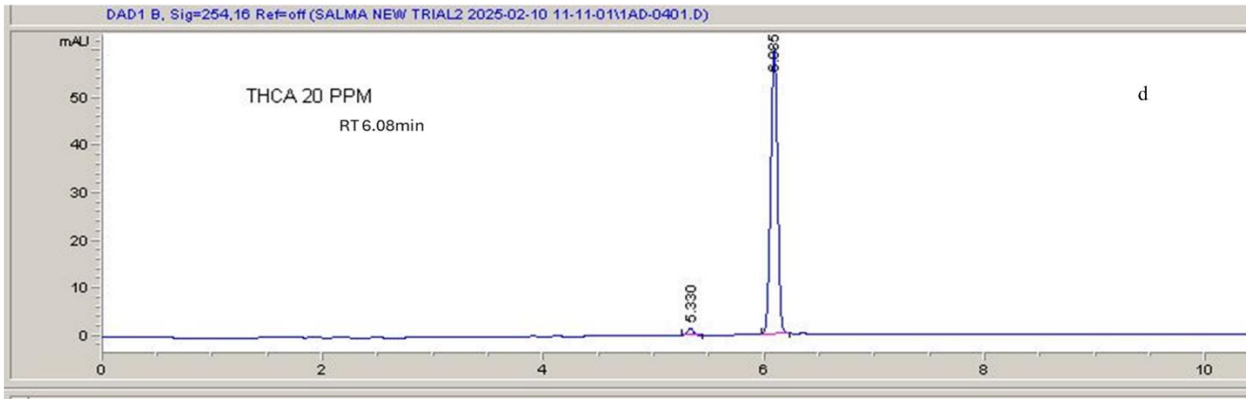
DAD1 B, Sig=254,16 Ref=off (SALMA NEW TRIAL2 2025-02-10 11-11-01\1AD-0401.D)
mAU
THCA 20 PPM
RT 6.08min
6.085
5.330
d

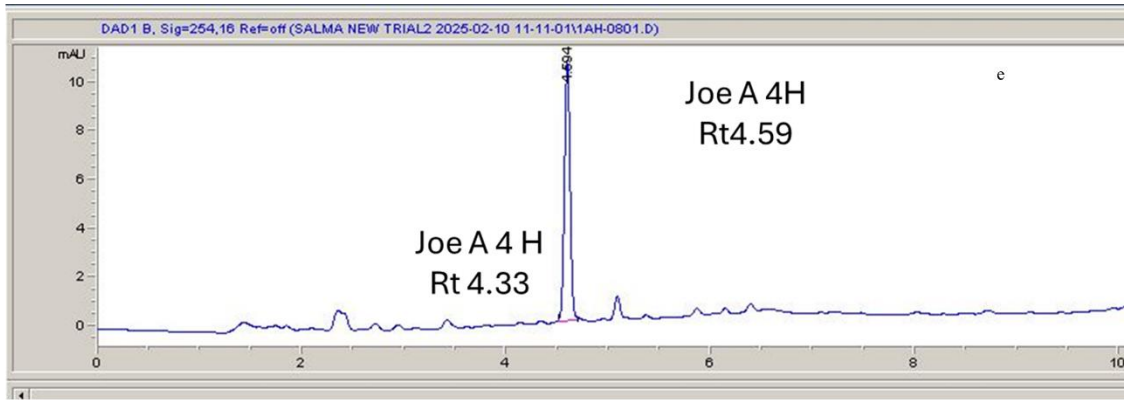
DAD1 B, Sig=254,16 Ref=off (SALMA NEW TRIAL2 2025-02-10 11-11-01\1AH-0801.D)
mAU
4.594
Joe A 4H
Rt4.59
Joe A 4 H
Rt 4.33
e

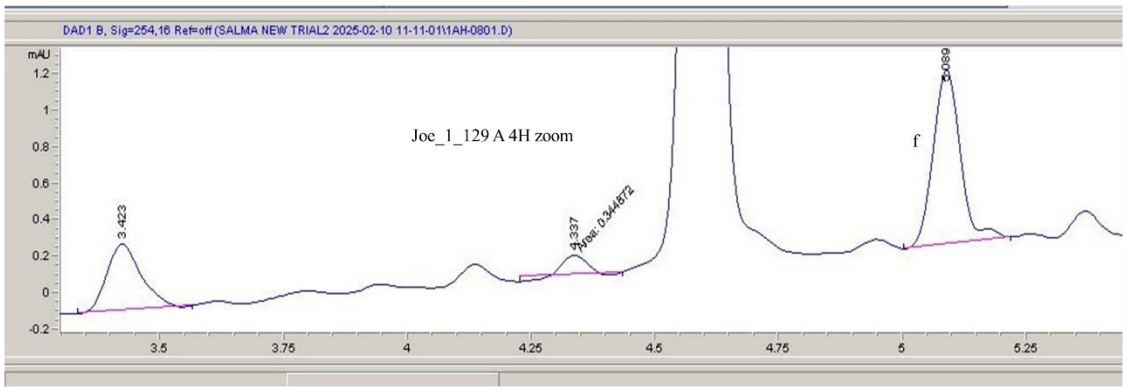
DAD1 B, Sig=254,16 Ref=off (SALMA NEW TRIAL2 2025-02-10 11-11-01\1AH-0801.D)
mAU
Joe_1_129 A 4H zoom
f
3.423
4.337
Area: 0.344572
5.089

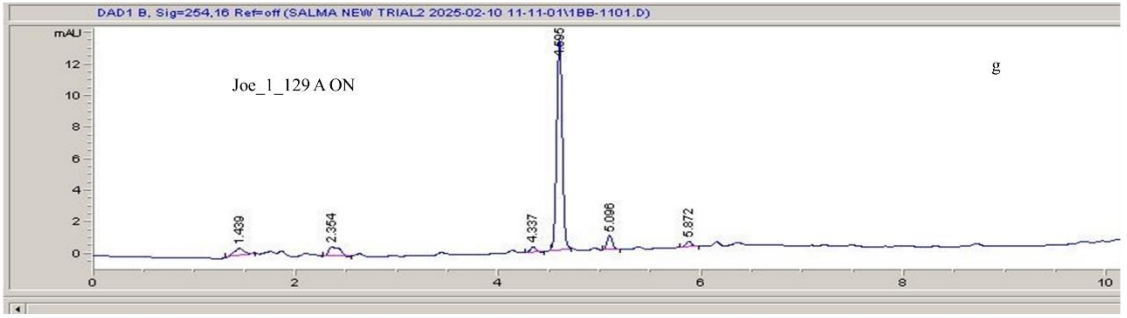
DAD1 B, Sig=254,16 Ref=off (SALMA NEW TRIAL2 2025-02-10 11-11-01\1BB-1101.D)
mAU
Joe_1_129 A ON
g
4.595
1.439
2.354
4.337
5.096
5.872

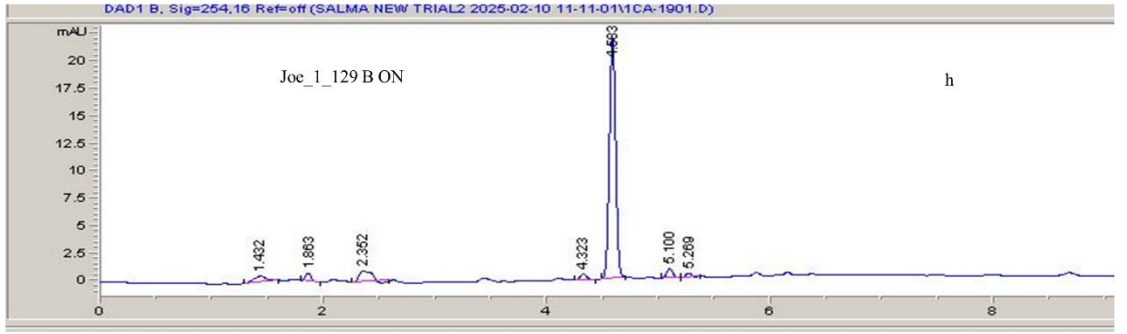
DAD1 B, Sig=254,16 Ref=off (SALMA NEW TRIAL2 2025-02-10 11-11-01\1CA-1901.D)
mAU
Joe_1_129 B ON
h
4.593
1.432
1.863
2.352
4.323
5.100
5.269

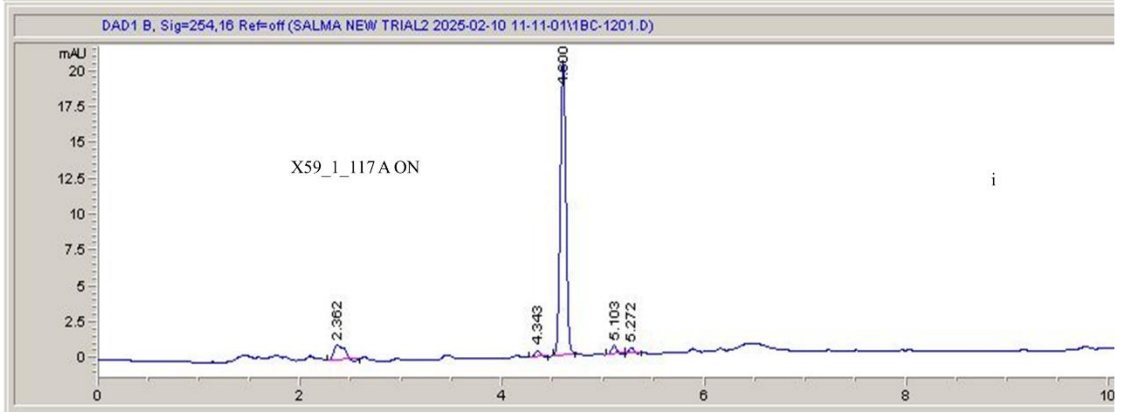
DAD1 B, Sig=254,16 Ref=off (SALMA NEW TRIAL2 2025-02-10 11-11-01\1BC-1201.D)
mAU
X59_1_117 A ON
i
4.600
2.362
4.343
5.103
5.272

Figure 17. Chromatographic evaluation of enzymatic activity tests for detecting CBGA and CBDA following HPLC analysis. The enzyme assay(4^{th}) was performed for 4 hours and overnight at 30°C, 500 rpm, utilizing 25 mM sodium acetate buffer for some samples. The chromatograms present the retention times for CBGA (4.59 minutes), CBDA (4.3 minutes), and THCA (6.08 minutes). (a) Chromatogram depicting the 20 ppm CBGA standard. (b) Chromatogram showing the 20 ppm CBDA standard. (c) Chromatogram of a combined standard comprising 10 ppm CBGA and 10 ppm CBDA. (d) Chromatogram illustrating the 20 ppm THCA standard. (e) Chromatogram of sample Joe_1_129 without buffer after 4 hours of incubation, revealing peaks for CBGA and CBDA. (f) Zoomed-in chromatogram of sample Joe_1_129(e). (g) Chromatogram of sample Joe_1_129 after overnight incubation, displaying peaks for CBGA and CBDA. (h) Chromatogram of sample Joe_1_129 with buffer and overnight incubation, showing peaks for CBGA and CBDA. (i) Chromatogram of sample X59_1_117 with buffer following overnight incubation, highlighting peaks for CBGA and CBDA. Peaks for CBGA and CBDA are observed in all four treatment groups, although the peak areas differ, indicating variations in enzymatic activity. No peaks for THCA were identified in any of the chromatograms.

The other CBDAS variant, X59_1_117 (A) (overnight), shows the peak coverage area for CBDA is 1.6, while for CBGA, it is 79.3. None of the other replicates of the X59_1_117 variant showed significant results for the final enzyme assay. These findings point out the need for further optimization of reaction conditions, such as enzyme concentration, pH, temperature, and incubation time, to achieve reliable and reproducible results in enzyme assays. Systematic optimization is crucial to improving the efficiency of CBGA-to-CBDA conversion.

4.1.10 Enzyme Activity and Conversion Efficiency

Since X59-1_117 (A-Overnight) and Joe_1_129 (A-Overnight) have nearly the same conversion efficiency, a detailed comparison of their enzyme activity and normalized protein intensity (Table 5) is necessary to determine which CBDAS variant is more effective. In our comparison of conversion efficiency and enzyme activity across various variants based on incubation time (enzyme assay), we found that the Joe_1_129 (A)

sample, when incubated with substrate CBGA for just 4 hours, had a lower conversion efficiency (0.84%) and enzyme activity (0.24) in contrast to another replicate of the same variant, which displays higher conversion efficiency (2.46%) and enzyme activity (0.89) after incubating CBDAS Overnight with CBGA. These findings emphasize that incubating CBDAS with CBGA overnight is the ideal condition for optimizing both conversion efficiency and enzyme activity (Table 6). The conversion efficiency of Joe_1_129(A-overnight) (2.46%) is slightly higher than that of X59-1_117 (A-overnight)) (1.98%) (Table 6)**.** However, when comparing enzyme activity**,** X59_1_117 (A-overnight) (1.14) outperforms Joe_1_129 (A-overnight) (0.89)**,** meaning that X59_1_117(A-overnight)) produces more CBDA per unit of the enzyme**,** making it a more efficient catalyst. Additionally, the normalized protein intensity of Joe_1_129 (A-overnight) was 1.46 (Table 5), which was slightly higher than that of X59_1_117 (A-overnight) 1.40, yet its enzyme activity was lower (Table 6). This suggests that although Joe_1_129 (A-overnight) produces slightly more enzyme**,** X59_1_117 (A-overnight) has better catalytic efficiency per unit of protein, meaning that it is functionally superior. Given that both samples were incubated under the same conditions, the data suggests that X59_1_117(A-overnight) is the more efficient CBDAS variant, as it exhibits higher enzyme activity despite similar conversion efficiency.

Table 5: A detailed normalized band intensity calculation for the *CBDAS* and *GAPDH* genes based on area and mean values obtained using ImageJ software

Sr #	Sample Name	Initial Protein Con.(ug/ul)	*CBDAS* Gene (Image J)		Area /Mean	*GAPDH* Gene (Image J)		Area /Mean	Normalized Band Intensity CBDAS (Area/Mean) /GAPDH (Area/Mean)
			Area	Mean		Area	Mean		
1	Del-1-108 P1	4.1	1,728	128.52	13.44	1,728	144.02	12.00	1.12
2	Del-1-108 P2	Out of range (High)	1,728	126.82	13.63	1,728	145.28	11.89	1.15
3	CRS1-105 P1	Out of range (High)	1,728	122.13	14.15	1,728	151.69	11.39	1.24
4	CRS1-105 P2	4.3	1,728	141.76	12.19	1,728	150.67	11.47	1.06
5	X59-1-117 P2	1.9	1,728	143.97	12.00	1,728	149.77	11.54	1.04
6	Joe-1-129 P1	3.5	1,728	128.59	13.44	1,728	150.26	11.50	1.17
7	X59-1-117 P1	1.7	1,728	112.60	15.35	1,728	157.77	10.95	1.40
8	Joe-1-129 P2	3.8	1,728	109.15	15.83	1,728	159.52	10.83	1.46

Table 6. A detailed enzyme activity and conversion ratio calculation, based on HPLC analysis and band normalization from Western blot data.

Sample #	HPLC Retention Time (CBGA)	HPLC Peak Area (CBGA)	HPLC Retention Time (CBDA)	HPLC Peak Area (CBDA)	Western membrane (Band intensity)	Enzyme Activity (CBDA / Normalized Intensity)	Conversion Efficiency (%)
Joe_1_129 A 4Hrs	4.59	40.8	4.3	0.34	1.46	0.24	0.84%
Joe_1_129 A Overnight	4.59	51.5	4.3	1.3	1.46	0.89	2.46%
Joe_1_129 B overnight	4.59	85.6	4.3	2	1.46	1.37	2.28%
X59_1_117 A overnight	4.6	79.3	4.3	1.6	1.4	1.14	1.98%

CHAPTER 5: DISCUSSION

5.1 Analysis of CBDAS Variants Activity

Industrial hemp (*Cannabis sativa* L.) is a dioecious diploid (2n = 20) plant that is mainly grown for fiber, seed, and oil (Deguchi et al., 2020). Evidence shows that human civilization historically used industrial hemp (*Cannabis sativa* L.) for its phytochemicals and lignocellulosic biomass. Hemp is a highly resourceful crop with industrial applications in fiber production, oil extraction, food processing, and animal feed, making it a crucial resource for sustainable manufacturing and economic growth. Given the increasing demand, it is crucial to adapt biotechnological approaches to cultivate new hemp varieties rich in valuable phytochemicals, thereby improving efficiency, quality, and overall industrial profitability.

In the study of cannabinoid biosynthesis, Taura et al. identified and isolated two key enzymes, THCA synthase and CBDA synthase, which are specifically active in drug-type (THCA-rich) and fiber-type (CBDA-rich) chemical varieties of *C. sativa* (Taura et al., 1995, 1996). These enzymes, the first cannabinoid synthases to be characterized, are of significant interest for biotechnological applications as they generate the direct precursors of pharmacologically active cannabinoids. Additionally, these enzymes carry out a unique biosynthetic step, the specific oxidative cyclization of the geranyl group in cannabigerolic acid (CBGA), a reaction not seen in any other known biochemical processes. Furthermore, the relationship between THCA synthase and CBDA synthase in terms of structure, function, and genetics is also very interesting and worth studying further.

CBD and THC are produced by decarboxylation from acid precursors, CBDA and THCA, that are themselves produced from cannabigerolic acid (CBGA) through enzymatic reactions by their respective enzymes, CBDAS and THCAS. Both enzymes are partially promiscuous. That is, each of them can convert CBGA to CBDA and THCA at different ratios, with the most common being 10:1 and 20:1. Therefore, even when a plant has no *THCAS* gene, it would still contain THCA. This poses a problem since many regulatory bodies in different countries, including Health Canada, regulate hemp varieties for cultivation by the maximum amount of THC produced by plants (0.3% of dry weight of flowers in Canada). These enzymes have many structural similarities. After initial bioinformatic work and analysis of available databases conducted by Dr. Aparna Singh, a postdoctoral researcher in Igor Kovalchuk's lab, 26 unique functional *CBDAS* variants were identified. It was hypothesized that some variants might convert CBGA to CBDA and THCA at ratios significantly higher than 20:1 or even produce only CBDA.

To enhance enzyme properties for cannabinoid production, all 26 sequences were analyzed, focusing on glycosylation patterns, the impact on the C-terminal berberine bridge (BBE) domain, active sites, and enzyme specificity. Notably, the analysis of variants expressed in yeast *Komagataella phaffii* showed that the S116A SNP at the activation site of CBDAS variants resulted in a 2.6-fold increase in CBDA production compared to the wild-type CBDAS (Zirpel et al., 2018). Through this study, I investigated these findings by examining the effects of the *CBDAS* variants isolated from several hemp cultivars (Joe_1_129, X59_1_117, Del_1_108, CRS1_105) on CBDA and THCA production. This was achieved by stably transforming the gene variants into *Nicotiana benthamiana* plants.

Extracts from these plants were prepared, and *in vitro* conversion reactions were performed to assess enzyme activity and product ratios.

The biosynthesis of cannabinoids has traditionally been limited to *Cannabis sativa*, but recent advances in metabolic engineering have enabled heterologous production of these compounds in alternative plant systems. Reddy et al. (2022) engineered *Nicotiana benthamiana* to serve as a platform for producing cannabinoid precursors and their analogues. They generated stable transgenic *N. benthamiana* plants expressing cannabis-derived acyl-activating enzyme (AAE) and olivetol synthase (OLS), enabling the biosynthesis of olivetol upon infiltration of hexanoic acid. Transient expression of olivetolic acid cyclase (OAC) in these transgenics further facilitated the production of olivetolic acid (OA). To expand the chemical diversity toward minor and novel cannabinoids, butanoic acid, propanoic acid, pentanoic acid, and heptanoic acid were infiltrated using Agrobacterium-mediated leaf infiltration, which led to the production of divarinic acid (DA) and various novel cannabinoid precursors with different side chains. Cell lines derived from these transgenic plants were also established, although whole plants produced higher olivetol levels than cell cultures. While cannabigerolic acid (CBGA), the central cannabinoid intermediate, was not detected, likely due to low precursor availability. The study demonstrates the feasibility of using *N. benthamiana* as a versatile host to investigate enzyme substrate specificity and to develop new-to-nature cannabinoids through synthetic biology (Reddy et al., 2022).

This study provides information that can be used to study the effects of SNP mutations (*CBDAS* variants) on the rate of conversion of CBGA into CBDA and THCA and the ratio of the final products. This research builds on the work of Zirpel et al., who studied the

recombinant expression of THCAS and CBDAS in *Komagataella phaffii* to explore their catalytic mechanisms, structural features, and potential for producing cannabinoids through biotechnology (Zirpel et al., 2018).

Using stable tobacco transgenics to study CBDAS variants offers several key advantages over yeast systems. Tobacco (*Nicotiana benthamiana*) provides a plant-based environment that more closely mimics the native context of CBDAS, including appropriate post-translational modifications like glycosylation, correct protein folding, and the presence of plant-specific cofactors. This increases the likelihood of proper enzyme functionality. Additionally, transgenic tobacco allows for *in planta* cannabinoid pathway reconstruction, enabling researchers to evaluate CBDAS activity in a whole-organism system. In contrast, yeast systems may misfold plant enzymes or fail to perform essential modifications, limiting the accuracy of functional studies. Additionally, in one of the studies, Gulck et al. (2020) investigated the heterologous production of cannabinoids and their glucosides in alternative host systems. The researchers identified and characterized genes from *Cannabis sativa* involved in cannabinoid biosynthesis, focusing on aromatic prenyltransferases of the UbiA superfamily and chalcone isomerase-like (CHIL) proteins. Among these, *CsaPT4* exhibited cannabigerolic acid synthase (CBGAS) activity in both *N. benthamiana* and *S. cerevisiae*, with co-expression of CHIL proteins not significantly affecting CBGAS catalytic efficiency. When exploring the potential for glucosylation, the study revealed that metabolic engineering of *N. benthamiana* resulted in intrinsic glucosylation of olivetolic acid and cannabigerolic acid. In contrast, *S. cerevisiae* was engineered to produce their respective glucosides, demonstrating its potential as a more controlled system for glucosylation processes. The *N. benthamiana* system showed advantages in its ability to

naturally perform glucosylation of cannabinoid intermediates, making it a valuable platform for more complex biosynthesis without additional modifications. Meanwhile, *S. cerevisiae* presented a more robust platform for precise metabolic engineering, enabling the production of cannabinoid glucosides that could be tailored for specific applications. These findings highlight the complementary strengths of both expression systems, *N. benthamiana* for natural glucosylation and *S. cerevisiae* for engineered production of cannabinoid glucosides, making them valuable platforms for cannabinoid biosynthesis and derivative output (Gulck et al., 2020).

Genetic modification of tobacco is well-documented, and its high biomass production (over 100,000 kg of tissue per hectare) makes it suitable for large-scale production of recombinant proteins (Tremblay et al., 2010; Twyman et al., 2003). Stable transformation is often preferred over transient transformation because it ensures the desired gene is integrated into the plant's genome, allowing the traits to be inherited by future generations. *Nicotiana benthamiana* is commonly used as a model plant for AMT due to its high susceptibility to *Agrobacterium* infection, ease of genetic modification, fast growth, and suitability for both stable and transient gene expression studies. These characteristics make it an excellent system for functional genomics and protein production research (Kasschau and Carrington, 1998).

Stable transformation is favored over transient transformation because it ensures the desired gene is integrated into the plant's genome, allowing future generations to inherit the traits. I also conducted transient transformation in this study by introducing the recombinant pORE-E2 vector, containing *CBDAS* variants gene, into *Nicotiana benthamiana* (data not shown).

I conducted agroinfiltration using both syringe infiltration and vacuum infiltration methods, but the best control results for *GUS* expression were achieved with syringe infiltration. In this method, the leaves were attached to the plant and placed in the dark. Samples were collected after 48 and 72 hours of agroinfiltration. However, when performing protein extraction for Western blot analysis, the intensity of the bands was very weak, or bands were undetectable. Consequently, I decided to shift focus from transient expression to stable transformation, aiming for high biomass from transformed leaves to ensure sufficient protein extraction and detection material. To develop transgenic plants, I utilized the 35S constitutive promoter (Amack and Antunes, 2020) that drives *CBDAS* gene expression at all stages of plant development.

During the stable transformation process, I faced several troubleshooting challenges. Specifically, when explants were transferred to shooting media and placed in a growth chamber (25°C, 16/8-hour light/dark cycle), the explants began to turn yellow continuously. To address this, I modified the infection media, extended the incubation time of explants in the infection media from 30 minutes, added 200 µM acetosyringone to the co-cultivation media, and adjusted the plant growth regulators (PGRs). Initially, I used 6-benzylaminopurine (6BAP) and indole-3-acetic acid (IAA) but later switched to naphthaleneacetic acid (NAA) instead of IAA, along with the introduction of silver nitrate (AgNO3). Despite these changes, the explants continued to show yellowing.

I then moved some of the explants to a lab desk with a room temperature of approximately 25°C, where I could not control the day length or light period. Although callus formation started, after several weeks, the explants mainly formed callus-like structures without developing proper leaves. Finally, I relocated all the explants to a growth chamber with the

same conditions as before, but with a light spectrum comprising both white and red lights. In this chamber, I was able to achieve successful plant regeneration within a few weeks. This series of events highlights the critical role that light spectra play in the healthy regeneration and development of transgenic plants, as emphasized by Gomes et al. (2023) and Yuejing et al. (2023), who demonstrated how light intensity and spectral composition influence both transient and stable transformation processes as well as gene expression in regenerated plants.

Subcellular localization is a key factor in the efficient biosynthesis of cannabinoids, as the positioning of enzymes within specific cellular compartments can impact their stability, activity, and post-translational modifications. Enzymes such as Δ^9-tetrahydrocannabinolic acid synthase (THCAS) and cannabidiolic acid synthase (CBDAS) require proper targeting to organelles like the endoplasmic reticulum to ensure correct folding and glycosylation, which are essential for their functionality. Optimizing the intracellular location of these enzymes is therefore critical for enhancing the production of cannabinoids like tetrahydrocannabinolic acid (THCA) and cannabidiolic acid (CBDA) in heterologous expression systems. In one of the studies, Geissler et al. (2018), focused on the production of Δ^9-tetrahydrocannabinolic acid synthase (THCAS), a key enzyme in cannabinoid biosynthesis, by transiently expressing it in *Nicotiana benthamiana*, a model plant system. A modular cloning strategy was used to construct expression vectors, allowing the THCAS gene to be directed to various compartments within the plant cell, including the cytosol, plastids, and endoplasmic reticulum (ER). Protein expression was observed to be successful only when the enzyme was targeted to the ER, suggesting that this subcellular location supports proper folding or stabilization. The enzyme also appeared to undergo

glycosylation, indicating the plant host's capacity to apply post-translational modifications that might influence protein activity and durability. Functional assays using cannabigerolic acid as the substrate confirmed that the recombinant enzyme could catalyze the production of both tetrahydrocannabinolic acid (THCA) and cannabichromenic acid (CBCA), with significantly higher activity levels for THCA. These findings demonstrate the feasibility of using *N. benthamiana* for the expression of complex cannabinoid biosynthetic enzymes, while also highlighting the importance of targeting strategies within the cell to ensure effective enzyme production and activity (Geissler et al., 2018).

In this study, CBDAS enzyme assays were optimized to evaluate CBDAS activity and compare results under varying conditions. The assay initially followed the protocol described by Taura et al. (2007), using 0.1% (w/v) Triton X-100 and 100 mM sodium citrate buffer (pH 5.0). Triton X-100, a commonly used non-ionic detergent, helps solubilize membrane proteins without denaturing them. However, I suspected that Triton X-100 might interfere with CBDAS activity, prompting me to exclude detergents from the enzyme assay. Despite this, NP-40 detergent was used during total protein extraction from transgenic *Nicotiana benthamiana* plants and for the IP of CBDAS-expressed protein. NP-40, another non-ionic detergent, is well-suited for extracting membrane and cytosolic proteins in a non-denaturing way, ensuring that proteins like CBDAS remain functionally active after extraction. This is essential for studying their role in the phenylpropanoid pathway. However, to remove any remaining contaminants or detergents, Sephadex-25 gel filtration was carried out using 25 mM sodium acetate buffer (pH 4.5).

Various buffers were assessed to determine their impact on CBDAS activity, including 100 mM sodium citrate at pH 5.0 (Taura et al., 2007), 0.1 M sodium citrate buffer at pH 5.0

(Dai et al., 2024), and 25 mM sodium acetate buffer at pH 4.85. Although this was not a strictly controlled comparative experiment, enzyme activity was noted in the 25 mM sodium acetate buffer at pH 4.86. Given that other reaction parameters varied, it is challenging to make conclusive statements regarding the influence of buffers; nevertheless, the detected activity in sodium acetate suggests it may create optimal conditions for CBDAS functionality. Likely because its lower ionic strength helps maintain enzyme stability and activity. In comparison, citrate, especially at higher concentrations, may bind to essential metal cofactors or disrupt protein interactions. Acetate also performed better during Sephadex gel filtration, improving separation and enzyme efficiency. Similar experiments by Zirpel et al. (2018) confirmed that the best pH for CBDAS activity is 4.5, with activity being lost at pH levels above 6.5.

To find the ideal temperature for CBDAS enzyme activity, experiments were performed at 37°C, as suggested by Zirpel et al. (2018) and Dai et al. (2024), as well as at 30°C, in accordance with Taura et al. (2007) and Fantino et al. (2025). Although the study was not intended to be a direct comparison, higher activity levels of CBDAS were identified at 30°C. This is probably because CBDAS is an enzyme derived from plants, which functions best under the moderate growth conditions characteristic of *Cannabis sativa*. At 37°C, the enzyme may become less stable or experience partial denaturation, which can result in decreased activity.

To further optimize the incubation time, enzyme activity was tested over different durations: 30 minutes, 2 hours (Taura et al., 1996), 4 hours (Zirpel et al., 2018), and overnight (Dai et al., 2024; Fantino et al., 2025). Strong enzymatic activity was observed at 4 hours and overnight incubation, suggesting that CBDAS has a slow catalytic rate. This

likely reflects the need for extended time to allow proper enzyme folding, cofactor interactions, and the accumulation of detectable products.

After optimizing pH, incubation time, buffer composition, and temperature, I detected very low enzyme activity in only two *CBDAS* variants: Joe_1_129 and X59_1_117. The conversion of CBGA resulted in the production of CBD only, with no THC peak observed during HPLC analysis. The other two variants, CRS1_105 and Del_1_108, showed no detectable enzymatic activity.

I also got seeds from transgenic plants expressing the *CBDAS* variations, which could be cultivated F1 and F2 generations. These seeds offer a rich source for additional research on enzyme activity throughout several plant generations. Analyzing the F1 and F2 plants helps us to evaluate the stability and inheritance of the *CBDAS* gene, assess any variations in enzyme activity, and ascertain whether the intended features are regularly expressed.

CHAPTER 6: CONCLUSION AND FUTURE SIGNIFICANCE

This study successfully developed transgenic *Nicotiana benthamiana* plants that overexpressed *CBDAS* variants linked with SNPs and optimized assay conditions to evaluate their enzymatic activity. The findings highlight the critical role of buffer composition, pH, temperature, and incubation time in maintaining CBDAS stability and function. The observed differences in enzymatic activity between the variants suggest that specific SNPs may influence *CBDAS* functionality, which could have significant applications for metabolic engineering and cannabinoid biosynthesis.

Future research should aim to elucidate these SNPs' structural and functional impact on *CBDAS* activity, consider alternative expression systems to boost yield, and examine

cofactor necessities and protein-protein interactions that may influence CBDAS efficiency. Gaining insight into these mechanisms could enhance genetic engineering approaches for maximizing CBDA production, which holds significance for both pharmaceutical and industrial sectors.

Additionally, by optimizing several assay conditions, such as pH, temperature, buffer composition, and incubation time, the enzyme activity of CBDAS was detected in two variants, Joe_1_129 and X59_1_117. HPLC analysis verified the conversion of CBGA to the production of CBDA without any detectable peak for THCA. In contrast, the other two variants, CRS1_105 and Del_1_108, showed no measurable enzymatic activity, indicating possible structural or functional constraints.

Despite these observations, the overall enzyme activity was still low, highlighting the necessity for further refinement. Future enhancements could concentrate on fine-tuning buffer conditions, enzyme purification methods, and cofactor addition to improve stability and catalytic effectiveness. Additionally, investigating alternative detergents or lipid-based environments that more closely resemble the native membrane-associated state of *CBDAS* may enhance solubility and activity. Further structural and kinetic investigations, potentially involving site-directed mutagenesis, could assist in pinpointing crucial residues that affect enzyme efficiency, ultimately advancing *CBDAS* performance for biotechnological uses.

This study holds significant implications for the development of regulatory-compliant hemp strains by identifying CBDAS variants that produce only cannabidiolic acid (CBDA) without generating tetrahydrocannabinolic acid (THCA), thus helping ensure THC levels remain below the legal threshold of 0.3% in regions such as Canada, the United States, and

the European Union. Achieving stable and optimized CBDA expression in hemp not only minimizes legal risks associated with THC contamination but also enhances crop value for farmers. Furthermore, the production of F1 and F2 seeds from transgenic lines enables the long-term evaluation of gene inheritance, expression consistency, and the stability of desired traits. Importantly, this study is the first to employ a stable plant-based expression system using *Nicotiana benthamiana* to assess CBDAS variant activity in a biological context more closely related to *Cannabis sativa*, providing a novel and relevant platform for future functional analyses.

REFERENCES

1. Ahmed MZ, Ahmed O, Aibao Z, Hanbin S, Siyu L, Ahmad A. (2020). Epidemic of COVID-19 in China and associated Psychological Problems. *Asian J Psychiatr*. ;51:102092. doi: 10.1016/j.ajp.2020.102092.

2. Ahmed, S., Gao, X., Jahan, M.A., Adams, M., Wu, N., Kovinich, (2021). Nanoparticle-based genetic transformation of *Cannabis sativa. J. Biotechnol*. 326, 48–51. https://doi.org/10.1016/j.jbiotec.2020.12.014.

3. Amack, S. C., & Antunes, M. S. (2020). CaMV35S promoter – A plant biology and biotechnology workhorse in the era of synthetic biology. Current Plant Biology, 24, 100179. https://doi.org/10.1016/j.cpb.2020.100179

4. Andre, C. M., Hausman, J., & Guerriero, G. (2016). *Cannabis sativa*: The Plant of the Thousand and One Molecules. *Front. Plant Sci. 7,* 174167. https://doi.org/10.3389/fpls.2016.00019.

5. Arya, S.S., Rookes, J.E., Cahill, D.M., Lenka, S.K. (2020). Next-generation metabolic engineering approaches towards development of plant cell suspension cultures as specialized metabolite producing biofactories. *Biotechnol. Adv*. 45, 107635. https://doi.org/10.1016/j.biotechadv.2020.107635.

6. Beard, K.M., Boling, A.W.H., Bargmann, B.O.R. (2021). Protoplast isolation, transient transformation, and flow-cytometric analysis of reporter-gene activation

in *Cannabis sativa* L. *Ind. Crop. Prod*. 164, 113360. https://doi.org/10.1016/j.indcrop.2021.113360.

7. Bharadwaj, R., Kumar, S.R., Sharma, A., Sathishkumar, R. (2021). Plant metabolic gene clusters: evolution, Organization, and their applications in synthetic biology. *Front. Plant Sci*. 12, 697318. https://doi.org/10.3389/fpls.2021.697318.

8. Bócsa I., Máthé P., and Hangyel L. (1997). Effect of nitrogen on tetrahydrocannabinol (THC) content in hemp (*Cannabis sativa* L.) leaves at different positions. *J. Int. Hemp. Assoc*. **4**(2): 78–79.

9. Bohlmann, J., Gershenzon, J. (2009). Old substrates for new enzymes of terpenoid biosynthesis. *Proc. Natl. Acad. Sci*. U.S.A. 106 (26), 10402–10403. https://doi.org/ 10.1073/pnas.0905226106.

10. Callaway, J. C. (2004). Hempseed as a nutritional resource: An overview. *Euphytica*, 140(1–2), 65–72.

11. Campbell, L.G., Dufresne, J., Sabatinos, S.A. (2020). Cannabinoid inheritance relies on complex genetic Architecture. *Cannabis and Cannabinoid Res*. 5 (1), 105–116. https://doi.org/10.1089/can.2018.0015.

12. Casano, Salvatore & Grassi, Gianpaolo & Martini, V & Michelozzi, Marco. (2011). Variations in Terpene Profiles of Different Strains of *Cannabis sativa* L. *Acta hortic*. 925. 115-121. 10.17660/ActaHortic.2011.925.15.

13. Chandra S, Bandopadhyay R, Kumar V, Chandra R. (2010). Acclimatization of tissue cultured plantlets: from laboratory to land. *Biotechnol Lett*. 32(9):1199-205. doi: 10.1007/s10529-010-0290-0.

14. Chandra, S., Lata, H., Khan, I.A., ElSohly, M.A. (2017). *Cannabis sativa* L.: Botany and Horticulture. In: Chandra, S., Lata, H., ElSohly, M.A. (Eds.), *Cannabis Sativa L*. Botany and Biotechnology. Springer International Publishing, pp. 79–100. https://doi.org/10.1007/978-3-319-54564-6_3.

15. Chen, T., Hao, J., He, J., Zhang, J., Li, Y., Liu, R., Li, L. (2013). Cannabisin B induces autophagic cell death by inhibiting the AKT/mTOR pathway and S phase cell cycle arrest in HepG2 cells. *Food Chem*. 138 (2–3), 1034–1041. https://doi.org/10.1016/j.foodchem.2012.11.102.

16. Clarke, R.C., Merlin, M.D. (2016). Cannabis Domestication, breeding history, present-day genetic diversity, and future prospects. *Crit. Rev. Plant Sci*. 35 (5–6), 293–327. https://doi.org/10.1080/07352689.2016.1267498.

17. Constantin MJ, Henke RR, Mansur MA. (1977). Effect of activated chappellrcoal on callus growth and shoot organogenesis in tobacco. *In vitro*. 13:293-296. doi: 10.1007/BF02616173.

18. Coutu, C., Brandle, J., Brown., K. Brown., B. Miki., J.simmonds., D. Hegedus. (2007). pORE: a modular binary vector series suited for both monocot and dicot plant transformation. *Transgenic Res* **16**, 771–781 (2007). https://doi.org/10.1007/s11248-007-9066-2.

19. Cox, C. (2018). The Canadian Cannabis Act legalizes and regulates recreational cannabis use in 2018. *Health Pol*. 122 (3), 205–209. https://doi.org/10.1016/

20. Dai, L., Niu, T., Luo, R., Zhang, L., Zhang, S., Kang, Y., Chi, J., Feng, X., Shi, J., Tian, Y., Gao, B., & Li, Z. (2024). Improvement of cannabidiolic acid synthetase activity through molecular docking and site-directed mutagenesis. *Industrial Crops and Products*, *208*, 117860. https://doi.org/10.1016/j.indcrop.2023.117860

21. Davis, E.M., Croteau, R. (2000). Cyclization enzymes in the biosynthesis of monoterpenes, sesquiterpenes, and Diterpenes. In: Leeper, F.J., Vederas, J.C. (Eds.), Biosynthesis: Aromatic Polyketides, Isoprenoids, Alkaloids. Springer, pp. 53–95. https://doi.org/10.1007/3-540-48146-X_2.

22. Davis WM, Hatoum NS. Neurobehavioral actions of cannabichromene and interactions with delta 9-tetrahydrocannabinol. *Gen Pharmacol*. 1983;14(2):247-52. doi: 10.1016/0306-3623(83)90004-6. PMID: 6301931.

23. DeLong, G. T., Wolf, C. E., Poklis, A., & Lichtman, A. H. (2010). Pharmacological evaluation of the natural constituent of *Cannabis sativa*, cannabichromene and its modulation by Δ9-tetrahydrocannabinol. *Drug and Alcohol Dependence*, 112(1-2), 126-133. https://doi.org/10.1016/j.drugalcdep.2010.05.019

24. de Meijer, E.P.M., Bagatta, M., Carboni, A., Crucitti, P., Moliterni, V.M.C., Ranalli, P., Mandolino, G. (2003). The inheritance of chemical phenotype in *Cannabis sativa* L. *Genetics* 163 (1), 335–346. https://doi.org/10.1093/genetics/163.1.335.

25. de Meijer, E.P.M., Hammond, K.M., Micheler, M. (2009). The inheritance of chemical phenotype in *Cannabis sativa* L. (III): variation in cannabichromene proportion. *Euphytica* 165 (2), 293–311. https://doi.org/10.1007/s10681-008-9787-1.

26. Deguchi, M., Kane, S., Potlakayala, S., George, H., Proano, R., Sheri, V., Curtis, W. R., & Rudrabhatla, S. (2020). Metabolic Engineering Strategies of Industrial Hemp (*Cannabis sativa* L.): A Brief Review of the Advances and Challenges. *Front. Plant Sci*, 11, 580621. https://doi.org/10.3389/fpls.2020.58062

27. Devsi, A., Kiyota, B., Ouellette, T., Hegle, A.P., Rivera-Acevedo, R.E., Wong, J., Dong, Y., Pugsley, M.K., Fung, T. (2020). A pharmacological characterization of *Cannabis sativa* chemovar extracts. *J. Cannabis Res*. 2, 17. https://doi.org/10.1186/s42238-020-00026-0.

28. Divashuk M.G., Alexandrov O.S., Razumova O.V., Kirov I.V., and Karlov G.I. (2014). Molecular cytogenetic characterization of the dioecious *Cannabis sativa* with an XY chromosome sex determination system. *PLoS ONE*. **9**(1): doi: 10.1371/journal.pone.0085118.

29. Dudareva, N., Klempien, A., Muhlemann, J.K., Kaplan, I. (2013). Biosynthesis, function and metabolic engineering of plant volatile organic compounds. *New Phytol*. 198 (1), 16–32. https://doi.org/10.1111/nph.12145.

30. Eisohly HN, Turner CE, Clark AM, Eisohly MA. Synthesis and antimicrobial activities of certain cannabichromene and cannabigerol related compounds. *J Pharm Sci*. 1982 Dec;71(12):1319-23. doi: 10.1002/jps.2600711204. PMID: 7153877.

31. ElSohly, M. A., & Slade, D. (2005). Chemical constituents of marijuana: The complex mixture of natural cannabinoids. *Life Sciences*, 78(5), 539–548.

32. Fantino, E., Messaabi, A., Mérindol, N., Awwad, F., Sene, N., Gélinas, S., Custeau, A., Rhéaume, K., Meddeb-Mouelhi, F., & Desgagné-Penix, I. (2025). Extrachromosomal expression of functional *Cannabis sativa* cannabidiolic acid synthase in Phaedodactylum tricornutum. *Algal Research*, *85*, 103889. https://doi.org/10.1016/j.algal.2024.103889

33. Feeney, M., Punja, Z.K., 2003. Tissue culture and *Agrobacterium*-mediated transformation of hemp (*Cannabis sativa* L.). *In Vitro Cell Dev. Biol. Plant* 39 (6), 578–585. https://doi.org/10.1079/IVP2003454.

34. Fellermeier, M., Zenk, M.H. (1998). Prenylation of olivetolate by a hemp transferase yields cannabigerolic acid, the precursor of tetrahydrocannabinol. *FEBS (Fed. Eur. Biochem. Soc.)* Lett. 427 (2), 283–285. https://doi.org/10.1016/s0014-5793(98)00450-5.

35. Fetterman, P.S., Keith, E.S., Waller, C.W., Guerrero, O., Doorenbos, N.J., Quimby, M.W., (1971). Mississippi-grown *Cannabis sativa* L: Preliminary observation on chemical definition of phenotype and variations in tetrahydrocannabinol content versus age, sex, and plant part. *J. Pharmaceut. Sci*. 60 (8), 1246–1249. https://doi.org/10.1002/jps.2600600832.

36. Flemming, T., Muntendam, R., Steup, C., and Kayser, O. (2007). Chemistry and biological activity of tetrahydrocannabinol and its derivatives. *In* Bioactive Heterocycles IV. *Edited by* M.T.H. Khan. Springer. pp. 1–42 10.1016/j.jmb.2012.06.030.

37. Gallily, R., Yekhtin, Z., Hanuš, L.O.(2018). The Anti-inflammatory properties of terpenoids from cannabis. *Cannabis and Cannabinoid Res*. 3 (1), 282–290. https://doi.org/10.1089/can.2018.0014.

38. Gaoni, Y., Mechoulam, R. (1964). Isolation, structure, and partial synthesis of an active constituent of hashish. *J. Am. Chem. Soc*. 86 (8), 1646–1647. https://doi.org/10.1021/ja01062a046.

39. García-Pe˜nas, J.J., Gil Nagel-Rein, A., S´anchez-Carpintero, R., Villanueva-Haba, V. (2021). Cannabidiol for the treatment of Lennox-Gastaut syndrome and Dravet syndrome: experts' recommendations for its use in clinical practice in Spain. *Rev. Neurol*. 73(S1), S1-S8. https://doi.org/10.33588/rn.73S01.2021250.

40. Geissler, M., Volk, J., Stehle, F. Kayser,O. Warzecha, H. Subcellular localization defines modification and production of Δ^9-tetrahydrocannabinolic acid synthase in transiently transformed *Nicotiana benthamiana*. *Biotechnol Lett* **40**, 981–987 (2018). https://doi.org/10.1007/s10529-018-2545-0

41. Gerasymchuk, M., Robinson, G.I., Groves, A., Haselhorst, L., Nandakumar, S., Stahl, C., Kovalchuk, O., Kovalchuk, I. (2022). Phytocannabinoids stimulate rejuvenation and prevent cellular senescence in human dermal fibroblasts. *Cells. 11* (23). https://doi.org/10.3390/cells11233939. Article 23

42. Gomes.M., M. Aragão., H. Pereira., E. Matto., P. Peixoto., M.Martins., M.Santos. (2023). Evaluation of led light on transgenic *Nicotiana benthamiana* production of a recombinant antibody fragment scFvanti-BAP1. PREPRINT (Version 1) available at Research Square [https://doi.org/10.21203/rs.3.rs-3433165/v1]

43. Gosal SS and SH Wani. (2018). Plant genetic transformation and transgenic crops: methods and applications. In Biotechnologies of Crop Improvement, Volume 2 (pp. 1-23). Springer, Cham.

44. Grassa, C.J., Wenger, J.P., Dabney, C., Poplawski, S.G., Motley, S.T., Michael, T.P., Schwartz, C.J., Weiblen, G.D. (2018). A complete cannabis chromosome assembly and adaptive admixture for elevated cannabidiol (CBD) content. *bioRxiv*, 458083.https://doi.org/10.1101/458083.

45. Groom, Q., Clarke, R.C., Merlin, M.D. (2014). Cannabis: Evolution and ethnobotany. 2013. *Plant Ecol. Evol*. 147 (1), 1. https://doi.org/10.5091/plecevo.2014.933.

46. Gülck, T., Booth, J. K., Carvalho, A., Khakimov, B., Crocoll, C., Motawia, M. S., Møller, B. L., Bohlmann, J., & Gallage, N. J. (2020). Synthetic biology of cannabinoids and cannabinoid glucosides in *Nicotiana benthamiana* and *Saccharomyces cerevisiae*. *Journal of Natural Products*, 83(10), 2877–2893. https://doi.org/10.1021/acs.jnatprod.0c0024.

47. Hesami, M., Jones, A.M.P. (2020). Application of artificial intelligence models and optimization algorithms in plant cell and tissue culture. *Appl. Microbiol. Biotechnol*. 104 (22), 9449–9485. https://doi.org/10.1007/s00253-020-10888-2.

48. Hesami, M., Pepe, M., Alizadeh, M., Rakei, A., Baiton, A., Phineas Jones, A.M. (2020b). Recent advances in cannabis biotechnology. *Ind. Crop. Prod*. 158, 113026. https://doi.org/10.1016/j.indcrop.2020.113026.

49. Hillig K.W. (2005). Genetic evidence for speciation in Cannabis (*Cannabaceae*). *Genet. Resour. Crop Evol*. **52**(2): 161–180. doi: 10.1073/pnas.0803601105.

50. Hurgobin, B., Tamiru-Oli, M., Welling, M.T., Doblin, M.S., Bacic, A., Whelan, J., Lewsey, M.G. (2021). Recent advances in *Cannabis sativa* genomics research. *New Phytol*. 230 (1), 73–89. https://doi.org/10.1111/nph.17140. j.healthpol.2018.01.009.

51. Kasschau, K. D., & Carrington, J. C. (1998). A Counter defensive Strategy of Plant Viruses. *Cell*. 95(6), 891–897. https://doi.org/10.1016/S0092-8674(00)81756-0.

52. Kearsey, L.J., Prandi, N., Karuppiah, V., Yan, C., Leys, D., Toogood, H., Takano, E., Scrutton, N.S. (2020). The structure of the *Cannabis sativa* olivetol-producing enzyme reveals cyclization plasticity in type III polyketide synthases. *FEBS J*. 287 (8), 1511–1524. https://doi.org/10.1111/febs.15089.

53. Kovalchuk, I., Pellino, M., Rigault, P., van Velzen, R., Ebersbach, J., Ashnest, J.R., Mau, M., Schranz, M.E., Alcorn, J., Laprairie, R.B., McKay, J.K., Burbridge, C., Schneider, D., Vergara, D., Kane, N.C., Sharbel, T.F. (2020). The genomics of cannabis and its close relatives. *Annu. Rev. Plant Biol*. 71 (1), 713–739. https://doi.org/ 10.1146/annurev-arplant-081519-040203.

54. Laverty, K.U., Stout, J.M., Sullivan, M.J., Shah, H., Gill, N., Holbrook, L., Deikus, G., Sebra, R., Hughes, T.R., Page, J.E., Bakel, H. van. (2019). A physical and genetic map of *Cannabis sativa* identifies extensive rearrangements at the THC/CBD acid synthase loci. *Genome Res*. 29 (1), 146–156. https://doi.org/10.1101/gr.242594.118.

55. Lercker, G., Bocci, F., Frega, N., Bortolomeazzi, R. (1992). Cannabinoid acids analysis. *Farmaco* 47 (3), 367–378.

56. Linder, E.R., Young, S., Li, X., Henriquez Inoa, S., Suchoff, D.H. (2022). The effect of transplant date and plant spacing on biomass production for floral hemp (*Cannabis sativa* L.). *Agronomy.* 12 (8). https://doi.org/10.3390/agronomy12081856. Article 8.

57. Liu S., Ma J., Liu H., Guo Y., Li W., Niu S. (2020). An efficient system for *Agrobacterium*-mediated transient transformation in *Pinus tabuliformis*. *Plant Methods* 16:52. 10.1186/s13007-020-00594-5

58. Livingston, S.J., Quilichini, T.D., Booth, J.K., Wong, D.C.J., Rensing, K.H., Laflamme-Yonkman, J., Castellarin, S.D., Bohlmann, J., Page, J.E., Samuels, A.L. (2020). Cannabis glandular trichomes alter morphology and metabolite content during flower maturation. *Plant J: Cell. Mol. Biol*. (Sarreguemines, Fr., Online) 101 (1), 37–56. https://doi.org/10.1111/tpj.14516.

59. Ma L, Lukasik E, Gawehns F, Takken FL. (2012). The use of agroinfiltration for transient expression of plant resistance and fungal effector proteins in *Nicotiana benthamiana* leaves. *Methods Mol Biol.* 835:61-74. doi: 10.1007/978-1-61779-501-5_4.

60. Mahlberg, P.G., Hammond, C.T., Turner, J.C., Hemphill, J.K. (1984). In: Rodriguez, E., Healey, P.L., Mehta, I. (Eds.), Structure, Development and Composition of Glandular Trichomes of *Cannabis Sativa* L. Springer *US*, pp. 23–51. https://doi.org/10.1007/978-1-4899-5355-1_2.

61. McPartland, J.M. (2018). Cannabis systematics at the levels of family, genus, and species. *Cannabis and Cannabinoid Res.* 3 (1), 203–212. https://doi.org/10.1089/can.2018.0039.

62. Ming, R., Bendahmane, A., Renner, S.S. (2011). Sex chromosomes in land plants. *Annu. Rev. Plant Biol*. 62, 485–514. https://doi.org/10.1146/annurev-arplant-042110- 103914.

63. Morimoto S., Komatsu K., Taura F., and Shoyama Y. (1998). Purification and characterization of cannabichromenic acid synthase from *Cannabis sativa*. *Phytochem*, **49**(6): 1525–1529. doi: 10.1016/s0031-9422(98)00278-7.

64. Mücke, M., Phillips, T., Radbruch, L., Petzke, F., H¨auser, W. (2018). Cannabis-based medicines for chronic neuropathic pain in adults. *Cochrane Database Syst. Rev*. 3 (3). https://doi.org/10.1002/14651858.CD012182.pub2.

65. Murray MG, Thompson WF. (1980). Rapid isolation of high molecular weight plant DNA. Nucleic Acids Res. Oct 10;8(19):4321-5. doi: 10.1093/nar/8.19.4321.

66. Nagegowda, D.A. (2010). Plant volatile terpenoid metabolism: biosynthetic genes, transcriptional regulation and subcellular compartmentation. *FEBS (Fed. Eur. Biochem. Soc.) Lett*. 584 (14), 2965–2973. https://doi.org/10.1016/j.febslet.2010.05.045.

67. Onofri, C., de Meijer, E.P.M., Mandolino, G. (2015). Sequence heterogeneity of cannabidiolic- and tetrahydrocannabinolic acid-synthase in *Cannabis sativa L*. and its relationship with chemical phenotype. *Phytochem.* 116, 57–68. https://doi.org/10.1016/j.phytochem.2015.03.006.

68. Owen, L.C., Suchoff, D.H., Chen, H. (2023). A novel method for stimulating *Cannabis sativa L*. Male flowers from female plants. *Plants*. 12 (19), 3371. https://doi.org/ 10.3390/plants12193371.

69. Pacifico D., Miselli F., Micheler M., Carboni A., Ranalli P., and Mandolino G. (2006). Genetics and marker-assisted selection of the chemotype in *Cannabis sativa* L. *Mol. Breed*. 17(3): 257–268.

70. Pacula, R.L., Smart, R. (2017). Medical marijuana and marijuana legalization. *Annu. Rev. Clin. Psychol*. 13, 397–419. https://doi.org/10.1146/annurev-clinpsy-032816- 045128.

71. Page, S.R.G., Monthony, A.S., Jones, A.M.P. (2021). DKW basal salts improve micropropagation and callogenesis compared with MS basal salts in multiple commercial cultivars of *Cannabis sativa*. *Botany*. 99 (5). https://doi.org/10.1139/cjb-2020-0179. Article 5.

72. Pattnaik, F., Nanda, S., Mohanty, S., Dalai, A. K., Kumar, V., Ponnusamy, S. K., & Naik, S. (2022). Cannabis: Chemistry, extraction and therapeutic applications. *Chemosphere*, *289*, 133012. https://doi.org/10.1016/j.chemosphere.2021.133012

73. Pichersky, E., Noel, J.P., Dudareva, N. (2006). Biosynthesis of plant volatiles: nature's diversity and ingenuity. *N.Y.Sci J*. 311 (5762), 808–811. https:// doi.org/10.1126/science.1118510.

74. Quimby M.W., Doorenbos N.J., Turner C.E., and Masoud A. (1973). Mississippi-grown marihuana: *Cannabis sativa* cultivation and observed morphological variations. *Econ. Bot*. **27**: 117–127. https://doi.org/10.1007/BF02862224.

75. Rahn, B., Pearson, B.J., Trigiano, R.N., Gray, D.J., 2016. The derivation of modern cannabis varieties. *Crit. Rev. Plant Sci*. 35 (5–6), 328–348. https://doi.org/10.1080/ 07352689.2016.1273626.

76. Reddy, V. A., Leong, S. H., Jang, C., & Rajani, S. (2022). Metabolic Engineering of Nicotiana benthamiana to Produce Cannabinoid Precursors and Their Analogues. *Metabolites*, *12*(12), 1181. https://doi.org/10.3390/metabo12121181

77. Rupasinghe, H. P. V., Davis, A., Kumar, S. K., Murray, B., & Zheljazkov, V. D. (2020). Industrial Hemp (*Cannabis sativa* subsp. *sativa*) as an Emerging Source for Value-Added Functional Food Ingredients and Nutraceuticals. *Molecules*, 25(18), 4078. https://doi.org/10.3390/molecules25184078

78. Russo, E.B., Marcu, J. (2017). Cannabis pharmacology: the usual suspects and a few promising leads. *Adv. Pharmacol*. 80, 67–134. https://doi.org/10.1016/

79. Sakamoto K., Akiyama Y., Fukui K., Kamada H., and Satoh S. (1998). Characterization; genome sizes and morphology of sex chromosomes in hemp (*Cannabis sativa* L.). Cytologia, 63(4): 459–464.

80. Salami SA, Martinelli F, Giovino A, Bachari A, Arad N, Mantri N. (2020). It Is Our Turn to Get Cannabis High: Put Cannabinoids in Food and Health Baskets. *Molecules*. 4;25(18):4036. doi: 10.3390/molecules25184036.

81. Sawler J, Stout JM, Gardner KM, Hudson D, Vidmar J, Butler L, Page JE, Myles S. (2015). The Genetic Structure of Marijuana and Hemp. *PLoS One*.26;10(8):e0133292. doi: 10.1371/journal.pone.0133292.

82. Schachtsiek, J., Hussain, T., Azzouhri, K., Kayser, O., Stehle, F. (2019). Virus-induced gene silencing (VIGS) in *Cannabis sativa* L. *Plant Methods*. 15 (1), 157. https:// doi.org/10.1186/s13007-019-0542-5.

83. Schultz, C.J., Lim, W.L., Khor, S.F., Neumann, K.A., Schulz, J.M., Ansari, O., Skewes, M.A., Burton, R.A. (2020). Consumer and health-related traits of seed from selected commercial and breeding lines of industrial hemp, *Cannabis sativa* L. *J AGR FOOD RES*2, 100025. https://doi.org/10.1016/ j.jafr.2020.100025.

84. Shoyama, Y., Tamada, T., Kurihara, K., Takeuchi, A., Taura, F., Arai, S., Blaber, M., Shoyama, Y., Morimoto, S., Kuroki, R. (2012). Structure and function of Δ1-tetrahydrocannabinolic acid (THCA) synthase, the enzyme controlling the psychoactivity of *Cannabis sativa. J. Mol. Biol*. 423 (1), 96–105. https://doi.org/10.1016/j.jmb.2012.06.030.

85. Singh, A., Bilichak, A., Kovalchuk, I. (2021). The genetics of Cannabis-genomic variations of key synthases and their effect on cannabinoid content. *Genome*. 64 (4), 490–501. https://doi.org/10.1139/gen-2020-0087.

86. Sirikantaramas S, Morimoto S, Shoyama Y, Ishikawa Y, Wada Y, Shoyama Y, Taura F. (2004). The gene controlling marijuana psychoactivity: molecular cloning and heterologous expression of Delta1-tetrahydrocannabinolic acid synthase from *Cannabis sativa L. J Biol Chem*. 279: 39767–39774.doi: 10.1074/jbc.M403693200. Epub 2004 Jun 9.

87. Small, E., Beckstead, H.D. (1973). Common cannabinoid phenotypes in 350 stocks of Cannabis. *Lloydia*. 36 (2), 144–165.

88. Small, E., & Marcus, D. (2002). Hemp: A new crop with new uses for North America. In *Trends in new crops and new uses* (pp. 284–326).

89. Sorokin, A., Yadav, N.S., Gaudet, D., Kovalchuk, I. (2020). Transient expression of the β-glucuronidase gene in *Cannabis sativa* varieties. *Plant Signal Behav*. 15 (8), 1780037. https://doi.org/10.1080/15592324.2020.1780037.

90. Staginnus, C., Zorntlein, S., de Meijer, E. (2014). A PCR marker linked to a THCA synthase polymorphism is a reliable tool to discriminate potentially THC-rich plants of *Cannabis sativa* L. *J. Forensic Sci*. 59 (4), 919–926. https://doi.org/10.1111/1556-4029.12448.

91. Steinbrecher, T., Zhu, C., Wang, L., Abel, R., Negron, C., Pearlman, D., Feyfant, E., Duan, J., Sherman, W. (2017). Predicting the effect of amino acid single-point mutations on protein stability-large-scale validation of MD-based relative free energy calculations. *J. Mol. Biol*. 429 (7), 948–963. https://doi.org/10.1016/j.jmb.2016.12.007.

92. Tahir, M.N., Shahbazi, F., Rondeau-Gagne, S., Trant, J.F. (2021). The biosynthesis of the cannabinoids. *J. Cannabis Res*. 3 (1), 7. https://doi.org/10.1186/ s42238-021-00062-4

93. Tan, Z., Clomburg, J.M., Gonzalez, R. (2018). Synthetic pathway for the production of olivetolic acid in *Escherichia coli*. *ACS Synth. Biol*. 7 (8), 1886–1896. https:// doi.org/10.1021/acssynbio.8b00075

94. Taura F. (2009). Studies on tetrahydrocannabinolic acid synthase that produces the acidic precursor of tetrahydrocannabinol, the pharmacologically active cannabinoid in marijuana. *Drug Discov Ther*.3(3):83-7.

95. Taura, F., S. Morimoto, Y. Shoyam. (1996). Purification and characterization of cannabidiolic-acid synthase from *Cannabis sativa* L. Biochemical analysis of a novel enzyme that catalyzes the oxidocyclization of cannabigerolic acid to cannabidiolic acid. *J. Biol. Chem*. 271 pp. 17411-17416. doi: 10.1074/jbc.271.29.17411

96. Taura, F., Sirikantaramas, S., Shoyama, Y., Shoyama, Y., & Morimoto, S. (2007). Phytocannabinoids in *Cannabis sativa*: Recent Studies on Biosynthetic Enzymes. *Chemistry & Biodiversity*, *4*(8), 1649-1663. https://doi.org/10.1002/cbdv.200790145

97. Taura, F., Sirikantaramas, S., Shoyama, Y., Shoyama, Y., Morimoto, S. (2007a). Phytocannabinoids in *Cannabis sativa*: recent studies on biosynthetic enzymes. *Chem. Biodivers*. 4 (8), 1649–1663. https://doi.org/10.1002/cbdv.200790145.

98. Taura, F., Sirikantaramas, S., Shoyama, Y., Yoshikai, K., Shoyama, Y., Morimoto, S. (2007b). Cannabidiolic-acid synthase, the chemotype-determining enzyme in the fiber-type *Cannabis sativa*. *FEBS (Fed. Eur. Biochem. Soc.) Lett*. 581 (16), 2929–2934. https://doi.org/10.1016/j.febslet.2007.05.043.

99. Taura, F., S. Morimoto, Y. Shoyama, R. Mechoulam. (1995). First direct evidence for the mechanism of Δ^1-tetrahydrocannabinolic acid biosynthesis. *J. Am. Chem. Soc*., pp. 9766-9767

100. The Ultimate Guide to Cannabis Terpenes: Understanding Flavor Profiles, Effects on the Body and Activation Temperature - BeTheHippy

101. Tholl, D. (2006). Terpene synthases and the regulation, diversity and biological roles of terpene metabolism. *Curr. Opin. Plant Biol*. 9 (3), 297–304. https://doi.org/10.1016/j.pbi.2006.03.014

102. Toth, J.A., Stack, G.M., Cala, A.R., Carlson, C.H., Wilk, R.L., Crawford, J.L., Viands, D.R., Philippe, G., Smart, C.D., Rose, J.K.C., Smart, L.B. (2020). Development and validation of genetic markers for sex and cannabinoid chemotype in *Cannabis sativa* L. *GCB Bioenergy*. 12 (3), 213–222. https://doi.org/10.1111/gcbb.12667.

103. Tremblay R, Wang D, Jevnikar AM, Ma S. (2010) Tobacco, a highly efficient green bioreactor for production of therapeutic proteins. *Biotechnol Adv*. 28(2):214-21. doi: 10.1016/j.biotechadv.2009.11.008.

104. Turner CE, Elsohly MA. Biological activity of cannabichromene, its homologs and isomers. *J Clin Pharmacol*. 1981 Aug-Sep;21(S1):283S-291S. doi: 10.1002/j.1552-4604.1981.tb02606.x. PMID: 7298870.

105. Twyman RM, Stoger E, Schillberg S, Christou P, Fischer R. (2003). Molecular farming in plants: host systems and expression technology. *Trends Biotechnol*.21: 570-578. 10.1016/j.tibtech.2003.10.002.

106. van Bakel, H., Stout, J.M., Cote, A.G., Tallon, C.M., Sharpe, A.G., Hughes, T.R., Page, J.E. (2011). The draft genome and transcriptome of *Cannabis sativa*. *Genome Biol*. 12 (10), R102. https://doi.org/10.1186/gb-2011-12-10-r102.

107. Vyskot B. and Hobza R. (2015). The genomics of plant sex chromosomes. *Plant Sci*. 236: 126–135. doi: 10.1016/j.plantsci.2015.03.019.

108. Wahby, I., Caba, J. M., & Ligero, F. (2017). Hairy root culture as a biotechnological tool in *C. sativa*. In S. Chandra, H. Lata, & M. A. ElSohly (Eds.), *Cannabis sativa* L. – Botany and Biotechnology (pp. 299-317). Springer, Cham.

109. Wahby, I., Caba, J.M., Ligero, F. (2013). *Agrobacterium* infection of hemp (*Cannabis sativa* L.): establishment of hairy root cultures. *J. Plant Interact*. 8 (4), 312–320. https://doi.org/10.1080/17429145.2012.746399.

110. Weiblen, G.D., Wenger, J.P., Craft, K.J., ElSohly, M.A., Mehmedic, Z., Treiber, E.L., Marks, M.D. (2015). Gene duplication and divergence affecting drug content in *Cannabis sativa*. *New Phytol*. 208 (4), 1241–1250. https://doi.org/10.1111/nph.13562.

111. Welling MT, Liu L, Kretzschmar T, Mauleon R, Ansari O, King GJ. (2020). An extreme-phenotype genome-wide association study identifies candidate cannabinoid pathway genes in Cannabis. *Sci Rep*. 29;10(1):18643. doi: 10.1038/s41598-020-75271-7.

112. Wrobel C, Dieter A, Huet A, Keppeler D, Duque-Afonso CJ, Vogl C, Hoch G, Jeschke M, Moser T. (2018). Optogenetic stimulation of cochlear neurons activates the auditory pathway and restores auditory-driven behavior in deaf adult gerbils. *Sci Transl Med*.11;10(449):eaao0540. doi: 10.1126/scitranslmed.aao0540.

113. Zhang Y, Ru Y, Shi Z, Wang H, Zhang J, Wu J, Pang H, Feng H. (2023). Effects of different light conditions on transient expression and biomass in *Nicotiana benthamiana* leaves. Open Life Sci. 14;18(1):20220732. doi: 10.1515/biol-2022-0732.

114. Zhang, X., Xu, G., Cheng, C., Lei, L., Sun, J., Xu, Y., Deng, C., Dai, Z., Yang, Z., Chen, X., Liu, C., Tang, Q., Su, J. (2021). Establishment of an *Agrobacterium*-mediated genetic transformation and CRISPR/Cas9-mediated targeted mutagenesis in hemp (*Cannabis sativa* L.). *Plant Biotechnol. J.* 19 (10), 1979–1987. https://doi.org/ 10.1111/pbi.13611.

115. Zirpel B, Kayser O, Stehle F. (2018). Elucidation of structure-function relationship of THCA and CBDA synthase from *Cannabis sativa* L. *J Biotechnol*. 20;284:17-26. doi: 10.1016/j.jbiotec.2018.07.031. Epub 2018 Jul 24. PMID: 30053500.